

## Knocking combustion in spark-ignition engines



Zhi Wang<sup>a,b,\*</sup>, Hui Liu<sup>a</sup>, Rolf D Reitz<sup>c</sup>

<sup>a</sup> State Key Laboratory of Automotive Safety and Energy, Tsinghua University, Beijing, 100084, China

<sup>b</sup> Center for Combustion Energy, Tsinghua University, Beijing 100084, China

<sup>c</sup> Engine Research Center, University of Wisconsin-Madison, Madison, WI 53706-1687, USA

### ARTICLE INFO

#### Article History:

Received 17 July 2016

Accepted 29 March 2017

#### Keywords:

Knocking combustion  
Spark ignition engine  
Auto-ignition  
Detonation  
Super-knock

### ABSTRACT

Knocking combustion research is crucially important because it determines engine durability, fuel consumption, and power density, as well as noise and emission performance. Current spark ignition (SI) engines suffer from both conventional knock and super-knock. Conventional knock limits raising the compression ratio to improve thermal efficiency due to end-gas auto-ignition, while super-knock limits the desired boost to improve the power density of modern gasoline engines due to detonation. Conventional combustion has been widely studied for many years. Although the basic characteristics are clear, the correlation between the knock index and fuel chemistry, pressure oscillations and heat transfer, and auto-ignition front propagation, are still in early stages of understanding. Super-knock combustion in highly boosted spark ignition engines with random pre-ignition events has been intensively studied in the past decade in both academia and industry. These works have mainly focused on the relationship between pre-ignition and super-knock, source analyses of pre-ignition, and the effects of oil/fuel properties on super-knock. The mechanism of super-knock has been recently revealed in rapid compression machines (RCM) under engine-like conditions. It was found that detonation can occur in modern internal combustion engines under high energy density conditions. Thermodynamic conditions and shock waves influence the combustion wave and detonation initiation modes. Three combustion wave modes in the end gas have been visualized as deflagration, sequential auto-ignition and detonation. The most frequently observed detonation initiation mode is shock wave reflection-induced detonation (SWRID). Compared to the effect of shock compression and negative temperature coefficient (NTC) combustion on ignition delay, shock wave reflection is the main cause of near-wall auto-ignition/detonation. Finally, suppression methods for conventional knock and super-knock in SI engines are reviewed, including use of exhaust gas recirculation (EGR), the injection strategy, and the integration of a high tumble - high EGR-Atkinson/Miller cycle. This paper provides deep insights into the processes occurring during knocking combustion in spark ignition engines. Furthermore, knock control strategies and combustion wave modes are summarized, and future research directions, such as turbulence-shock-reaction interaction theory, detonation suppression and utilization, and super-knock solutions, are also discussed.

© 2017 The Authors. Published by Elsevier Ltd.  
This is an open access article article under the CC BY-NC-ND license.  
(<http://creativecommons.org/licenses/by-nc-nd/4.0/>)

### Contents

1. Introduction .....	79
2. Conventional knock in SI engines .....	81
2.1. Basic characteristics of engine knocking combustion .....	81
2.2. Knock resistance and fuel chemistry.....	82
2.3. Intermediate species and auto-ignition front .....	83
2.4. Pressure oscillation and heat transfer .....	85
3. Super-knock in boosted SI engines.....	86
3.1. Relationship between super-knock and pre-ignition.....	86

\* Corresponding author at: State Key Laboratory of Automotive Safety and Energy, Tsinghua University, Beijing, 100084, China.

E-mail address: [wangzhi@tsinghua.edu.cn](mailto:wangzhi@tsinghua.edu.cn) (Z. Wang).

3.1.1. Distinguish pre-ignition and super-knock.....	86
3.1.2. Possible sources of pre-ignition before super-knock.....	88
3.2. Source analysis of pre-ignition.....	89
3.2.1. Oil droplets .....	89
3.2.2. Solid particle .....	89
3.3. The effect of oil and fuel properties on super-knock .....	91
3.3.1. Oil properties.....	91
3.3.1.1. Base stocks .....	91
3.3.1.2. Oil additives.....	91
3.3.2. Fuel properties.....	92
3.3.2.1. Composition.....	92
3.3.2.2. Octane number .....	92
3.3.2.3. Volatility .....	92
4. Combustion mode of engine knock .....	92
4.1. Visualization of combustion modes in the end gas .....	93
4.1.1. No-auto-ignition.....	93
4.1.2. End gas sequential auto-ignition .....	93
4.1.3. Detonation.....	93
4.2. Analysis of the process from pre-ignition to super-knock.....	94
4.2.1. Deflagration propagation .....	94
4.2.2. Detonation in unburned mixture.....	94
4.2.3. Pressure oscillation in combustion chamber.....	94
4.3. Effect of thermodynamic conditions on the combustion mode .....	96
4.3.1. Pressure and temperature .....	96
4.3.2. Energy density .....	96
4.3.3. Interaction of pressure - temperature - energy density .....	97
4.4. Discussion of engine knock with NTC.....	98
4.4.1. Phenomena of near-wall auto-ignition .....	98
4.4.2. Effect of shock compression on ignition delay.....	99
5. Suppression methods for engine knock.....	101
5.1. Control strategy for conventional knock.....	101
5.1.1. Retarding spark timing, improving octane number and enriching mixture .....	101
5.1.2. Exhaust gas recirculation .....	102
5.1.3. Stratified mixtures .....	102
5.1.4. Dual-fuel spark ignition with DI and PFI.....	102
5.1.5. Other methods.....	103
5.2. Control strategy for super-knock .....	104
5.2.1. Cooled EGR.....	104
5.2.2. Scavenging.....	104
5.2.3. Injection strategy .....	104
5.2.4. Integration of high tumble-high EGR-Atkinson/Miller cycle .....	105
6. Conclusions and future research directions .....	105
6.1. Conclusions .....	105
6.1.1. Conventional knock.....	105
6.1.2. Pre-ignition and super-knock.....	105
6.1.3. Knocking control strategies .....	106
6.1.4. Combustion wave modes .....	106
6.2. Future research directions .....	106
6.2.1. Fundamental theory relating to knocking combustion .....	106
6.2.2. Detonation suppression and utilization.....	106
6.2.3. Engine knock control and super-knock solution .....	107

## 1. Introduction

In recent years energy and environmental issues have become of more and more concern worldwide. In order to cut greenhouse gas exhaust, particularly CO<sub>2</sub> emissions, a series of emission standards on vehicle fuel consumption have been mandated in many countries. After 2025, even more stringent CO<sub>2</sub> emission regulations are under discussion. In Japan, industry and academia have started a project named the Research Association of Automotive Internal Combustion Engines (AICE), aiming at improving gasoline engine thermal efficiency to an unprecedented level of 50% by 2020. In Europe, major light-duty vehicle markets are moving toward about 95 g/km CO<sub>2</sub> by 2020. In the US, the average annual rate of CO<sub>2</sub> emission reduction for MYs (model year) 2017 through 2021 is 3.5 percent per year and

5 percent per year for MYs 2022 through 2025. In China, the current fuel consumption standard for domestically produced passenger cars is 6.9 L/100 km, which will be cut to 5.0 L/100 km in 2020, 4.0 L/100 km in 2025, and 3.2 L/100 km in 2030. Based on projections by the IEA (International Energy Agency), among light-duty vehicles and passenger cars in 2020, 70% will be powered by gasoline engines, and almost all vehicle models will use gasoline or diesel engines. By 2050, 58% of passenger cars will still be using internal combustion engines, among which 85% will be hybrid vehicles. Hybrid engines benefit from the advantages of internal combustion engines for high power density and battery electric motors for high energy conversion efficiency. The fundamental cause of fuel saving is due to the adoption of a high efficiency dedicated engine to convert fuel chemical energy to power. Therefore, internal combustion

## Abbreviations

AFR	Air Fuel Ratio
AKI	Anti-knock Index
ATDC	After Top Dead Centre
BDC	Bottom Dead Centre
BMEP	Brake Mean Effective Pressure
BTDC	Before Top Dead Center
BTE	Brake Thermal Efficiency
CA	Crank Angle
CFD	Computational Fluid Dynamics
CJ	Chapman-Jouguet
CN	Cetane Number
CR	Compression Ratio
DI	Direct Injection
DISI	Direct Injection Spark ignition
EGR	Exhaust Gas Recirculation
EOI	End of Injection
GDI	Gasoline Direct Injection
HCCI	Homogeneous Charge Compression ignition
HRR	Heat Release Rate
IMEP	Indicated Mean Effective Pressure
KI	Knock Index
KLSA	Knock Limit Spark Advance
KLT	Knock Limit Torque
KO	Knock Onset
LIVC	Late Intake Valve Closing
LSPI	Low Speed Pre-ignition
MON	Motor Octane Number
MPFI	Multipoint Port Fuel Injection
MPI	Multipoint Injection
NTC	Negative Temperature Coefficient
OI	Octane Index
PFI	Port Fuel Injection
PI	Pre-ignition
PIV	Particle Image Velocimetry
PLIF	Planar Laser Induced Fluorescence
MY	Model Year
PRF	Primary Reference Fuel
RCM	Rapid Compression Machine
ROI	Ratio of Injection
RON	Research Octane Number
RPM	Revolution per Minute
SAE	Society of Automotive Engineers
SI	Spark Ignition
SOI	Start of Injection
SPI	Stochastic Pre-ignition
SWRID	Shock Wave Reflection Induced Detonation
TDC	Top Dead Centre
THC	Total Hydrocarbon
TWC	Three Way Catalyst
VCR	Variable Compression Ratio
VVT	Variable Valve Timing

## Symbols

$a$	Sonic speed
$D_{CJ}$	Chapman-Jouguet detonation speed
$E$	Energy density
$h_u$	Lower heating value
$K$	Weighting factor
$m$	Mass
$p$	Pressure
$p_{ko}$	Pressure at knock onset
$p_{peak}$	Peak pressure

$Q$	Energy in the end gases
$S$	Sensitivity of the fuel
$T$	Temperature
$t$	Time
$u_f$	Normal flame speed
$u_{sp}$	Spontaneous reaction wave speed
$V_{cyl}$	Actual cylinder volume
$x_b$	Burned mass fraction
$Z$	Pressure related stochastic parameter
$\gamma$	Specific heat ratio
$\Delta p_{exp}$	Pressure rises by experiment
$\Delta p_{iso}$	Pressure rises by theoretical isochoric combustion
$\varepsilon$	Ratio of acoustic wave residence time in a hot spot to excitation time
$\theta$	Crank angle
$\xi$	Ratio of the acoustic speed to the localized autoignitive velocity
$\pi$	Pressure rise ratio
$\rho$	Density
$\tau_i$	Ignition delay
$\tau_e$	Excitation time for the chemical heat release
$\varphi$	Equivalence ratio

engines will likely be the mainstream of the world's transportation fleet for a very long time. With more stringent regulations on fuel economy, more efficient internal combustion engines are being developed worldwide.

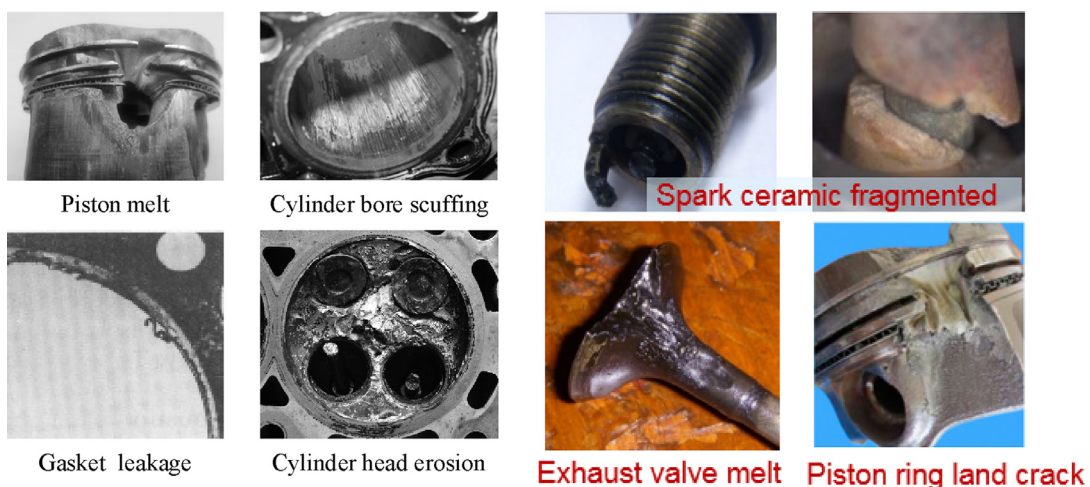
Currently, there are more than one billion vehicles in the world and more than 60% of them are equipped with gasoline spark ignition (SI) engines. Compared with diesel engines, gasoline engines using the non-expensive three-way catalytic converter (TWC) can meet the stringent emission regulations and have greater potential for further improvement in engine efficiency. However, the biggest obstacle for an SI engine to improve thermal efficiency is its knock tendency, which keeps engines from achieving optimized combustion phasing and higher compression ratio. Therefore, to meet future fuel economy and emission regulations, knock in high-efficiency engines must be well understood.

Knock is the name given to the noise associated with the auto-ignition of a portion of the fuel-air mixture ahead of the propagating flame front [1]. It is an inherent problem that plagues internal combustion engines, and it has been studied intensively for decades. In the literature, four terms are used to describe the phenomenon: knock, engine knock, knocking and knocking combustion. In order to uniformly describe it, "knocking combustion" is adopted in this review paper.

When knocking combustion occurs, high-frequency pressure oscillations can be observed. The SI engine can be damaged by knocking combustion in different ways: piston crown melting, piston ring sticking, cylinder bore scuffing, piston ring-land cracking, cylinder head gasket leakage and cylinder head erosion. To enhance power density and reduce fuel consumption, high boost with direct injection has become the mainstream technology in SI engines in recent years and a new knocking mode, called super-knock [2–4] has become a challenge for engine designers, especially with respect to direct injection engines in the low-speed, high-load operating regime. Fig. 1 shows typical damage resulting from conventional knock and super-knock.

In recent decades knocking combustion has been studied intensively not only with focus on conventional knock, but also on super-knock due to the desirable high boost technology in high efficiency gasoline engines, and the number of published papers relating to engine knock have increased greatly in the past 10 years (Tables 1 and 2).

In general, knocking combustion research is crucially important because it determines engine durability, fuel consumption, and



a) Conventional knock (adapted from [1]) b) Super-knock (Reprinted from [2] with permission of SAGE)

**Fig. 1.** Typical damage caused by engine knock.**Table 1**  
Papers related to engine knock (Web of Science indexed and SAE papers).

	Before 2005	2006	2007	2008	2009	2010	2011	2012	2013	2014	2015	2016 (up to July)
WOS	111	13	11	11	17	16	10	25	31	35	52	7
SAE	183	17	18	11	16	10	8	17	21	27	28	12

**Table 2**  
Categories and main content in WOS and SAE papers regarding engine knock.

Research aspects	Paper numbers	Representative research contents
Knock detection	72	Knock sensor development [5–8], knock characterization and detection [9–30], knock control logic and knock controller [31–39]
Numerical simulation	68	Knock prediction model [40–49], modelling of pressure oscillation [50–55], LES modeling of deflagration to detonation [56], application of LES model [57–59], 0D to 3D simulation of knock combustion [60–66], heat transfer prediction [67–70], emissions formation, effects of fuel or running conditions on knock occurrence [71,72]
Optical diagnostics	25	Visualization of pressure waves [73–76], visualization of end-gas auto-ignition [77–83], PLIF detection of HCHO evolution [84], chemiluminescence of intermediate species [85,86], end-gas temperature measurement [87–89], spectroscopic analysis [90]
Theoretical study	66	Auto-ignition prediction [91–93], modes of hot spot auto-ignition [2,4,94–99], reaction mechanism and chemistry [100,101], flame dynamics, acoustic and pressure analysis [102–105], heat transfer analysis [106]
Engine optimization	72	Knock and pre-ignition suppression [107–121], engine running conditions and performance [122–129]
Fuel properties oil additives	36	Octane number rating [3,130–134], high octane fuel (alcohols, furan, NG, LPG, etc) [135–139], fuel design [140–144], anti-knock additives [145,146], oil additives [147–153]

power density, as well as noise and emission performance. Rapid progress in combustion diagnostics and chemical kinetics in recent years has made it possible to improve the understanding of this complicated combustion process. Several possible mechanisms of knocking combustion have been proposed [83], and many researchers prefer either auto-ignition or detonation wave theories or a combined theory. In addition, flame acceleration [154] was also regarded as a cause of knocking. Currently, the maximum thermal efficiency of the SI engine is about 40% [155] and knocking combustion limits the maximum BMEP to 27 bar [156] in production engines.

This paper gives a comprehensive review of research progress and future trends in knocking combustion for high-efficiency engines based on engine testing, numerical simulation and optical diagnostics, with highlights of recent important progress in highly boosted SI engines. First, the basic characteristics of knocking combustion are summarized to achieve a deeper understanding of end-gas auto-ignition modes, which are related to conventional knock and super-knock. Then, influencing factors of auto-ignition and pressure oscillations are presented based on numerical simulation and optical diagnostics, including discussion of the source of pre-ignition, and the effect of oil/fuel properties, thermodynamic conditions and shock waves. Finally, suppression methods and future directions for conventional knock and super-knock are reviewed.

## 2. Conventional knock in SI engines

### 2.1. Basic characteristics of engine knocking combustion

Engine knock arises from auto-ignition of the end gas ahead of the propagating flame. Fig. 2 presents the pressure trace, pressure oscillation, heat release rate (HRR) and unburned gas temperature ( $T$ ) of a typical knocking case. The combustion process of the knocking case has two stages: flame propagation induced by spark ignition and end-gas auto-ignition causing pressure oscillation.

The flame propagation stage is from spark ignition to the crank angle of  $CA_{ko}$  (the onset of pressure oscillation), reaching the value of  $P_{ko}$ . The heat release rate shows an increasing tendency generally

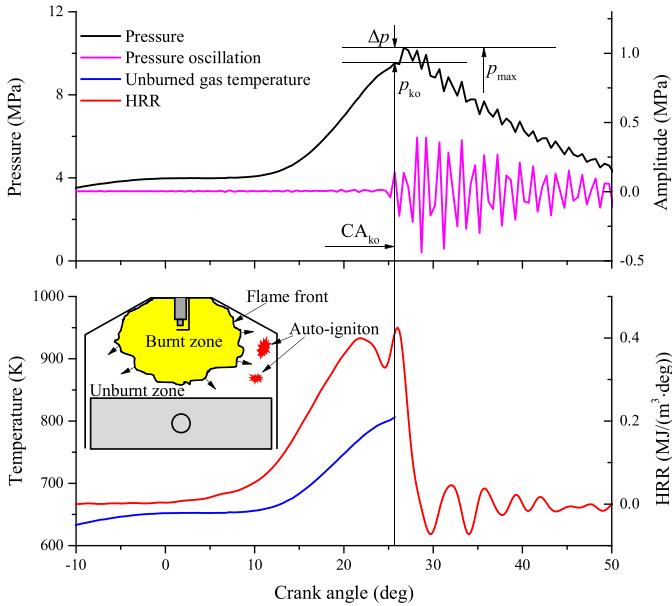


**Fig. 2.** Combustion parameters of engine knock cycle.

during this stage, with possibly a short term drop caused by the downward movement of the piston and heat transfer. The unburned gas temperature rises stably, caused by the compression heating effect of the burned gas and propagating flame, plus the compression or expansion due to the moving piston. The knock sensor signal shows no oscillations, since only flame propagation exists and there is no pressure oscillation in this stage. In the auto-ignition stage, the pressure trace at first increases dramatically, reaching a peak value, and then it oscillates with decaying amplitude. The knock sensor signal also oscillates from  $CA_{ko}$ . As for the combustion process, at  $CA_{ko}$ , the pressure and temperature of the end gas reaches a high level, causing the auto-ignition combustion phenomenon in the combustion chamber. Once auto-ignition is induced, a pressure wave can propagate into the chamber, reflecting back and forth from the walls, causing pressure oscillations.

Heat Release Rate (HRR), Temperature of the unburned gas ( $T_{unburned}$ ), maximum pressure rise ( $\Delta p$ ) and Knock Intensity (KI) are four important parameters that characterized knock behavior. HRR is calculated according to the first law of thermodynamics. In the calculation of  $T_{unburned}$ , the end-gas compression process is considered to be adiabatic. KI is integrated using the pressure oscillation obtained by high-pass filtering (HPF), as follows:

### 1) Heat release rate (HRR) [1]

$$HRR = \left( \frac{\gamma}{(\gamma-1)} \right) P \frac{dV}{d\theta} + \left( \frac{1}{(\gamma-1)} \right) V \frac{dP}{d\theta} \quad (1)$$

### 2) Temperature of the unburned gas ( $T_{unburned}$ ) [157]

$$\int_{T_0}^{T(t)} \frac{\gamma}{\gamma-1} d(\ln T) = \ln \frac{p(t)}{p_0} \quad (2)$$

### 3) Knock Intensity (KI) [158]

$$KI = \int |p_{HPF}| d\theta \quad (3)$$

## 2.2. Knock resistance and fuel chemistry

To reflect the knock resistance of fuels in SI engines, the research octane number (RON) and the motor octane number (MON) have been adopted for gasoline fuels since the 1920s [159]. A higher

octane number suggests more resistance to auto-ignition. The RON and MON tests have standard procedures on a single-cylinder engine [160]. During the measurements, different mixtures of Primary Reference Fuel (PRF), including n-heptane and iso-octane are tested until the knock behavior of the test fuel is matched. The operating conditions for the RON and MON test, as shown in Table 3, are different; MON is tested at a severer situation, where the intake temperature is higher and the engine speed is higher. RON is higher than MON for most non-PRF fuels and the sensitivity (S) of the fuel is defined as  $S = RON - MON$ . Since engine operating conditions vary greatly, RON and MON are designed as limiting operating conditions, but are not enough to describe the knock resistance of all fuels. To cover the whole operating range, Kalghatgi et al. [161,162] proposed the Octane Index (OI), defined as,

$$OI = K \cdot MON + (1 - K) \cdot RON. \quad (4)$$

K depends on the engine operating conditions and is supposed to be independent of fuel properties, and K tends to become negative for the most knock-limited regions in modern SI engines [161–168]. The development of engine design, such as use of an advanced cooling system, boost system, and injection system, have contributed to the decrease of K [167]. This means that the operating condition for modern engines tends to exceed the boundary defined by the operating conditions for both the RON and MON tests. Boot et al. plotted the correlation for K with unburnt gas temperature (e.g., at a compression pressure of 15 bar,  $T_{comp15}$  [164,169–171]) as shown in Fig. 3 [172]. Note that for RON and MON test conditions,  $T_{comp15}$  is roughly 700 and 850 K respectively. Values for K tend to be negative when  $T_{comp15}$  is lower than the corresponding temperature for the RON test. In modern SI engines,  $T_{comp15}$  tends to be lower is due to the lower intake temperature than that in the RON and MON tests, in which the engines are the same as the prototype in the 1930s, and

**Table 3**  
RON and MON engine operating conditions [173,174].

Parameter	RON	MON
Intake air temperature	52 °C	149 °C
Intake air pressure	atmospheric	atmospheric
Coolant temperature	100 °C	100 °C
Engine speed	600 rpm	900 rpm
Spark timing	13 °bTDC	14–26 °bTDC
Compression ratio	4–18	4–18

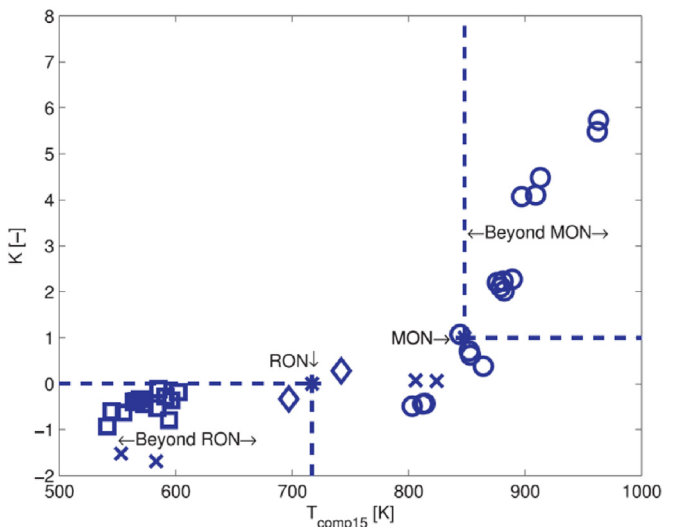


**Fig. 3.** K versus  $T_{comp15}$  (\*: RON and MON condition,  $\diamond$  [162],  $\square$  [175],  $\diamond$  [169],  $\circ$  [171]). (Reprinted from [172] with permission of Elsevier).

are fueled by heated carburetors [163] and fitted with inadequate cooling systems [167].

Although the above fuel ignition indices, RON, MON, and OI, have been used to describe fuel anti-knock properties in automotive engineering, the relationship between RON/MON and OI/K is still not clear. This is because auto-ignition in internal combustion engines is directly associated with the combustion chemistry of hydrocarbons at different operating conditions ( $T$ ,  $P$ ,  $\Phi$ , etc.).

Because of the competition of reaction pathways and the variation of predominant reaction classes at different conditions [176], the reactivity of a fuel molecule presents a complex behavior. Since  $\beta$ -scission [101] is slow at low temperatures, oxygen addition to the radical  $R\cdot$  is dominant, forming the  $RO_2\cdot$  radical. Then isomerization of  $RO_2\cdot$  forms  $\cdot QOOH$ , which can conduct a series of chain branching reactions to produce  $2\cdot OH$  radicals and oxygenated species ( $QOOH + O_2 \rightarrow OOQOOH \rightarrow HOOQ$ ,  $H_2O + OH \rightarrow OQ-H_2O + 2\cdot OH$ ). With increasing temperature, the oxygen addition reactions shift back to the decomposition direction, thus weakening the low-temperature chain branching. Meanwhile, at intermediate and higher temperatures, decomposition of the low-temperature intermediates (e.g.,  $RO_2\cdot$  and  $\cdot QOOH$ ) and the  $R\cdot$  radical gradually becomes more competitive and generates different products, including alkenes,  $HO_2$ , cyclic ethers, and other alkyl radicals. The enhanced decomposition of  $R\cdot$ ,  $RO_2\cdot$ , and  $QOOH$  radicals at intermediate temperatures, together with the backward shift of the low-temperature entrance channel, reduces the global chemical reactivity in the NTC regime [177–179]. A typical example of NTC phenomena on ignition delay times in an adiabatic homogeneous model is shown in Fig. 4 [180]. However, the oxidation of aromatic and olefinic molecules does not follow the general low-temperature reaction competition, thus NTC phenomena are not that prominent for these fuels.

For combustion researchers ignition delay times are usually used to investigate the reactivity in terms of auto-ignition propensity at various temperature and pressure conditions. There is an inherent correlation among the ignition index, ignition delay times, and the combustion chemistry. The difference between RON and MON is the octane sensitivity, and it is related to how the chemical reactivity of the fuel changes with pressure and temperature. The slope of the NTC region in the S-shaped ignition curve is another indicator of changing reactivity. Some scatter is present in the correlation between the sensitivity and the slope of the NTC region for a wide range of isoctane/*n*-heptane/toluene/1-hexene surrogate mixtures, as shown in Fig. 5(a) [160], but a definite trend that sensitivity increases with increasing slope can be observed. This can be explained by the fact that the unsaturated components (aromatics and olefins) have a larger impact on the sensitivity of gasoline fuels. On the other hand, a high overall reactivity, which is due to the avail-

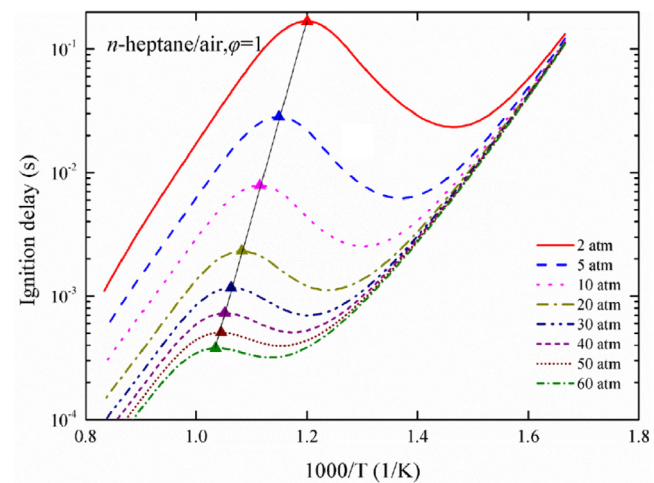


**Fig. 4.** Total ignition delay as a function of the initial temperature  $T$  for a stoichiometric *n*-heptane/air mixture under various pressure (Reprinted from [180] with permission of Elsevier).

ability of relatively rapid reaction pathways, can be reflected either by a low AKI (OI with  $K=0.5$ ), or by a short ignition delay time in the middle of the NTC region. A strong correlation between AKI and the ignition delay time can be observed in Fig. 5(b) [160]. This phenomenon indicates a possible reason why RON is larger than MON for gasoline and most non-PRF fuels. Namely, because the slope of the NTC region for most fuels is larger than that for isoctane and *n*-heptane. Thus, with increasing intake temperature, the operating condition shifts from the RON test to the MON test, the promotion of the overall reactivity before ignition is more significant for most fuels than for isoctane and *n*-heptane (There might even be a negative effect on reactivity for PRF due to the NTC region). To compensate for the extra reactivity, more *n*-heptane, which is more reactive than isoctane, is needed when matching the same knock behavior in the MON test compared with the RON test, which means that the composition of isoctane in a PRF mixture should be less, and the octane number is lower, too.

### 2.3. Intermediate species and auto-ignition front

Some important intermediate species ( $CH$ ,  $CHO$ ,  $CH_2O$  and  $OH$ ) can be used as markers of different combustion phases based on the fuel's low-temperature and high-temperature hydrocarbon oxidation chemistry. This information provides quantitative data of temperature and reactivity for understanding the knocking combustion process. Schießl et al. [87] investigated spatial species distributions and temperature fluctuations in the unburned end-

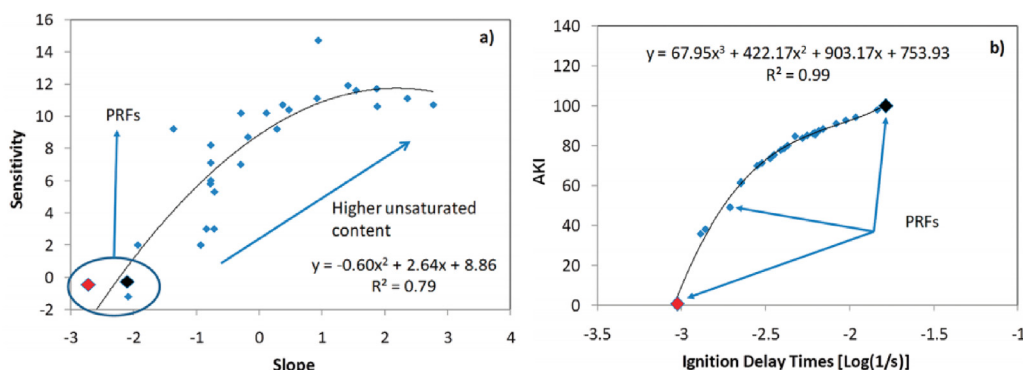


**Fig. 5.** Correlations for a wide range of isoctane/n-heptane/toluene/1-hexene surrogate mixtures between (a) sensitivity and slope of the NTC region and (b) the antiknock index (AKI) and ignition delay times at 825 K, 25 atm (Reprinted from [160] with permission of ACS). *n*-heptane (red, left) and isoctane (black, right) are highlighted in (a), *n*-heptane, PRF50 mixture, and isoctane are marked with the arrow in (b). (For interpretation of the references to color in this figure legend, the reader is referred to the web version of this article).

gas of a SI engine by laser-induced fluorescence, as shown in Fig. 6. The dark area indicates the burned zone due to an absence of fluorescing intermediate species and they identified auto-ignition hotspots at a few localized sites of increased temperature. Furthermore, the authors converted spatial formaldehyde ( $\text{CH}_2\text{O}$ ) concentration variations in the end gas to temperature fluctuations, and it was found that temperature fluctuations exceeding 20 K were present in the nominally homogeneous end-gas. This also provides quantitative evidence of temperature stratification in end-gas before engine knock.

Further investigations in optical engines using spectroscopic measurements [85] and chemiluminescence [86] were also conducted. Flame structures, intermediate species and pressure evolution during SI knocking combustion have been visualized. Radical species such as OH and CHO were detected and were correlated to the onset and duration of knock and the presence of hot-spots in the end gas [85]. It was found that the occurrence of the CHO radical in the end gas denoted the start of knocking combustion and OH marked the burned zone, as shown in Fig. 7. Using light emission and the absorption wavelengths of  $\text{CH}_2\text{O}$ , cool flame reactions in the unburnt gas were detected [90]. Using  $\text{CH}_2\text{O}$  and OH chemiluminescence synchronous with the pressure trace [86], it was found that the first auto-ignition occurs near the spark ignited flame front in slight knocking cases. Combustion images and heat release data indicate that a significant pressure gradient occurred in a local area because of end-gas auto-ignition with a constant volume-like heat release.

For auto-ignition front propagation during knocking combustion, studies have revealed different patterns. Besides near-wall

auto-ignition, as shown in Fig. 6, a flame-induced sequential auto-ignition (FIAI) pattern was also reported in a spark-ignition engine by high speed direct photography [86]. The auto-ignition occurs near the flame front with an apparent propagation speed of approximately 160 m/s, which is one order of magnitude higher than the normal turbulent flame speed in spark ignition engine, but much less than the local sound speed of approximately 700 m/s. Therefore, the local significant pressure increase does not occur due to pressure equilibrium, and no obvious pressure oscillation was observed in the combustion chamber. After spark ignition, a deflagrative flame propagates at the turbulent flame speed. With the compression of the deflagration, the unburned mixture temperature and pressure increase to the mode transition status. As a result, the flame front propagation abruptly accelerates to a high speed due to sequential auto-ignition. By using 1D simulations, similar phenomena have been revealed [181]. For reaction front-base temperatures below 1100 K, end-gas combustion was dictated by a transport-controlled deflagration processes. Beyond this reaction front-base temperature, transport had minimal effects on the front propagation rate and the combustion process could be described by a “spontaneous ignition front propagation regime”. Kawahara and Tomita et al. [182] investigated auto-ignited kernels during knocking combustion. They found that when the end gas was compressed due to the propagating flame front, auto-ignited kernels appeared near regions with negative curvature of the flame front, as shown in Fig. 8. The authors concluded that the negative curvature was caused by the initiation of the auto-ignited kernel.

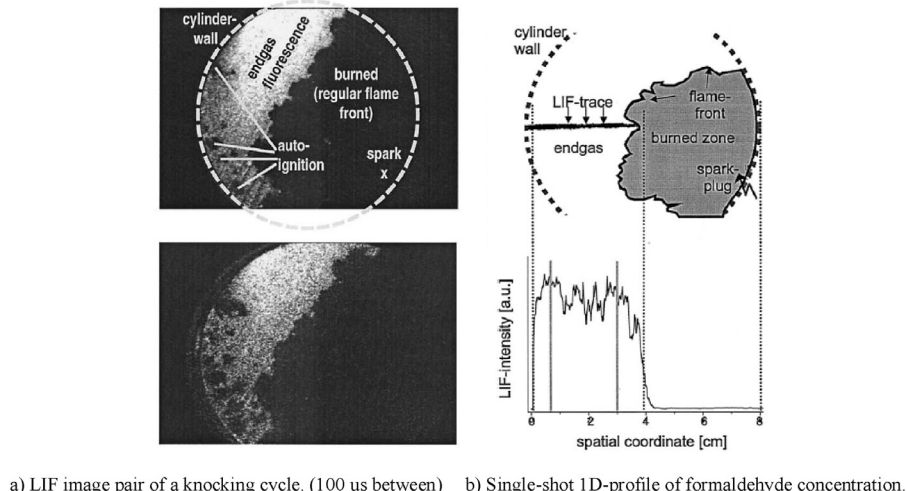


**Fig. 6.** Analysis of end-gas temperature fluctuations in an SI engine by laser-induced fluorescence (Reprinted from [87] with permission of Elsevier).

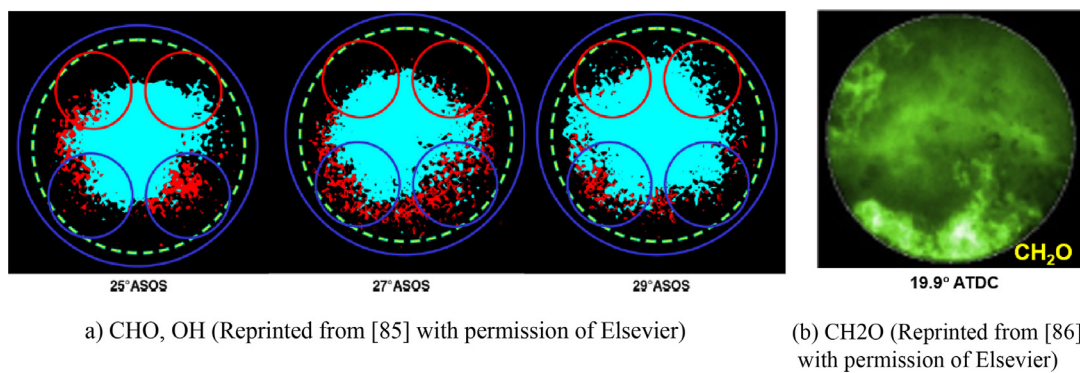


**Fig. 7.** CHO, OH and  $\text{CH}_2\text{O}$  spatial distributions during the knocking phase (red: CHO, cyan: OH, Green dashed line indicates optical window, blue solid line indicates the cylinder liner). (For interpretation of the references to color in this figure legend, the reader is referred to the web version of this article).

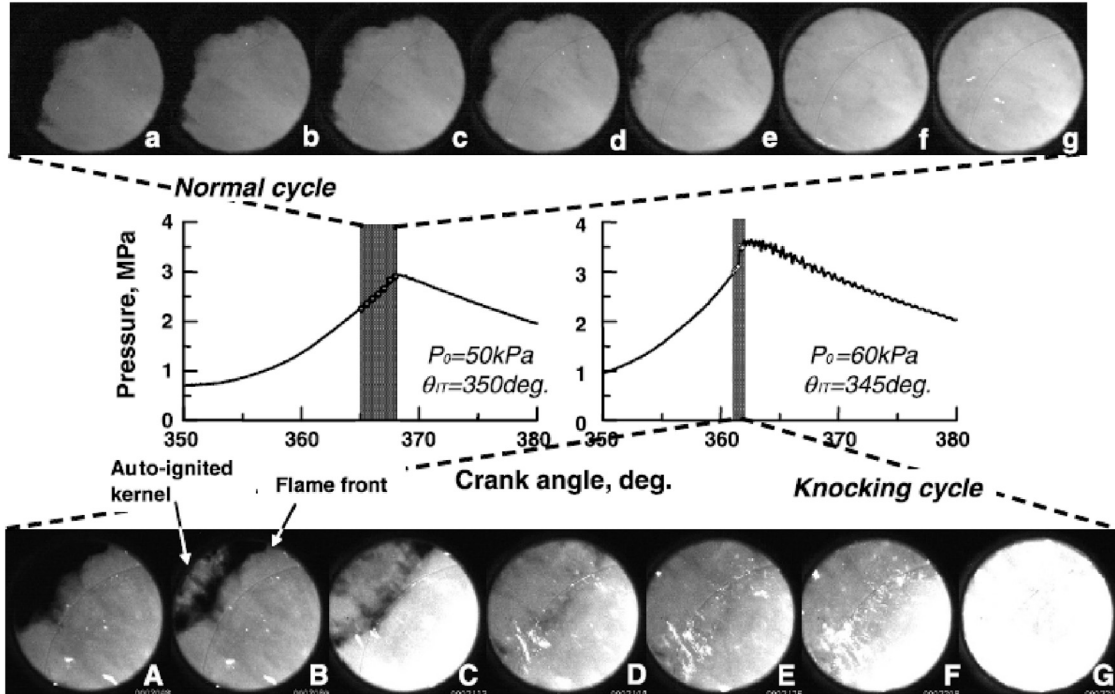


**Fig. 8.** Series of high-speed direct images and related in-cylinder pressure for normal and knocking engine cycles (Reprinted from [182] with permission of Elsevier).

Generally speaking, detonation is unlikely to occur in a naturally aspirated SI engine due to the low heat release rate, short chamber-wall distances and cool cylinder walls. From the literature, after the observations done by Miller and his colleagues [83], evidence about detonation during knock in engines was not published until 1991 by Spicher et al. [81]. It was found that high knock intensities seem to be related to shock waves. To observe the process at higher frequency, Pan et al. [183] recorded a set of images at 240,000 fps with the engine operating at 1000 rpm on a PRF90 fuel, and the ignition front from an auto-ignition center was observed developing at 896 m/s. Their numerical results showed that the development of the auto-ignition front could reach 1500 m/s. Both the experimental and numerical speeds were less than the Chapman-Jouguet (CJ) speed, but much higher than normal flame speeds in an engine. Supersonic waves propagated and reflected from the walls in the combustion chamber, which led to pressure oscillations.

#### 2.4. Pressure oscillation and heat transfer

Pressure oscillation in a cavity is a fundamental scientific phenomenon. For combustion systems, thermo-acoustic excitation is commonly observed, which may lead to pressure oscillations and combustion instabilities [184,185].

To capture oscillation patterns under IC engine-like conditions, a novel method was developed [76] using CH<sub>·</sub> emission based on high-speed chemiluminescence images during the combustion process. By reconstructing the images with the three basic color intensities of each pixel replaced by the amplitudes of the luminosity spectrum, mode shapes of the pressure oscillations in a cylindrical cavity were clearly obtained. Table 4 lists the first 5 modes, along with the theoretical ones (Draper's "drum mode" [186]). According to the amplitudes of the luminosity spectrum, pressure oscillation was mainly from the first resonant mode and the oscillating energy is focused at a fixed frequency (e.g. 7.2 kHz with bore of 79 mm [70]).

Pressure oscillation also influences heat transfer. To take the oscillating flow field into account, a new wall heat transfer model was developed using a pressure gradient correction [70]. In addition,

an energy source term was introduced to reflect the chemical heat release from near-wall reactions. The new wall heat flux formulation is given as [70],

$$q_w = \frac{\rho c_p u^* T \ln\left(\frac{T}{T_w}\right) + (2.1y^+ + 33.4) \frac{v}{u} \left( -\frac{1}{\gamma-1} \frac{\partial p}{\partial t} + Q_c \right)}{2.1 \ln(y^+) + 2.5} \quad (5)$$

where the first term in the numerator is the standard wall heat flux formulation of Han et al. [69] and the second term accounts for pressure fluctuations,  $\partial p/\partial t$ , and near-wall heat release,  $Q_c$ . Pressure oscillation-induced flows significantly enhance convective heat transfer. The energy loss via heat transfer was predicted to be nearly 40% of total fuel energy under heavy knocking conditions [70]. Therefore, heavy knock not only may lead to damage of engine components, but also significantly reduces thermal efficiency due to enhanced heat transfer.

Moreover, the pressure oscillation may couple with chemical kinetics. Fig. 9 shows pressure, temperature, fuel, CHO, and NOx distributions during the knocking combustion process [187]. A high concentration of OH radicals is formed in the center of the cylinder during the post-oxidation stage. A high concentration of CHO radicals is seen around the OH radicals, which indicates that auto-ignition of the end gas is about to take place. The local in-cylinder pressure is extremely uneven, as shown in the pressure distribution, during the knocking combustion process. The knocking combustion is related to local auto-ignition and pressure wave reflection near the walls. It was found that the 1st auto-ignition spot occurs ahead of the flame front because the end-gas mixture closer to the flame front has higher temperatures. Then the local pressure rises rapidly due to volumetric heat release, which generates a pressure wave, as shown in the pressure distribution. Pressure-wave induced negative curvature can be seen from the turbulent flame front (black curve captured by the G-equation combustion model) due to auto-ignited kernels near the flame front, as reported by Kawahara and Tomita et al. [182]. Then the pressure wave propagates and impinges on the cylinder wall. Note that this pressure wave is reflected with double its amplitude at walls, as shown in the pressure distribution. The double-amplitude pressure rapidly compresses the near wall

**Table 4**  
Mode shapes of the first 5 modes (adapted from [76]).

$(\alpha, \beta)$	$\rho_{(\alpha, \beta)}$	$f_{\text{theory}}$ (kHz)	$f_{\text{im}}$ (kHz)	$T_{\text{im}}$ (K)	Mode Shapes (theoretical)	Mode Shapes (image)
(1,0)	1.841	11.51	11.25	2731		
(2,0)	3.054	19.1	18.28	2621		
(0,1)	3.831	23.96	23.91	2849		
(3,0)	4.021	26.27	26.02	2806		
(4,0)	5.318	33.26	33.05	2825		

unburned gas to very high temperatures and significantly shortens its ignition delay. Thus, a 2nd auto-ignition occurs with much more pressure rise intensity near walls. This autoignition-induced flow pushes back the spark-ignited flame front and creates a further negative curvature. In addition, detonation could be initiated near the walls in IC engines if the energy density is high enough. This will be further elucidated in Sections 4 and 5.

### 3. Super-knock in boosted SI engines

In recent decades use of high boost has been developed to offer the potential of enhancing power density and reducing fuel consumption in gasoline SI engines [188]. The developments, especially in the low-speed and high-load regime, have however been challenged by the occurrence of a new mode of engine knock, super-knock [189], which has been variously termed as unwanted pre-ignition [190], mega knock [191], LSPI (low-speed pre-ignition) [192], deto-knock [2], SPI (stochastic pre-ignition) [193], developing detonation [194,195] or subsequent front propagation [196]. Such a single super-knock event can severely and instantaneously damage an engine due to the extremely high peak pressure and the associated pressure oscillations that are developed. Furthermore, super-knock events appear randomly with little direct relationship to engine control parameters, such as ignition timing, equivalence ratio, intake temperature, etc. Applying common knock suppression methods, such as retarding spark timing, cooling the intake charge and enhancing heat transfer, are not effective at avoiding super-knock. Therefore, super-knock is at present the major obstacle for further improving the boost level of turbocharged SI engines.

Fig. 10 shows the typical pressure trace and heat release rate of a normal combustion cycle, a conventional knock cycle, and a super-knock cycle. In highly boosted gasoline engines, the spark timing is usually retarded even after TDC to avoid conventional knock at low speed, high load conditions. The most significant difference between super-knock and conventional knock is the amplitude of the

pressure rise at knock onset. The amplitude of the maximum pressure rise of super-knock ( $\Delta p$ ) is more than an order of magnitude higher than for conventional knock.

#### 3.1. Relationship between super-knock and pre-ignition

Super-knock phenomena are significantly different from those of the conventional knock, indicating that they have a different combustion process. Many studies have been conducted to investigate super-knock [2–4,70,119,191,193,197–209], and it is generally accepted that super-knock originates from pre-ignition.

##### 3.1.1. Distinguish pre-ignition and super-knock

In the existing literature both “super-knock” and “pre-ignition” are used to describe the engine knock observed under low-speed, high-load conditions in boosted gasoline engines. Although sometimes interchangeable, they actually represent two different combustion phenomena. “Pre-ignition” represents the combustion of the air/fuel mixture triggered by a “hot spot”, other than an electric spark prior to the spark time. Researchers usually use “pre-ignition frequency” to evaluate the quality of a boosted gasoline engine combustion system. Peak pressure ( $p_z$ , higher than 10.5 MPa [153]) or peak-to-peak pressure oscillation ( $pp_{\max}$ , higher than 8.3 times of permitted knock amplitude [200]) was used as a criterion to capture pre-ignition events. However, pre-ignition may cause different combustion phenomena, including non-knocking combustion. It is difficult to identify pre-ignition using the above knock detection methods. “Super-knock” is named to distinguish itself from conventional knock. Conventional knock is due to end-gas auto-ignition before spark-triggered flame propagation consumes the end gas in the combustion chamber. Super-knock, however, is severe engine knock triggered by sporadic pre-ignition. Super-knock, which can be characterized using the peak pressure value ( $p_z$ ) or the amplitude of pressure rise ( $\Delta p$ ), as shown in Fig. 10(a), can be a direct inducer of engine damage. Moreover, super-knock occurs randomly.

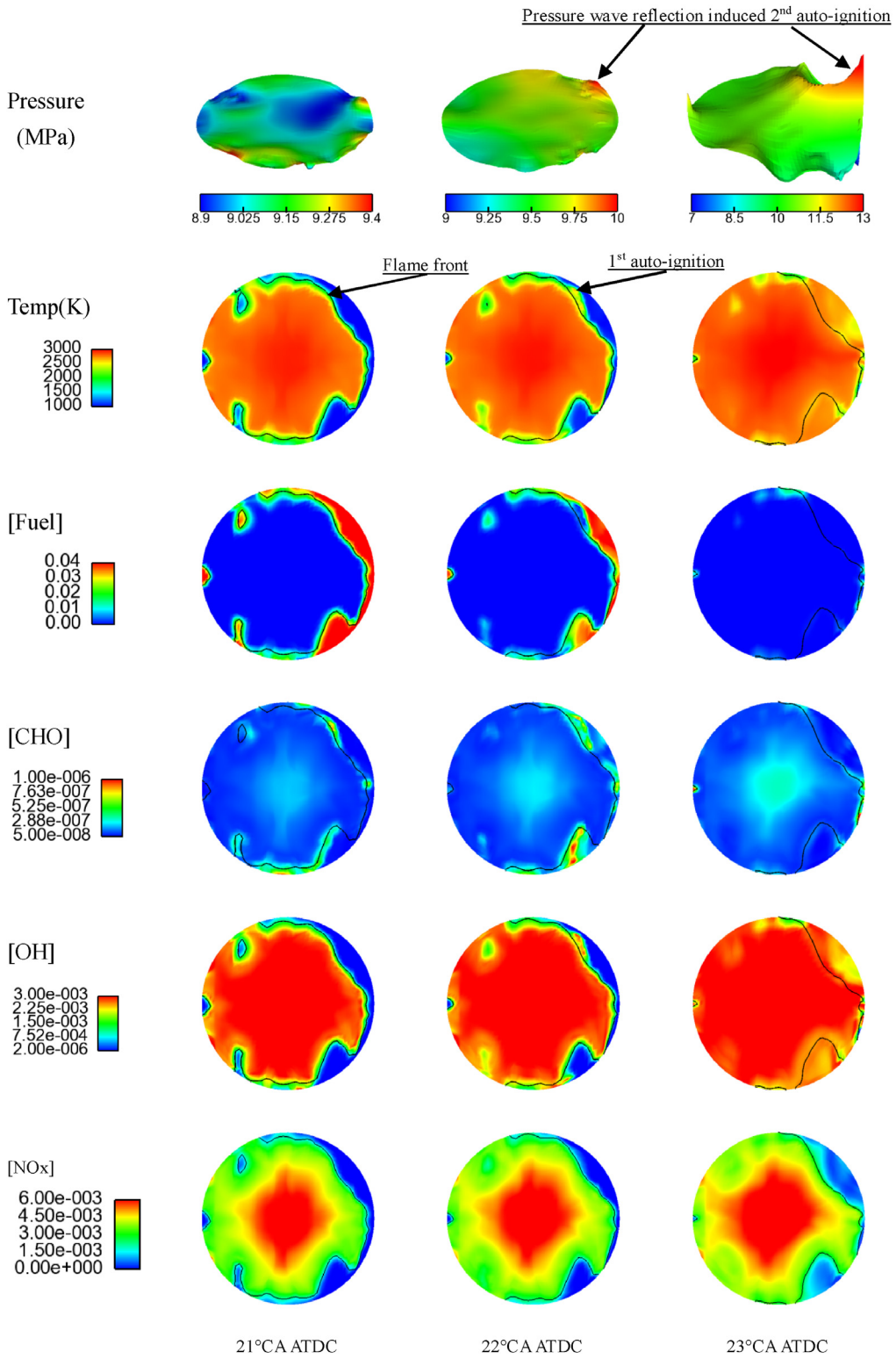
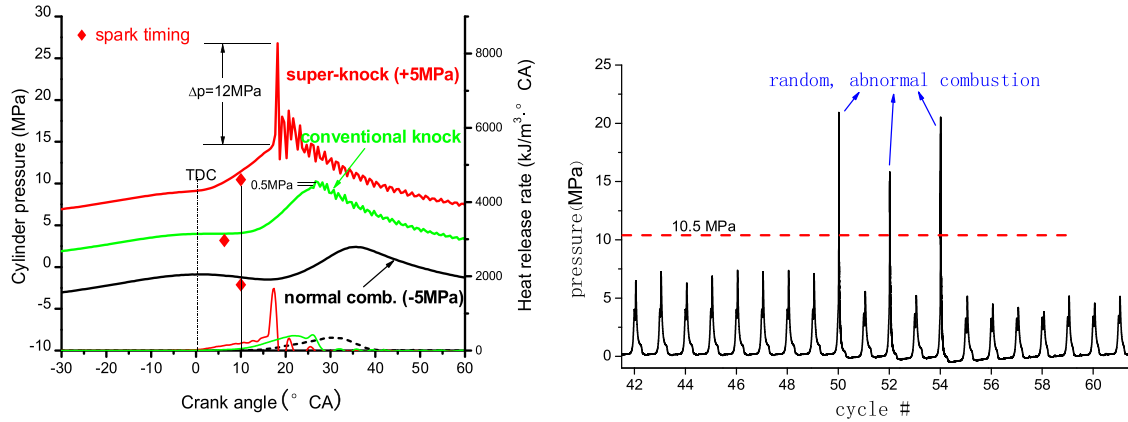


**Fig. 9.** SI combustion simulation at three representative timings during the knocking process (adapted from [187]) (Black curve: turbulent flame front).

To capture super-knock cycles, enough engine cycles (5000 cycles [2]) have to be recorded continuously, as shown in Fig. 10(b).

The relationship between pre-ignition, conventional knock, and super-knock in a boosted gasoline engine is summarized in Fig. 11. SI combustion can be divided into normal combustion and engine knock according to the value of the pressure oscillation. Engine knock can be classified into conventional knock and super-knock

according to the value of the peak pressure rise. Two types of super-knock are end-gas deflagration and end-gas detonation according to the precise combustion wave mode. Thus, pre-ignition is the origin of abnormal combustion. Pre-ignition can lead to end-gas detonation (super-knock), end-gas deflagration (super-knock, heavy knock, and slight knock) and normal flame propagation (non-knock). The combustion wave mode will be further discussed in Section 4.



a) Three typical combustion pressures traces

b) continuous engine cycles with random super-knock

**Fig. 10.** Comparison of super-knock, conventional knock and normal combustion (Reprinted from [2] with permission of SAGE).

To sum up, pre-ignition and super-knock are totally different combustion phenomena. Pre-ignitions do not always lead to super-knock. Pre-ignition may lead to super-knock, heavy-knock, slight-knock, and non-knock. Super-knock directly damages an engine while pre-ignition does not. Since super-knock combustion always has pre-ignition events occurring before spark timing, one of the effective ways to avoid super-knock is to eliminate pre-ignition.

### 3.1.2. Possible sources of pre-ignition before super-knock

Pre-ignition has been observed in gasoline spark ignited engines over the past 70 years [193,210–212]. According to the different sources of pre-ignition, the causes of pre-ignition can be divided into structured hot spots (such as the spark plug, valves, etc.) and unstructured hot spots (such as oil droplets, particles in the combustion chamber, etc.). When there is a structured hot spot in the combustion chamber, it can increase the local temperature, and this has been called run-away pre-ignition [1]. This kind of phenomenon can be avoided by optimizing the combustion chamber design. However, the pre-ignition, which can develop into super-knock, is not a homogeneous gas combustion process. It has been found that pre-ignition occurs via an obvious flame kernel growth and a flame propagation

process [3,202]. Simulation results also show that even in low speed pre-ignition (LSPI) cases, the ignition delay of the stoichiometric mixture is still long, and the mixture cannot pre-ignite spontaneously before spark ignition [119]. Therefore, LSPI is associated with hot spots. Super-knock is different from run-away pre-ignition in its combustion characteristics.

“Pre-ignition” is generally accepted to be due to three possible inducements, including surface ignition, lubricating oil, and carbon deposits. A protrusion on the chamber surfaces may become a hot-spot to induce pre-ignition. However, surface ignition cannot explain the occurrence of a random pre-ignition location in the combustion chamber and the occasional super-knock event.

Surface-ignition-induced pre-ignition can be ruled out in super-knock cycles. By evaluating endoscope data, Dahnz et al. [117] first excluded the theory that the spatial distribution of pre-ignition origins could be structured due to hot spots. Each black dot in Fig. 12 indicates the starting point of one optically registered auto-ignition site. To facilitate orientation, the visible combustion chamber outlines are also sketched on the background of the image. As can be seen, the pre-ignition origins are spread over a wide range in the plane of the cylinder head gasket. Detailed analyses showed no significant correlation between the engine operating conditions and the distributions of pre-ignition origin. Furthermore, the influence of the spark plug characteristics on super-knock was investigated [197] and it was concluded that the tendency for super-knock is not influenced by the location of the spark plug.

The causes of pre-ignition may relate to the lubricating oil, gasoline/oil mixing [2,191,203,213], floating deposits [202,204], gas-phase auto-ignition [189,205], and fuel properties [149,201,202]. Carbon deposit coatings increasing pre-ignition frequency has also

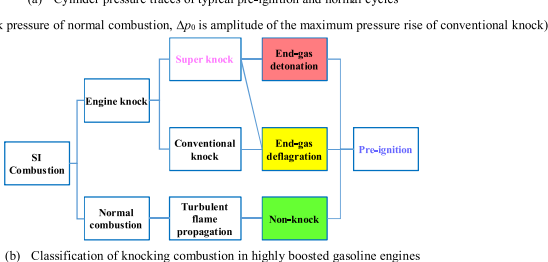
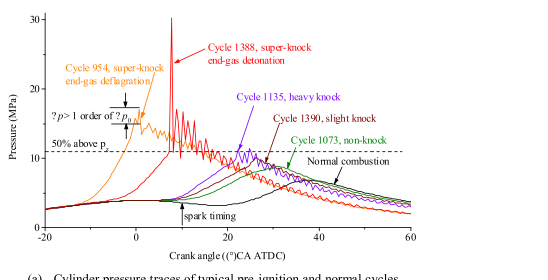


**Fig. 11.** Relationship between pre-ignition and super-knock: combustion (Reprinted from [2] with permission of SAGE).

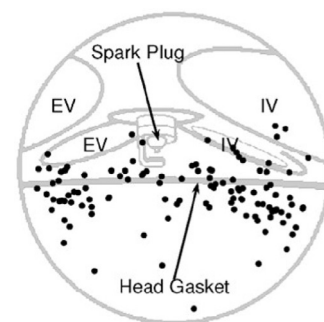


**Fig. 12.** Spatial distribution of pre-ignition origins (Reprinted from [117] with permission of SAGE).

been demonstrated. A clean combustion chamber without carbon deposits clearly shifts the pressure level at which pre-ignition occurs to higher values [200]. Injections too early during the intake stroke lead to spray impingement on the piston bowl and the corresponding increased soot emission has a strong relationship with the super-knock frequency [204]. Combustion visualizations and CFD simulations on the onset of pre-ignition, including liner wetting, injection targeting, stratification, mixture motion, and oil formulation, have identified oil mixing with the fuel as the leading reason for pre-ignition [153]. Moreover, the stochastic nature of oil intrusion into the combustion chamber may induce pre-ignition.

### 3.2. Source analysis of pre-ignition

#### 3.2.1. Oil droplets

The formulation of engine oil, which contains a base oil, detergent, dispersant, antioxidant, corrosion inhibitor and emulsifier, is complex. When an oil droplet enters the combustion chamber, it can become a hotspot because part of its component mixture may have a shorter ignition delay. The oil droplet can thus self-ignite before ignition under the proper temperature and pressure conditions, and this can initiate an air-fuel mixture which leads to pre-ignition, and finally super-knock.

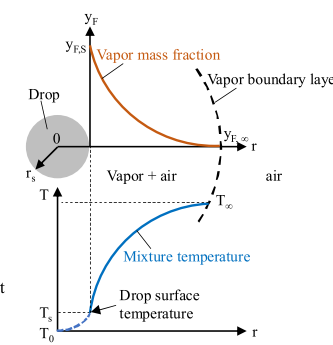
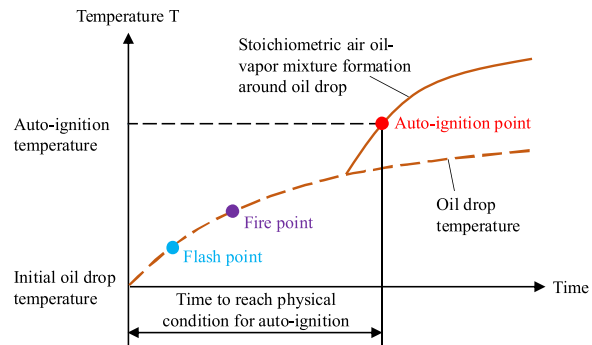
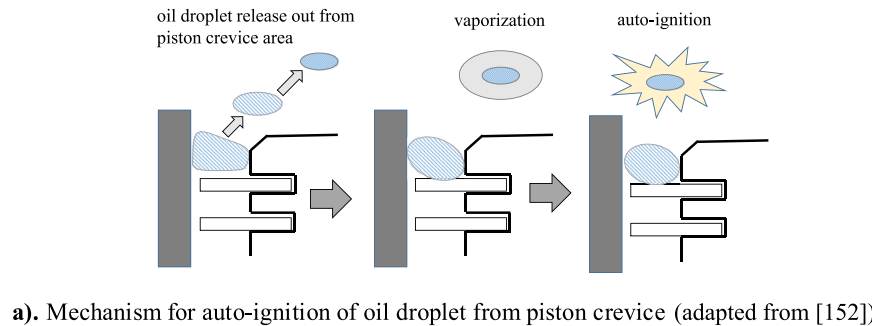
Dahnz et al. [202] first proposed the mechanism of lubricant oil droplet release from the cylinder liner, which has turned out to be the most probable explanation for the occurrence of pre-ignition. Pre-ignition is triggered by long-chain lubricating oil components that have shorter ignition delays [4]. The mechanism for auto-ignition of oil droplets from a piston crevice is shown in Fig. 13(a) [152]. Oil droplets accumulate in the piston crevice area and then vaporize in the combustion chamber. The process from an oil drop to the formation of a combustible mixture around an oil drop is illustrated in Fig. 13(b) [214]. An oil particle becomes an igniter only when a combustible gaseous mixture around it can be formed and the mixture temperature reaches that for auto ignition. Finally, oil/fuel/air mixture self-ignition in the cylinder causes pre-ignition.

The hypothesis about the relationship of knock and oil intrusion has been verified quite extensively. Oil intrusion before TDC could indeed induce pre-ignition and then knock; and slightly diluted oil (75% oil + 25% gasoline) caused the heaviest knock [215]. Lubricant-based, low-ignition delay components being carried into the combustion chamber during blow-down could survive to become a pre-ignition origin in a subsequent cycle [216]. Single oil droplet ignition that precedes the ignition of the fuel-air mixture has been observed in a rapid compression expansion machine [217]. Pre-ignition induced by lubricant has been observed when a lubricant is directly introduced into the combustion chamber [218]. Under 1.4 MPa and 710 K conditions, the oil droplet ignited first in a stoichiometric iso-octane / air mixture, and then initiated combustion in the surrounding air-fuel mixture leading to flame propagation [219]. This phenomenon is not observed when oil droplets are absent as the combustion phase occurs distinctly earlier with oil droplets ignition.

#### 3.2.2. Solid particle

Oil droplets are not the only inducement of pre-ignition. Floating solid particles in the combustion chamber also have a close connection with pre-ignition. Particle formation is related to the nature of the fuel, engine design and the operating conditions. As a product of incomplete combustion, particles can stay in the combustion chamber and participate in surface oxidation reactions in the next cycle. In addition, they can also serve directly as high temperature spots to ignite the mixture.

Pre-ignition is associated with the conditions to increase the accumulation rate of deposits. Less pre-ignition is observed after clean preconditioning than in a dirty engine combustion chamber [200]. Increasing spray/wall interaction strongly increases the probability of pre-ignition events [151]. The pre-ignition is presumably caused by self-ignition of some (still unidentified) substances originating from the lubricant or from lubricant/fuel spray interaction. The relevant species may not initially be present in the fuel or in the lubricant, but could be formed in the combustion chamber by incomplete combustion. At certain



b). Process for an oil drop in cylinder to ignite the mixture (adapted from [214])

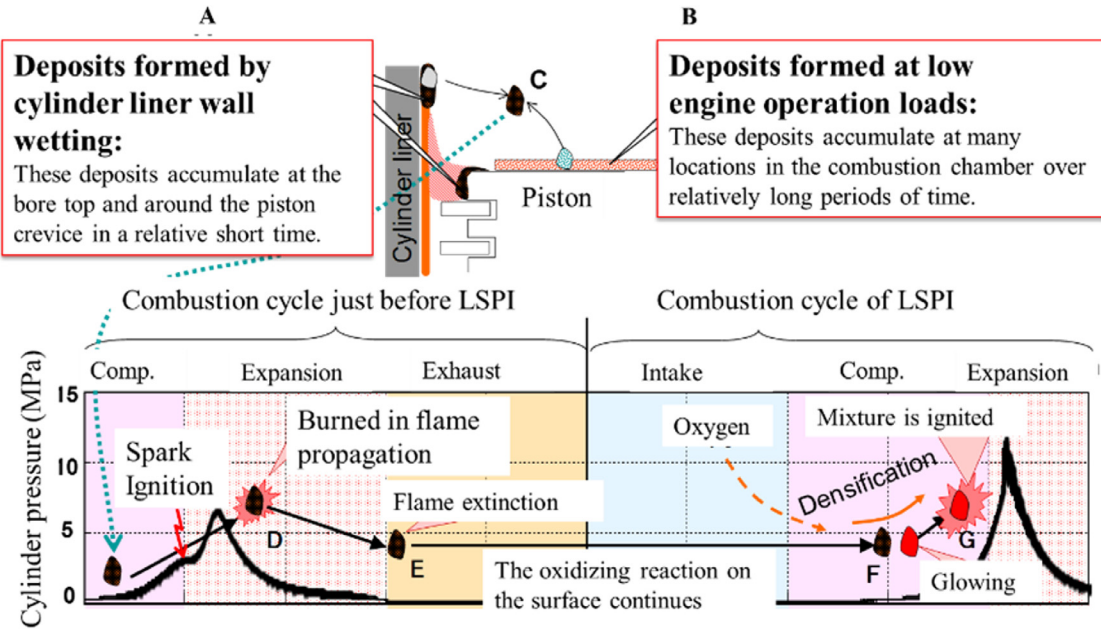
Fig. 13. Process from oil droplet release to vaporization to ignition.

injection timings, cylinder liner wall wetting was noticeably present, and a large amount of deposits were observed after the engine was operated under those conditions [220]. The number of LSPIs in a sequence increased under conditions that caused large amounts of cylinder liner wall wetting.

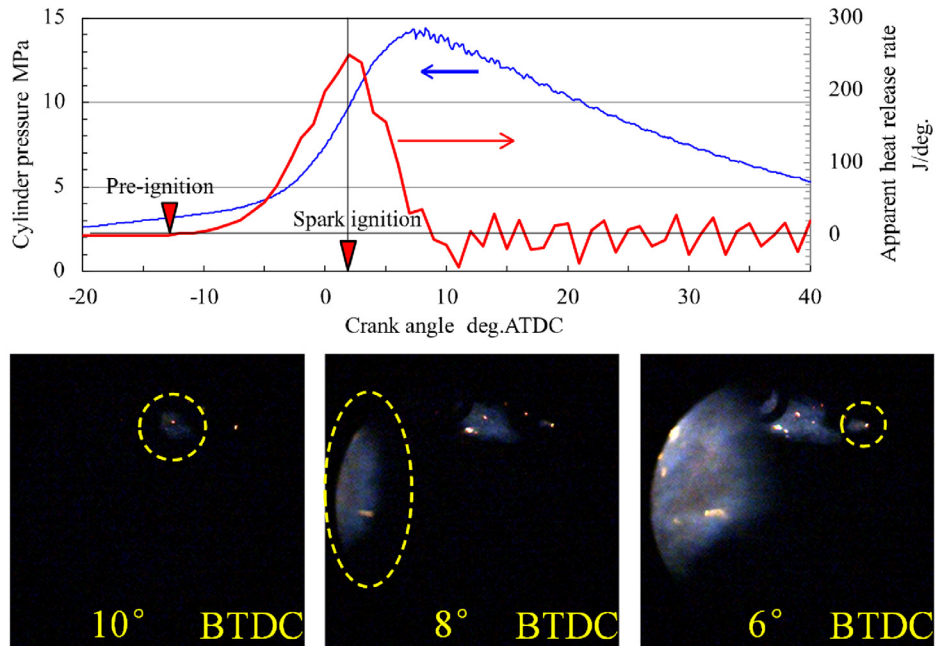
Based on these test results and considerations, Fig. 14 shows a new proposed LSPI mechanism [207]. Deposits formed by cylinder liner wall wetting (A) and deposits formed at low engine loads over extended periods of time (B) peel off and float in the combustion chamber space (C). Deposits exposed to combustion are burned and increase in temperature (D). However, although the flame is extinguished between the expansion and exhaust strokes (E), gradual

surface reactions with unburned oxygen continue. High-temperature deposits in the residual gases that remain in the next cycle are exposed to new oxygen in the intake stroke of the next cycle. The high-pressure and high-temperature of the compression stroke combine with the internal heat to accelerate the surface oxidizing reactions, creating the glowing particles that were observed (F). When the energy required for ignition of the surrounding mixture is discharged, the mixture starts to combust (i.e., flame propagation occurs) (G).

Similar findings can be found in Kuboyama et al. [221], Lauer et al. [222], Moriyoshi et al. [223], and Magar et al. [224]. In the research of Ref. [221], pre-ignition caused by glowing particles was



a). Schematic of new LSPI mechanism (adapted from [220])



b). In-cylinder pressure, heat release rate and direct photographs during a pre-ignition cycle induced by glowing particles (adapted from [221])

Fig. 14. Mechanism of deposit-induced pre-ignition.

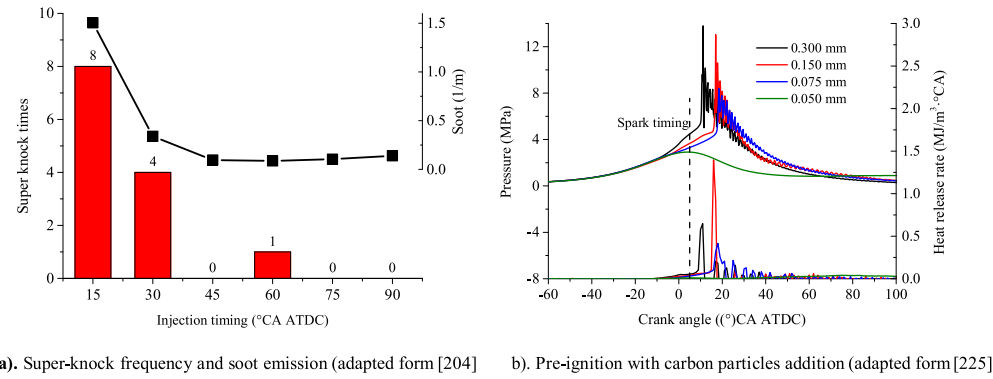


**Fig. 15.** Mechanism of carbon particle induced the pre-ignition.

observed by direct photography, as shown in Fig. 14(b). The glowing particles induced pre-ignition followed by heat release and pressure oscillation. In the research of Magar et al. [224], evidence enabling the identification of the trigger of premature, local auto-ignition was found. Their optical results reveal that pre-ignition is initiated in the immediate vicinity of glowing solid particles. The particles are either a result of the flaking of deposits, or of contamination of the combustion chamber.

There is a correlation between soot emissions and super-knock. Higher in-cylinder soot emission correlated well with the frequency of pre-ignition and super-knock cycles in a GDI production engine (Fig. 15(a)) [204]. To validate the hypothesis of soot particle-induced pre-ignition, carbon particles with different temperatures and sizes were introduced into the combustion chamber to trigger pre-ignition and super-knock, as shown in Fig. 15(b) [225]. The results indicate that large-diameter carbon particles directly lead to pre-ignition and super-knock phenomena. This can be explained by the fact that the bigger carbon particles could form an ignition kernel, and be more prone to be the source of heat imbalances. An incipient flame must reach a critical radius before it becomes self-sustaining [226]. When the kernel size is larger than the laminar flame thickness at the local temperature and pressure, pre-ignition is initiated [4,226]. The experimental data suggest that agglomerated soot particles with higher temperatures and larger sizes detached from the piston bowl surface could be one of the inducements of pre-ignition and super-knock.

In addition to deposits and soot, sulphated ash [227] and wear metals such as Fe and Cu [148], also contribute to increased pre-ignition frequency due to catalytic effects.

### 3.3. The effect of oil and fuel properties on super-knock

Research on super-knock has indicated that the composition and physicochemical properties of the oil and fuel also affect seriously the frequency of super-knock.

#### 3.3.1. Oil properties

**3.3.1.1. Base stocks.** Pre-ignitions were thought to arise from local auto-ignition of areas in the cylinder which are rich in low ignition delay “contaminants”, such as engine oil and/or heavy ends of gasoline [228]. These contaminants are introduced into the combustion chamber at various points in the engine cycle. In general, less reactive base stocks (i.e., those with a long ignition delay) appeared to have the lowest ignition tendency. The calculated ignition index (CII), which is an estimate of heavy hydrocarbon reactivity based on empirical measurements from bunker fuels, was found to predict the ignition tendency of group I-IV lubricant base stocks (Fig. 16).

**3.3.1.2. Oil additives.** Many researchers have noted that oil additives correlated directly with the frequency of super-knock due to possible catalytic reactions. The frequency of LSPI (super-knock) increased with the content of additives [151,153]. The detergent Ca has a contributory effect, and MoDTC or ZnDTP have a preventative effect on LSPI [148,152,229,230]. A new engine oil formulation has been developed [147], which reduced LSPI frequency to less than 10% of that of conventional ILSAC certified gasoline engine oils. High quality base oils and optimized additive components were formulated in which the amount of calcium-based detergent was reduced to levels lower than that in general ILSAC oils, and anti-oxidants were added. Based on these findings, a correlation to estimate LSPI frequency (relative) was obtained:

$$\text{LSPI frequency} = 6.59 \cdot \text{Ca[wt\%]} - 26.6 \cdot \text{P[wt\%]} - 5.12 \cdot \text{Mo[wt\%]} + 1.69 \quad (6)$$

In an assessment of engine oil degradation effects, the influence of wear metals and engine oil degradation was also investigated. It was found that addition of Fe and Cu compounds clearly showed contributory effects on LSPI frequency [148]. In addition, the observed auto-ignition frequency decreased with increasing viscosity and density, which is related to the physical property of the additives [228].

However, so far the reported work does not provide an explicit conclusion about the effect of oil additives. For example, there is no consensus on whether Zn and Mo have effects on pre-ignition [152,231]. This is because pre-ignition in engine production is random and oil additive effects are only one of the possible pre-ignition sources. To isolate the effect of oil additive on pre-ignition, a single factor experimental method needs to be developed to reproduce pre-ignition and super-knock in a research engine [149]. This represents a promising area for future research work, as developing inhibited additives could provide solutions for suppressing pre-ignition and super-knock.

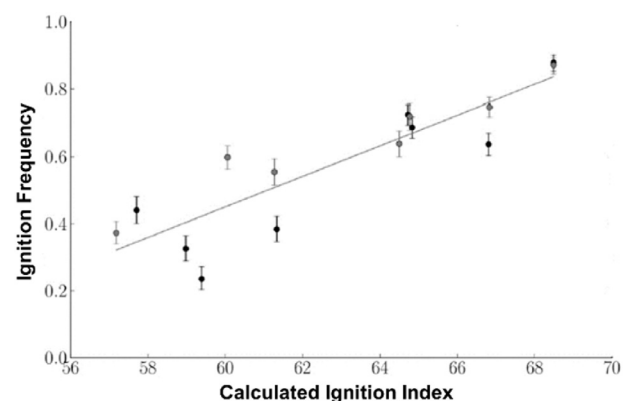


**Fig. 16.** The effect of base stock on LSPI (adapted from [228]).

### 3.3.2. Fuel properties

The fuel's chemical composition, octane number and volatility have effects on the frequency of super-knock. On one hand, the quality of the fuel directly influences the ignition properties of the mixture. On the other hand, fuel droplets may play a role in the origin and progress of pre-ignition.

**3.3.2.1. Composition.** The effect of fuel composition on super-knock was experimentally investigated in a boosted direct-injection gasoline engine [201,232,233]. Despite similar RON and MON ratings, the super-knock characteristics of the test fuels in direct injection SI engines were different. Fuel blends with high levels of aromatics increase super-knock frequency, whereas a low aromatic fuel and E10 (10% mass of ethanol) reduced super-knock frequency under different test conditions of A/F ratios and EGR levels, as shown in Fig. 17. For the aromatic content, it was found to correlate strongly with super-knock frequency. Moreover, a lower limit for the aromatic content was found by Andrew et al. [232]: as aromatic content was increased from 15 to 35% the super-knock frequency increased from zero to ~100 events in 135,000 cycles. Below 15% no super-knock behavior was detected even for the highest load conditions.

In essence, the fact that a high aromatic content increases the super-knock frequency can be explained by two main reasons. Aromatic combustion leads to soot formation and enhanced deposits, and these solid particles are possible sources of pre-ignition for super-knock, as discussed in Section 3.2.2: Solid particle. Moreover, soot and deposits also coat the surface of the combustion chamber, which resists heat transfer from walls. The reduced heat transfer leads to higher temperatures and pressures in-cylinder before spark timing, which also promotes pre-ignition. For ethanol addition, this influences the latent heat and flame propagation and will be further discussed in the following Section: Octane number.

**3.3.1.2. Octane number.** Fuel octane number has comprehensive effects on pre-ignition and super-knock. Most experiments in the literature show that there is no correlation between pre-ignition propensity and RON or MON. Some experiments show that pre-ignition frequency decreases with increased octane number [202,234]. Pre-ignition temperature tends to be higher with increasing RON, and pre-ignition temperature is more related to RON than MON [199]. However, it was found that ethanol had a relatively high pre-ignition tendency with high intake manifold pressure, although its octane numbers (RON and MON) are particularly high [235]. This can be explained by the fact that fuels like ethanol and hydrogen are very susceptible to pre-ignition because of their high laminar burning velocities [3,236,237] and smaller laminar flame thickness. A stable flame can be established if the kernel radius is sufficiently larger

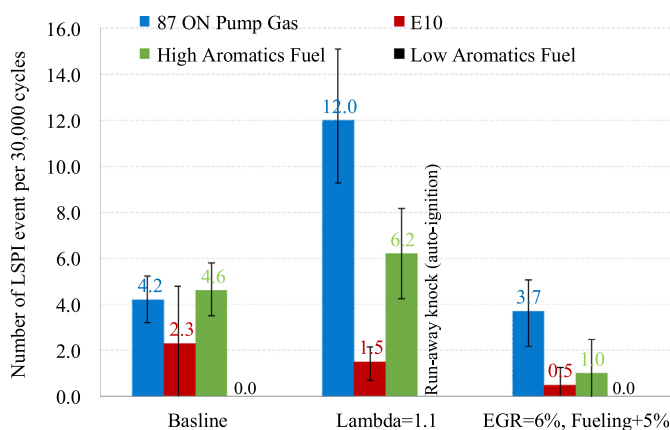


Fig. 17. The effect of fuel composition on super-knock (adapted from [201]).

than the laminar flame thickness [238]. On the other hand, lower super-knock tendency with ethanol fuel than gasoline fuel may be thanks to the higher heat of evaporation of ethanol. To sum up, pre-ignition with a high octane number fuel might not lead to super-knock due to its higher resistance to auto-ignition.

**3.3.1.3. Volatility.** A higher frequency of pre-ignition was observed for a fuel featuring a higher fraction of low volatility compounds. Fuels that had a distillation point of T50 below 103 °C showed a lower number of stochastic pre-ignition (SPI) events [193], as shown in Fig. 18. Fuel distillation points (T90 and T95) also have effects on LSPI frequency. It was concluded that a heavier fuel could lead to an increase in LSPI tendency [229]. This conclusion is consistent with the theory that high boiling point fuel components can cause more liner wetting [239] due to poorer atomization of the fuel spray and slower evaporation after adhesion on the wall, potentially leading to more fuel accumulation in crevices and higher LSPI frequency. More references on the effect of oil volatility on pre-ignition can be found in Palaveev et al. [151], Zheng et al. [240], Dahnz et al. [202], Zahdeh et al. [153], Sasaki et al. [241], Hamilton et al. [242], Chan et al. [243], and Li et al. [234].

Fuel additives also affect pre-ignition. A cleaning detergent was added to standard RON 95 pump fuel with the intention of reducing the deposits in the combustion chamber. However, pre-ignitions were found to be higher by a factor of 3 because a kerosene type solvent was used as part of the additive package. The poor evaporation with an evaporation range of 150–300 °C was thought to be the major driver for the increased soot formation and the resulting high pre-ignition frequency [153].

## 4. Combustion mode of engine knock

As discussed above, engine knock is associated with auto-ignition in the end gas [1]. In terms of auto-ignition evolution in a reactive gas, Zel'dovich [244] classified four modes: (1) near thermal explosion without a shock wave: where  $u_{sp} > D_{cj} \gg a$ , (2) detonation propagating supersonically:  $D_{cj} \geq u_{sp} > a$ , (3) deflagration propagating subsonically:  $a > u_{sp} > u_f$ , and (4) a normal flame propagating by molecular diffusive and conductive mechanisms:  $u_{sp} \approx u_f$ . Gu and Bradley et al. [98] extended the auto-ignition theory to consider temperature gradients (hot spots). Using 1-D DNS for syngas/air with detailed chemistry, they demonstrated five propagation modes of auto-ignition fronts: (1) thermal explosion, (2) supersonic auto-ignitive deflagration, (3) developing and developed detonation, (4) subsonic autoignitive deflagration, and (5) conventional laminar burning deflagration. Bradley [98] proposed two dimensionless

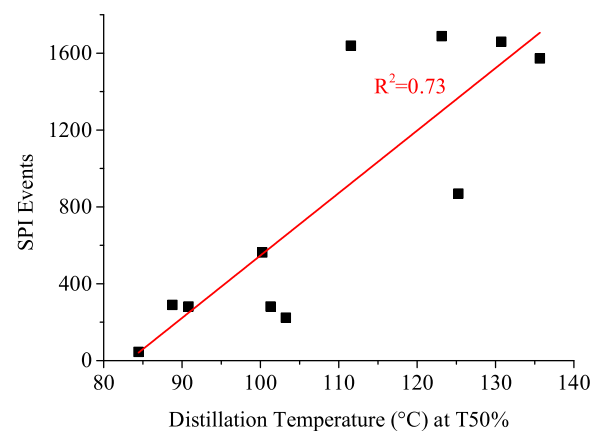


Fig. 18. SPI events per 240,000 firing cycles vs. distillation temperature of the fuel (adapted from [193]).

parameters,  $\varepsilon$  and  $\zeta$ .  $\varepsilon$  is the ratio of the residence time of the acoustic wave in the hot spot to the short excitation time in which most of the chemical energy is released, and  $\zeta$  is the ratio of the acoustic speed to the localized autoignitive velocity. The hot spot induced combustion mode can be plotted by a peninsula on the  $\varepsilon$ - $\zeta$  diagram. Kalghatgi et al. [4] applied the above method to super-knock analysis, and pointed out super-knock cases were located in the “developing detonation” zone in the  $\varepsilon$ - $\zeta$  diagram (see Fig. 19). In addition to the above two parameters, Rudloff et al. [95] proposed a third parameter,  $\pi$ , which is the ratio of the experimental pressure rise after super-knock to the theoretical pressure rise based on isochoric combustion, to discern super-knock. It was found that super knock is often located in the region with high  $\varepsilon$  and low  $\zeta$ .

Based on the above theoretical framework, numerical simulation and experimental investigations on the combustion modes of engine knock were also carried out to explain super-knock occurrence. To consider large hydrocarbon fuels with negative temperature coefficient (NTC) behavior, Dai and Chen [99] carried out 1-D CFD numerical experiments on reaction front propagation in n-heptane/air mixtures. It was found that shock compression of the mixture between the deflagration wave and the leading shock wave produces an additional ignition kernel, which determines the autoignition modes. To consider high-octane fuels in highly boosted gasoline engines, Wang and He et al. [2] carried out engine tests with gasoline fuel under high-temperature and high-pressure conditions. It was found that a hot-spot in the unburned end-gas mixture at temperature and pressure conditions above a so-called “deto-curve” may induce detonation. Kalghatgi and Bradley [4] attributed super-knock to developing detonations which originate from a resonance between acoustic waves emitted by an auto-igniting “hot spot” and a reaction wave, which propagates along negative temperature gradients in the fuel-air mixture. Robert et al. [56] placed the calculated  $\varepsilon$  and  $\zeta$  for the grid points close to autoignition on  $\varepsilon$ - $\zeta$  diagram in a LES study on knock prediction, and found that the possible existence of a DDT seems to be in good agreement with the evolution of knock intensity with spark timing. Bates et al. [245] used another parameter,  $\bar{E}$ , which is defined by  $\bar{E} = (\tau_i/\tau_e)(E/RT)$ , to insert contours of hot spot temperature elevations on the  $\varepsilon$ - $\zeta$  diagram. The different regimes for hot spot auto-ignition, extending from controlled auto-ignition at one limit, through the development of knock to super-knock, could be identified through the values of  $\tau_i$ ,  $\tau_e$ , and  $\bar{E}$  on the  $\varepsilon$ - $\zeta$  diagram.

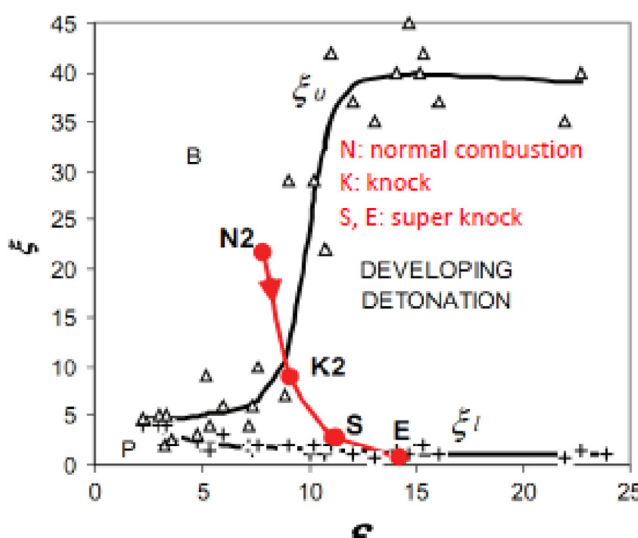


Fig. 19. Two dimensionless parameters for different combustion modes (Reprinted from [4] with permission of Elsevier).

Super-knock is stochastic phenomena and should be explained based on the nature of cyclical changes, including for example, temperature gradients, species stratification, and turbulent mixing in the mixture. Kalghatgi et al. [238] indicated that stochastic processes can affect knock intensity (KI) which will be dependent on both  $Z$  (a parameter that depends on the pressure at knock onset timing) and  $\partial x/\partial T$  (temperature gradient in a hot spot) with cycle-to-cycle variations. However, Peters et al. [205] ascribed the stochastic occurrence of pre-ignition and the resulting “super-knock” events to the stochastic nature of turbulence based on a 2D Direct Numerical Simulation (DNS).

To provide deep insights into the combustion process and reveal the combustion mode in the end gas, combustion visualization is the most direct method, as described next.

#### 4.1. Visualization of combustion modes in the end gas

Although numerous efforts to visualize the pre-ignition to super-knock process in SI engines have been conducted [153,203,218,220,222], very few direct experimental observations have been reported that would allow quantitative analysis of a super-knock event because super-knock occurs at high loads, which are usually beyond the operating conditions of optical engines. This problem can be solved by using a Rapid Compression Machine (RCM) with optical accessibility to simulate conditions similar to those within internal combustion engines.

Recently, Tsinghua University [77,78,179,246,247] carried out extensive RCM experiments to study the auto-ignition of isoctane. While most of the experiments exhibited HCCI-like combustion, a few combustion processes with pre-ignition and detonation induced by unknown randomly distributed particles were observed [248]. Enlightened by the randomly observed detonation process, a systematic study of reproducing the super-knock combustion process [78] was conducted using a spark to create pre-ignition in the RCM (Fig. 20) to capture the deflagration-to-detonation transition. It was found the amplitude of the pressure oscillations varies depending on the thermodynamic conditions. Different combustion modes of the end gas, including no-autoignition, sequential autoignition, and detonation were observed. Fig. 21 shows three typical image sequences corresponding to three combustion modes. Fig. 22 shows the corresponding pressures, heat releases and detonation waves.

##### 4.1.1. No-auto-ignition

When the initial pressure is low, the pressure trace is smooth. After spark ignition, a flame propagates out from the cylinder center. Once the flame front arrives at the cylinder walls, the combustion ends. Thus, no auto-ignition was observed in the end gas as shown in Fig. 21(a). This is a flame propagation case, like in the normal engine combustion cycle.

##### 4.1.2. End gas sequential auto-ignition

As the initial pressure increases, the heat release rate shows a second peak before the end of combustion. This 2nd heat release peak leads to a several bar pressure oscillation, which is similar to that in the conventional knock cycle. Such an amplitude pressure oscillation causes a small variation in image luminosity. The increases in image luminosity and pressure oscillation are due to the end-gas autoignition, as shown in Fig. 21(b) in the blue areas on the top right of the images from (3) to (6). No flame front propagation was observed after auto-ignition, which is due to the sequential autoignition of the surrounding gases.

##### 4.1.3. Detonation

For the case of high initial pressure, a steep pressure rise of more than 10 MPa occurs within a short time of 0.02 ms. Then, significant pressure oscillations were observed with an amplitude exceeding

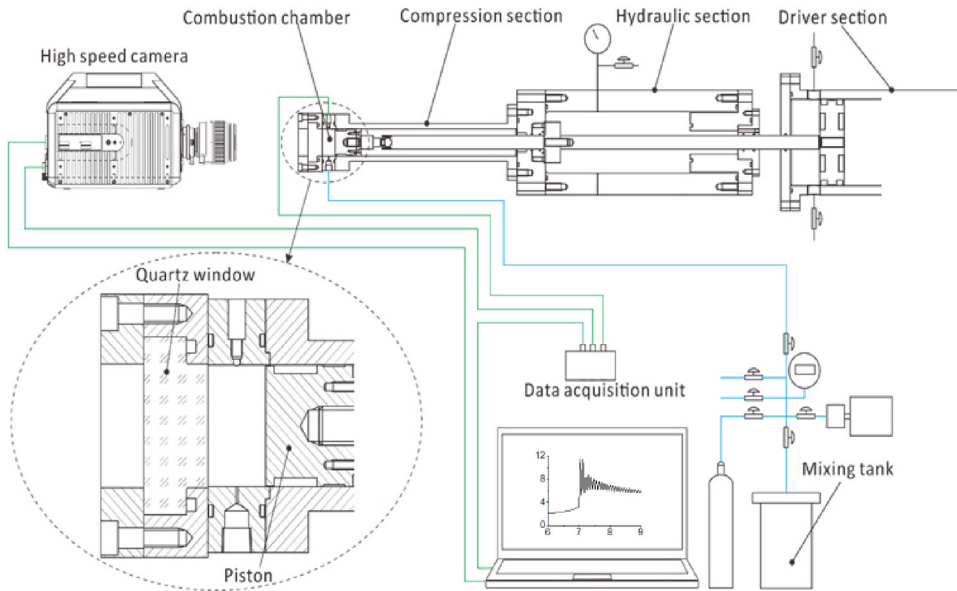


**Fig. 20.** Schematic of the RCM experimental setup (Reprinted from [248] with permission of Elsevier).

8 MPa. This phenomenon is a typical super-knock. Consecutive images near the start of the pressure oscillation are shown in Fig. 21 (c). A bright area appears near the top of the cylinder at the time of Image B, indicating a auto-ignition zone. At the time of Image C, a clear flame front with bright blue color is observed which propagates downward.

Fig. 22 also presents the propagation paths of the combustion wave. From image C to F, the average propagation speed swept by the left wing of the combustion wave front along the wall is 1847 m/s (Path 1). The propagation speed swept by the right wing of the combustion wave front along the wall is 1917 m/s (Path 4). Since the Chapman-Jouguet detonation speed ( $D_{CJ}$ ) for the end gas is predicted to be 1867 m/s, the bright blue flame from Image C to Image H is clearly a self-sustained detonation wave.

In SI engines the end gas can be subjected to isentropic compression until knock onset by assuming that heat loss is negligible. For the typical super-knock cycle [2], both  $p_{ai}$  and  $T_{ai}$  of super-knock in the engine are higher than for the detonation case in the RCM, and the super-knock engine cycle exhibits even higher amplitudes of pressure oscillations, thus the high pressure oscillation of the super-knock is due to detonation. This conclusion is also supported by the intensity parameter proposed by Rudloff et al. [95], which was calculated using pressure ratio to characterize a super-knock:

$$\pi = \frac{\Delta p_{exp}}{\Delta p_{iso}} = \frac{p_{peak\_exp} - p_{ko}}{p_{peak\_iso} - p_{ko}} = \frac{p_{peak\_exp} - p_{ko}}{\frac{(\gamma-1)Q}{V_{cyl}}} \quad (7)$$

The calculated  $\pi$  in the RCM case (Fig. 21(c)) is 1.97. The pressure rise is much higher than that of isochoric combustion. Correspondingly, the calculated  $\pi$  for the engine super-knock cycle (Cycle 1388 in Fig. 11(a) in Ref. [2]) is 2.58, even higher than the confirmed detonation case in the RCM. Thus, the 1388 engine super-knock cycle is identified as detonation.

#### 4.2. Analysis of the process from pre-ignition to super-knock

To further analyze the process of super-knock, a random pre-ignition event and the following super-knock combustion process under high temperature and high pressure conditions by high speed photography and pressure measurements was successfully captured [77], as shown in Fig. 23, from deflagration to detonation. Also shown are selected images at specific instances over the pressure

trace, which clearly demonstrate the three distinguishing stages of the combustion process: deflagration, detonation, and the resulting pressure oscillations.

##### 4.2.1. Deflagration propagation

The first stage in the combustion process is deflagration. The combustion event is initiated by a random pre-ignition particle that first appears in the center in this case and ignites the mixture. A deflagration is initiated and the resulting blue flame propagates outward at a subsonic flame speed. The chemical heat release from the deflagration leads to thermal expansion of the burned zone, which compresses the surrounding unburned mixture to high pressure and high temperature.

##### 4.2.2. Detonation in unburned mixture

The second stage is detonation. Three distinct blue flames are initiated near the wall with two clearly identified merging boundaries near the cylinder wall. Since the mixture in the center of the cylinder has already been burned, the newly-initiated flames propagate in the surrounding unburned mixture along the periphery of the cylinder.

A rapidly propagating wave travels from this region to the bottom-right corner. The passage occurs in a short time with a propagation speed of 3080 m/s in the unburned mixture near the wall. This supersonic wave propagates with a Mach number of 5.5. Indeed, the Chapman-Jouguet theory yields a C-J detonation velocity ( $D_{CJ}$ ) of 2325 m/s. This clearly indicates that the bright blue flame is a strong detonation wave, which rapidly sweeps past the pressure transducer, leading to a rapid pressure rise of 8.0 MPa in a short time period of 0.04 ms, as is evident from the pressure “discontinuity” in Fig. 23.

##### 4.2.3. Pressure oscillation in combustion chamber

The third stage is pressure oscillation. After the initiation of the detonation the propagating fronts collide at the bottom of the cylinder, forming an incandescent zone. The merged waves are then reflected from the bottom of the wall and bounce back towards the top. Since all the reactants in the combustion chamber have been consumed at this stage, the velocity of the resulting wave is 1155 m/s, which matches the sound speed of the burned gas. The frequency of the pressure oscillation is 11 kHz, as shown in

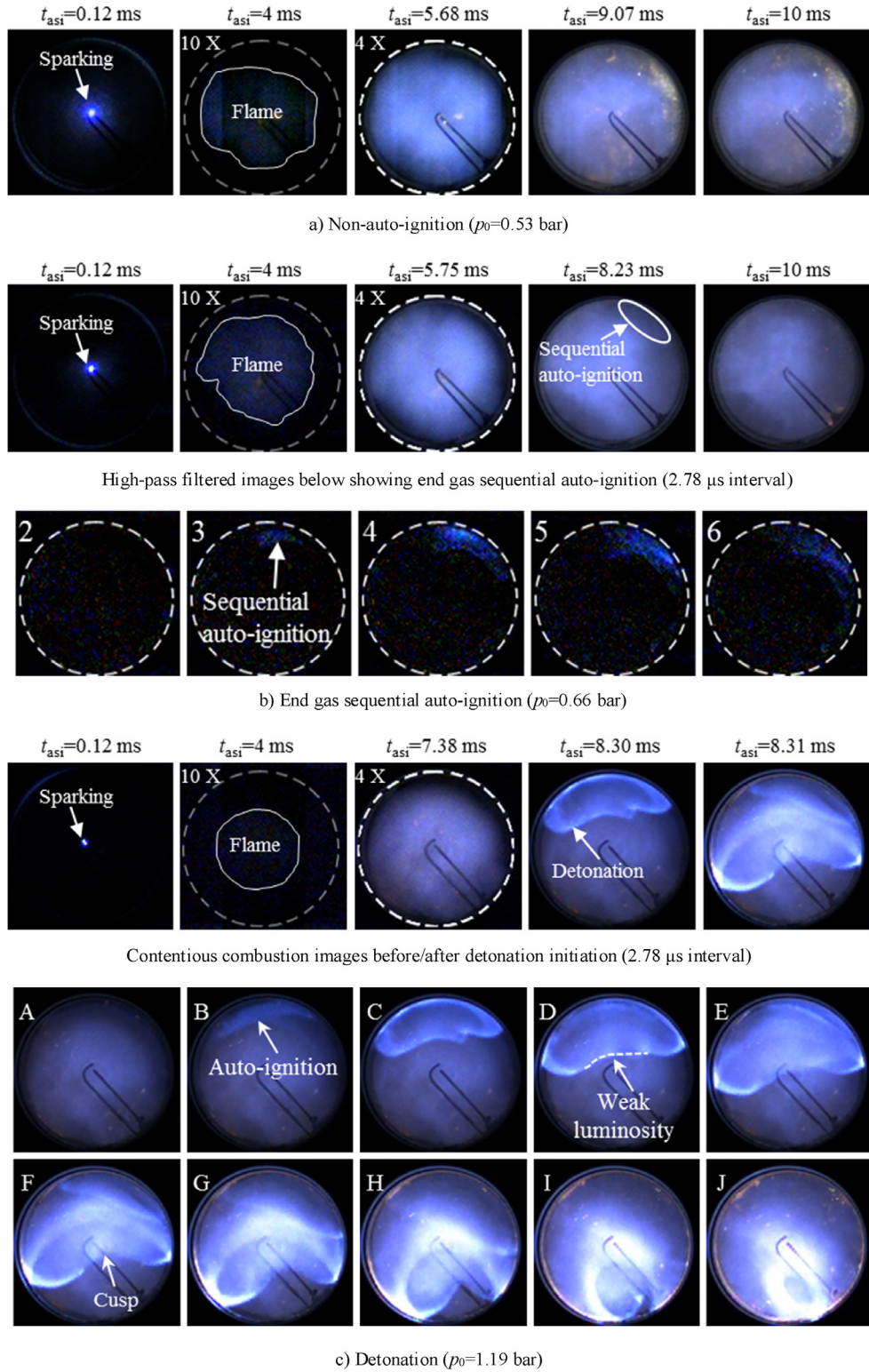
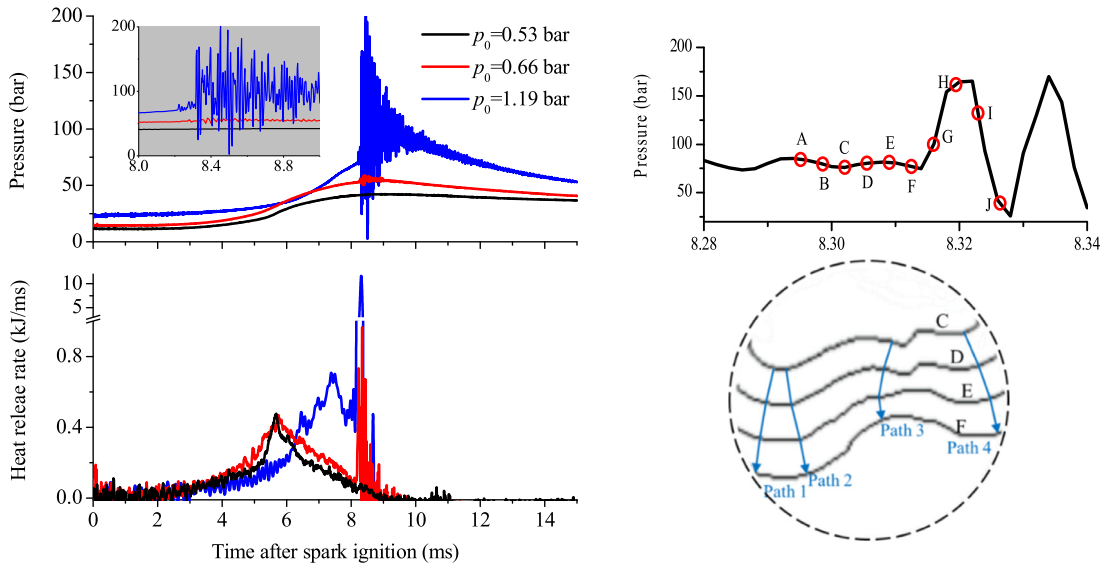


**Fig. 21.** Combustion process of three end-gas combustion modes (Reprinted from [78] with permission of Elsevier).

Fig. 23(b), which is consistent with the first radial resonant mode of Draper's "drum mode", as shown in Table 4 [76].

The above high-speed combustion imaging from the above RCM experiment demonstrates that the mechanism of super-knock consists of hotspot-induced deflagration-to-detonation transition followed by high-pressure oscillation. A deflagration starts the combustion and leads to detonation, which is similar

to the pre-ignition observed in gasoline engines. However, it is significant to note that the deflagration does not self-accelerate to detonation. Instead, it is the "hot spots" located in the unburned mixture at high pressure and high temperature conditions that initiate detonation, and which consume the unburned mixture rapidly and causes the large-magnitude pressure rise and the following pressure oscillations.



a). Pressure traces and heat release rates of 3 combustion modes b) Pressure trace and flame front locations of the detonation case

**Fig. 22.** Pressure traces, heat release rates and detonation wave (Reprinted from [78] with permission of Elsevier).

The above mechanism obtained in the RCM can also be used to explain the phenomena of super-knock in boosted gasoline engines, as shown in Fig. 24. First, pre-ignition occurs before TDC due to a local hot-spot (oil, deposit, oil-gasoline, etc.) in the combustion chamber during the compression stroke. A pre-ignition-triggered flame propagates from the hot-spot to the rest of the mixture. Then, the spark ignition occurs, and the 2nd flame front may propagate if the spark ignition is in an unburned zone. The rapid expansion of the burned gas rapidly compresses the unburned mixture to higher temperature and pressure (about 1000 K, 10 MPa). Finally, a second hot-spot (or multiple hot-spots) in the end gas induces the detonation of the un-burned mixture at high temperature and high pressure, as indicated in Fig. 24.

As the timing of the “hot spot” combustion in the unburned mixture is crucial to detonation, this mechanism also helps to explain why an earlier pre-ignition does not always lead to a higher knock intensity. If the “hot spot” appears too early, the in-cylinder pressure and temperature are relatively low. It may turn out to be a deflagration, similar to the combustion processes in the 1st stage. If the “hot spot” appears too late, the majority of the mixture has already been consumed by the deflagration, and pressure tends to decrease with the downward movement of the piston. As a result, the pressure rise and pressure oscillation will be smaller. If the “hot spot” starts near TDC, it is likely to trigger detonation under high pressure and high temperature conditions.

#### 4.3. Effect of thermodynamic conditions on the combustion mode

##### 4.3.1. Pressure and temperature

Since super-knock typically occurs near TDC at high loads, the pressure and temperature have significant impact on super-knock or the end-gas combustion mode. A systematically investigated effect of pressure and temperature on auto-ignition behavior in a RCM was conducted using a stoichiometric isoctane/O<sub>2</sub>/N<sub>2</sub> mixture [78], as shown in Fig. 25(a). The magnitude of the pressure oscillation increases with increasing initial pressure.

To explore the sole effect of the temperature on combustion mode, Fig. 25(b) gives pressure traces at different compression ratios with the same pressure at the end of compression. The auto-ignition timing advances as the compression ratio increases. This is attributed to the reduction of the end-gas ignition delay due to the

temperature increase. It is interesting to note that the end-gas combustion mode for the low temperature case is detonation; as the temperature increases, the mode changes to sequential auto-ignition. This indicates that temperature has less impact on detonation formation than pressure does. This phenomenon is related to the mixture density. Since detonation needs high heat release to initiate, a mixture with higher density is more prone to detonation due to the higher energy.

The above data can be plotted in Gu and Bradley's detonation peninsula [98], as shown in Fig. 26 using Kalghatgi and Bradley's method [249]. The parameters of  $\varepsilon$  and  $\xi$  at the time of knock onset for the above test cases are calculated by the following equations:

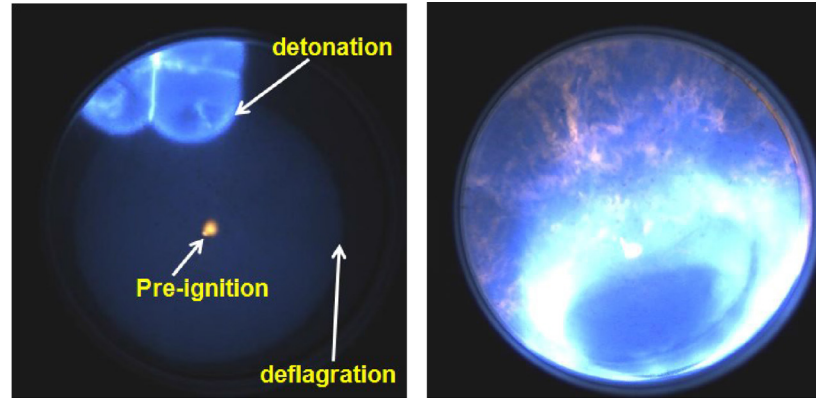
$$\varepsilon = \frac{r_0/a}{\tau_e} \quad (8)$$

$$\xi = a \frac{\partial \tau_i}{\partial T} \frac{\partial T}{\partial r} \quad (9)$$

$\tau_e$  and  $\tau_i$  are calculated using Chemkin software and the Wisconsin PRF mechanism [250],  $r_0$  and  $\partial T/\partial r$  are assumed to be 5 mm and -2 K/mm, which are the same as those adopted by Kalghatgi and Bradley [4]. It is obvious that the case of  $p_0 = 0.53$  bar (normal flame propagation) is located in the deflagration area, and the case of  $p_0 = 1.19$  bar (detonation) is located in the detonation area, while the case of  $p_0 = 0.66$  bar (sequential auto-ignition) is located very close to the boundary. It also shows that the propagation of detonation outside the hot spot is entirely possible under low  $\varepsilon$  conditions relevant to a boosted gasoline engine.

##### 4.3.2. Energy density

Since  $\rho^\infty p/T$ , and the mixture density can thus be used to represent the coupling effect of pressure and temperature. Fig. 27 shows the relationship between mixture density and combustion modes. Here  $E_{end}$  is the energy density at the end of the compression. It should be noted that combustion mode is closely related to the mixture energy density. Detonation tends to occur at higher mixture energy density instead of temperature. The boundary between the auto-ignition and non-auto-ignition modes is also obvious according to the engine density. This is consistent with the results of SI combustion engine tests, in which knock is unlikely to occur at low load with low intake pressure, i.e., low energy density.



a). Natural luminosity image including Pre-ignition, deflagration and detonation

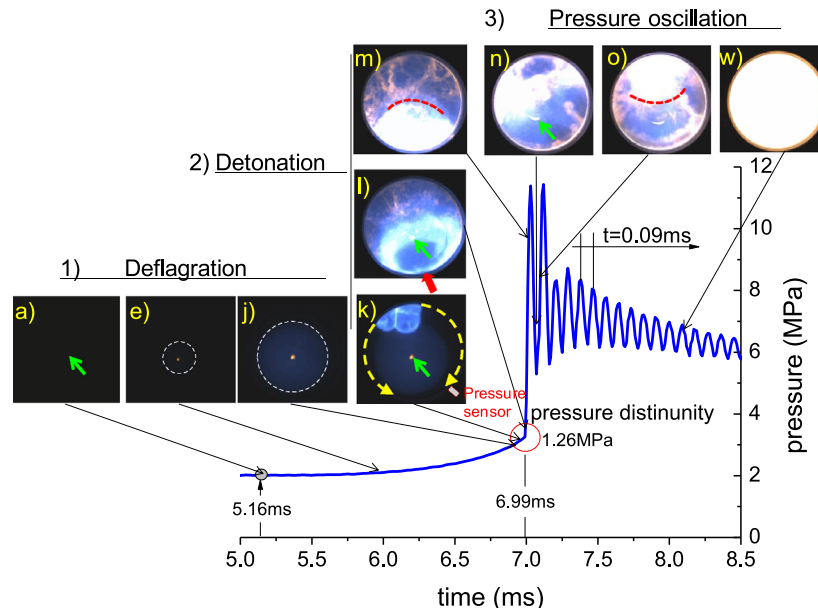


Fig. 23. A random pre-ignition induced super-knock combustion process (Reprinted from [77] with permission of Elsevier).

In SI engines under stoichiometric conditions, as the intake pressure increases the mixture energy density also increases, which increases the probability of knock, and ultimately leads to super-knock [153,192]. This shows that, as the energy density increases, the combustion mode in the end gas gradually transitions from non-auto-ignition, sequential auto-ignition to detonation.

#### 4.3.3. Interaction of pressure - temperature - energy density

Pressure, temperature and energy density are related parameters. To obtain the correlation, a significantly advanced spark timing to simulate pre-ignition from 8 to  $-50^{\circ}\text{CA}$  ATDC was conducted [251] at different boost pressures, as shown in Fig. 28. The results show that early spark ignition triggered flame propagation, which could lead to super-knock when the mixture state was above a critical condition. At high boost pressure, advancing the spark timing caused transitions from normal combustion to conventional knock, then to super-knock and then back to conventional knock and to normal combustion. The transition between knocking conditions was well correlated with the thermodynamic state at the start of the in-cylinder pressure oscillations. At the same intake temperature and naturally aspirated conditions, only slight knock was observed by advancing spark timing, which indicates that the thermodynamic

state dominates the conditions of knocking or non-knocking combustion.

Based on the experimental results, a pressure-temperature-energy density (P-T-E) diagram was developed to define super-knock, knock and normal combustion criteria [251]. Fig. 29 presents the knocking intensity results from the engine study as a function of the characteristic pressure and temperature. The super-knocking conditions are associated with high pressures and temperatures; however, as noted above, these values do not uniquely identify super-knocking conditions.

Ignition delay time was identified as a criterion to distinguish non-knocking conditions from knocking and super-knocking conditions. Generally, an ignition delay time higher than 1.1 ms (corresponding to  $9.9^{\circ}\text{CA}$  at 1500 rpm) correlated well with non-knocking results and ignition delay times lower than 1.1 ms correlated well with knocking and super-knocking conditions.

The energy density of the unburned end-gas mixture at the onset of knock was identified as a criterion for super-knock. For gasoline fuel in the test engine, when the energy density of the unburned end-gas mixture exceeded  $30 \text{ MJ/m}^3$ , super-knock was always observed. For lower energy densities, knock or non-knock was observed.

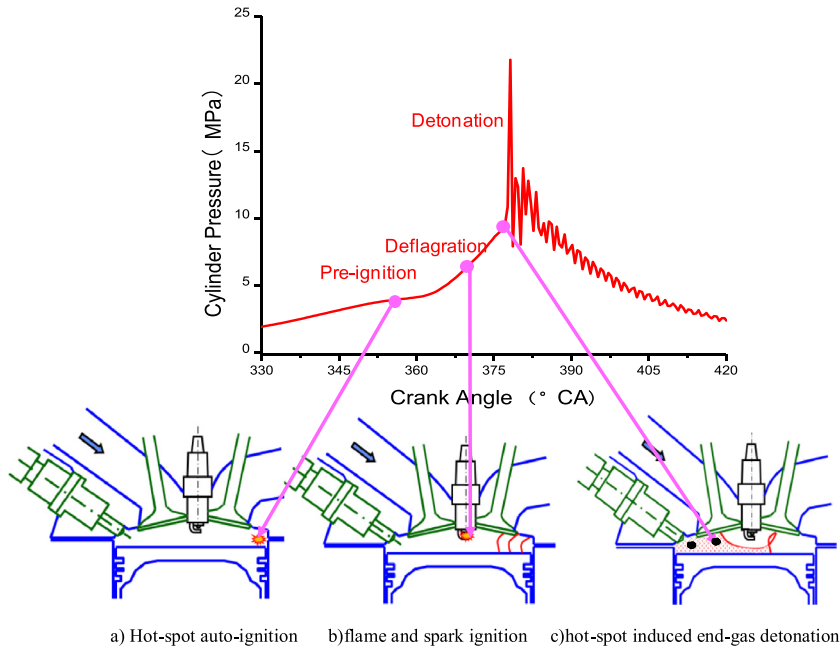


**Fig. 24.** Possible process of pre-ignition to super-knock (Reprinted from [2] with permission of SAGE).

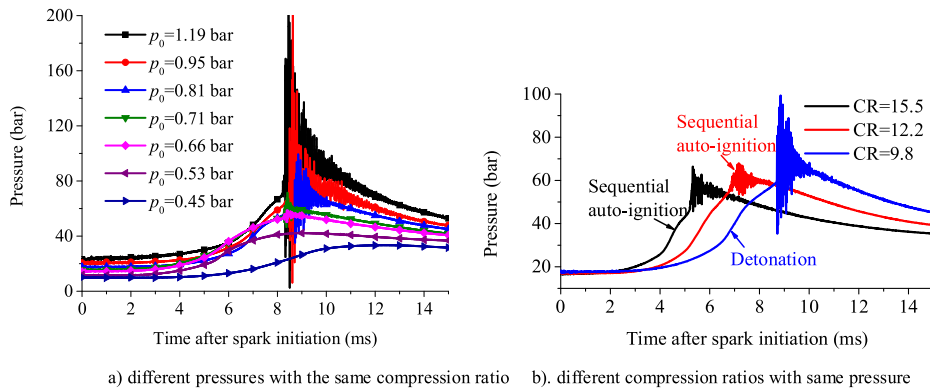


**Fig. 25.** Pressure traces of different pressure and temperature conditions (Reprinted from [78] with permission of Elsevier).

#### 4.4. Discussion of engine knock with NTC

##### 4.4.1. Phenomena of near-wall auto-ignition

Since higher temperatures occur ahead of the flame front, it is more likely for end-gas auto-ignition to occur near the flame front. However, many studies have shown that auto-ignition usually occurs in the end gas near the wall [1,80–82,252,253]. Some researchers propose that engine knock may be related to the negative temperature coefficient (NTC). Griffiths et al. [253] investigated n-pentane homogeneous charge compression ignition (HCCI) in a RCM to identify the behavior of end-gas auto-ignition in SI engines. Because of the local pressure rise caused by rapid heat release due to hot stages of ignition, the authors inferred that the knock observed in a RCM originates from the localized development of the hot stages of ignition. Its origin from near the combustion chamber walls may due to NTC behavior, as shown in Fig. 30(a), and an inhomogeneous temperature field, as shown in Fig. 30(b). The authors also pointed out that the rapidity and severity of the onset of high temperature ignition is probably associated with the transition in these non-homogeneous regions to vigorous chain branching through O atom generation.

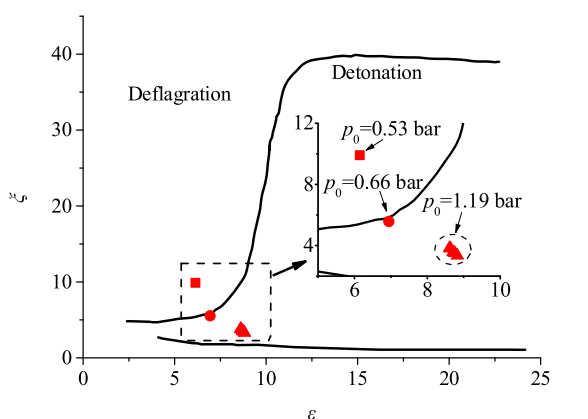


**Fig. 26.** Location of the tests with different initial pressures in Gu and Bradley's  $\epsilon$ - $\xi$  diagram (Reprinted from [78] with permission of Elsevier).

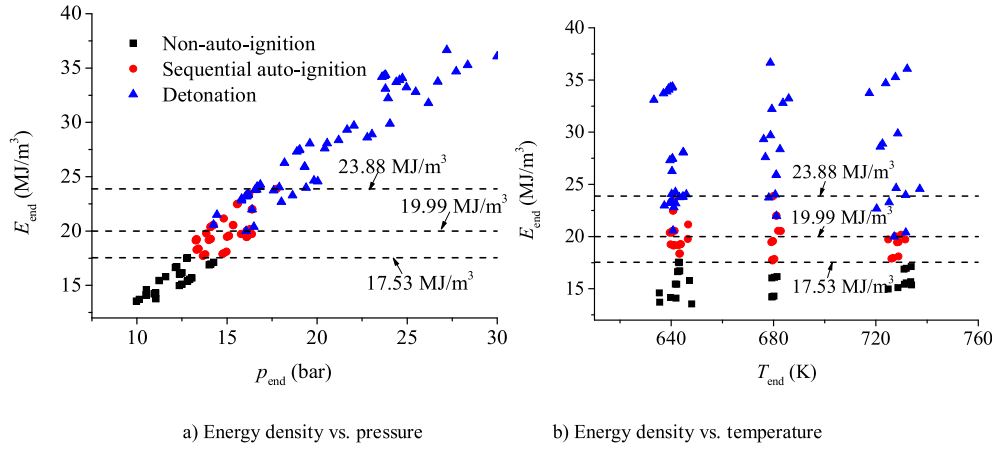


**Fig. 27.** Relationship between energy density at the end of compression and combustion mode (Reprinted from [78] with permission of Elsevier).

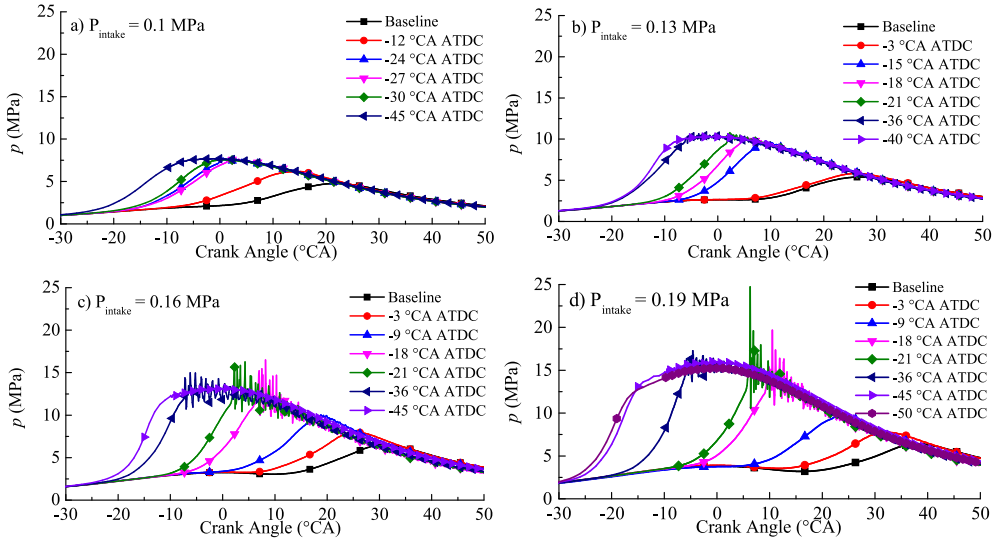


**Fig. 28.** Experimental results for in-cylinder pressure showing the transition between combustion modes as a result of spark timing changes at different intake pressures. The intake temperature was set to 20 °C for all cases (adapted from [251]).

In contrast to this point, Pöschl et al. [80] investigated the influence of temperature inhomogeneities on the reaction kinetics of knocking combustion using a primary reference fuel (PRF) which exhibited strong NTC. The research octane number (RON) of the fuel used was 69. The observed results showed that NTC does not play any role in the evolution of knock. The authors concluded that the initiation of a detonative combustion includes three stages: (1) Sequential auto-ignition due to low temperature kinetics, which leads to a fast-propagating reaction front along the temperature gradient, as shown in Fig. 31. The cool flame travels with speeds of 50–200 m/s. (2) Subsequently, a second reaction front due to main heat release follows, with average speeds up to 500 m/s. (3) Shock waves are generated by the fast-propagating reaction front. If the shock wave is strong and the gas mixture is reactive enough, the pressure wave couples with heat release. This detonation exhibits an intensely illuminating flame that travels at speeds up to 1400 m/s.

Near-wall auto-ignition was also observed using fuel which exhibited non-NTC and weak NTC. Wang and co-authors [77,78,247] investigated end-gas auto-ignition using a pure isoctane fuel. The authors found that near-wall auto-ignition is the reproducible mode observed in a closed cylinder under high temperature and high pressure conditions. The detailed flame structures are slightly different because the deflagrative flame front after spark ignition is wrinkled

due to obstruction by the spark electrode. Fig. 32 shows selected images after the end-gas auto-ignition of continuous five tests under the same initial conditions [78]. The images exhibit very similar combustion processes from deflagration to detonation and the same transition mode from the near-wall auto-ignition (NWAI) to detonation. NWAI is related to pressure wave reflection and chemical reaction. It was found that weak pressure oscillations with amplitudes of several bar were detected before detonation initiation due to the fast propagating deflagration wave in the center, as shown in Fig. 22. The first observed auto-ignition occurs near the wall and this could be explained as follows: (1) a pressure wave/shock wave reflects with double its amplitude at the wall, which compresses the near-wall unburned gas to higher temperature and shortens the ignition delay. (2) Turbulence-chemistry interaction shortens the ignition delay due to relatively strong eddy dissipation near the wall at TDC in the RCM. Local explosion is likely to occur in the corner vortices near the wall.

#### 4.4.2. Effect of shock compression on ignition delay

Since shock waves and temperature inhomogeneities always occur in the engine knocking combustion process, the effect of both shock waves and NTC on the ignition delay should be considered to understand near-wall auto-ignition. Qi et al. [254] calculated

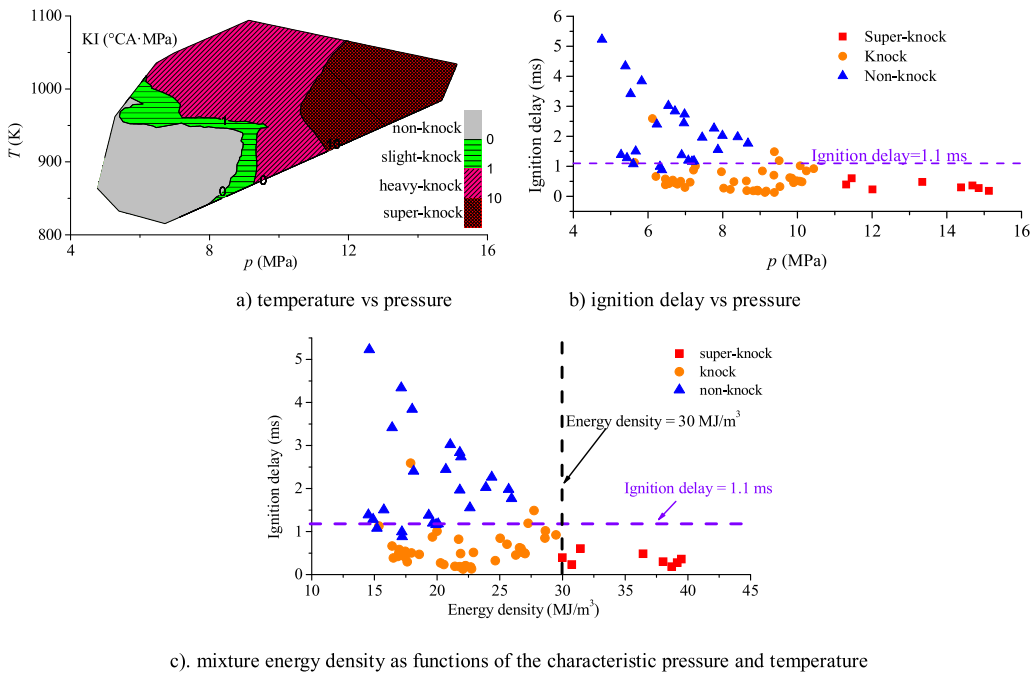


Fig. 29. P-T-E as functions of the characteristic pressure and temperature in the engine (adapted from [251]).

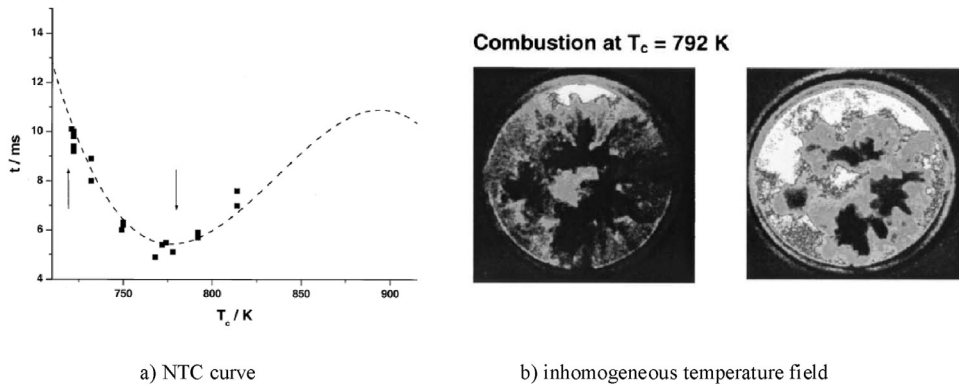


Fig. 30. Knock originates from near the combustion chamber walls due to NTC behavior (Reprinted from [253] with permission of Elsevier).

ignition delay variation in RCM tests [78] based on their experimental pressure traces. Their chemical-kinetics-calculated results show that auto-ignition near the wall is unlikely to be affected by NTC. The ignition delay traces of isoctane/air calculated according to their experimental pressure traces almost do not pass through the NTC region (Fig. 33), especially for low temperature at the end of compression ( $T_{end}$ ) cases.

A recent RCM study revealed that the reason why super-knock is usually initiated near the wall is due to shock wave reflection near the cylinder wall [247]. The mechanism of the near wall detonation initiation can be described as shock wave reflection induced detonation (SWRID). SWRID has the following features: (1) the end gas was compressed due to the heat release of spark-triggered turbulent flame propagation (Fig. 34(a)); (2) a relatively strong local end gas auto-ignites (local explosion), which causes a sudden local pressure rise and generates an incident shock wave (Fig. 34(b)). The incident shock wave propagates into the unburned mixture; (3) the incident shock wave propagates in the mixture and interacts with the curved wall. When the shock wave travels in the first half of the cylinder, the area of the shock wave increases, as shown in Fig. 34(b). (4) when the incident shock wave propagates in the second half of

the cylinder, the area of the shock wave decreases. In these cases, a reflected shock wave is generated near the wall. As the shock wave moves along the circular sidewall, the incident angle changes continuously. Therefore, the reflection of the shock wave evolves from Mach reflection to reverse Mach reflection, and then to transitional regular reflection, and eventually to regular reflection [255,256], during which a Mach stem is generated. The Mach stem further elevates the pressure and temperature of the unburned mixture, and initiates detonation (Fig. 34(c)) [247]. The detonation wave then propagates in the surrounding unburned mixture (Fig. 34(d)), causing an extremely high pressure rise in the cylinder.

The auto-ignition-initiated shock wave elevates the unburned mixture's pressure and temperature. However, the ignition delay of the mixture after the incident shock wave compression is still long, even under higher pressure and temperature conditions. Only after the Mach stem develops will the mixture pressure and temperature be further elevated, and then detonation initiation occurs. The heat release of the mixture couples with the shock wave reflection near the wall, resulting in detonation, which propagates at a speed faster than the C-J detonation velocity. Based on high-speed images, the detonation is typically initiated near the cylinder wall [77,78,247].

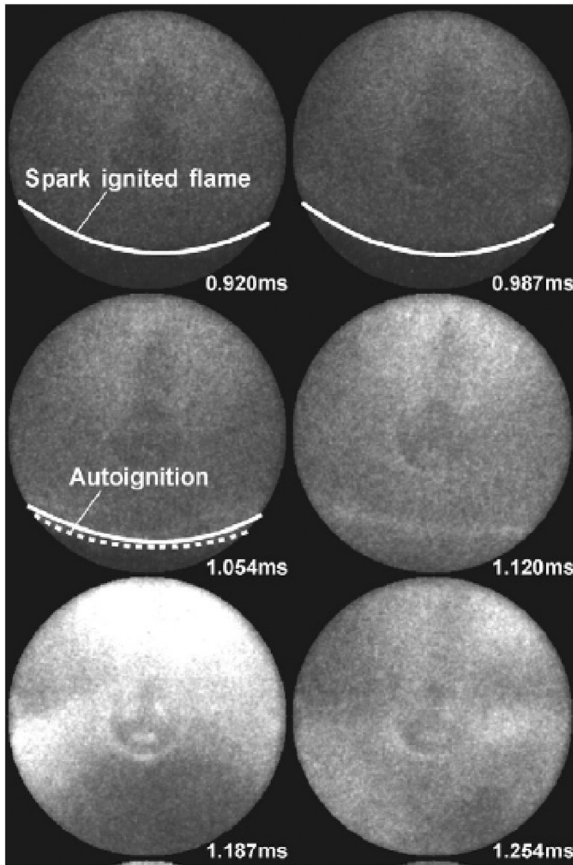


**Fig. 31.** Sequence of flame luminescence of knocking combustion (Reprinted from [80] with permission of Elsevier).

## 5. Suppression methods for engine knock

### 5.1. Control strategy for conventional knock

Conventional knock is a race between the flame in the engine and the thermal auto-ignition of the unburned “end gas” [1]. The

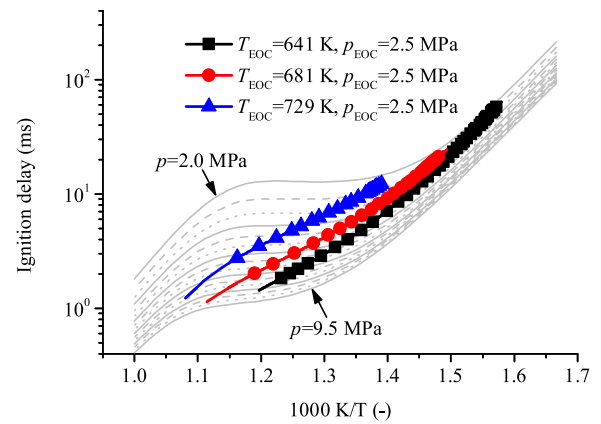


**Fig. 33.** Ignition delay variation of RCM tests based on experimental pressure traces (Reprinted from [254]).

principle for avoiding engine knock is that the time of flame propagation to the end gas ( $\tau_1$ ) is less than the time of the end-gas auto-ignition ( $\tau_2$ ). Possible control strategies present in SI engines are summarized next.

#### 5.1.1. Retarding spark timing, improving octane number and enriching mixture

Retarding spark timing [257–259], improving octane number [258,260–262] and enriching the mixture [258,263] are commonly applied approaches for knock suppression in production engines without component modifications. Retarding spark timing is the most effective method to simultaneously reduce the end-gas temperature and pressure. Lower end-gas temperature and pressure prolong the ignition delay ( $\tau_2$ ). However, late spark timing usually leads to an un-optimized combustion phase with lower thermal efficiency. It also may deteriorate engine performance due to the decrease in mean combustion chamber temperature and pressure [264–266]. Increasing the fuel octane number can be achieved by introducing antiknock additives to the fuel, like ethers, etc. In addition, adding alcohols or even water into the combustion chamber could also increase the time for the end-gas auto-ignition ( $\tau_2$ ) and

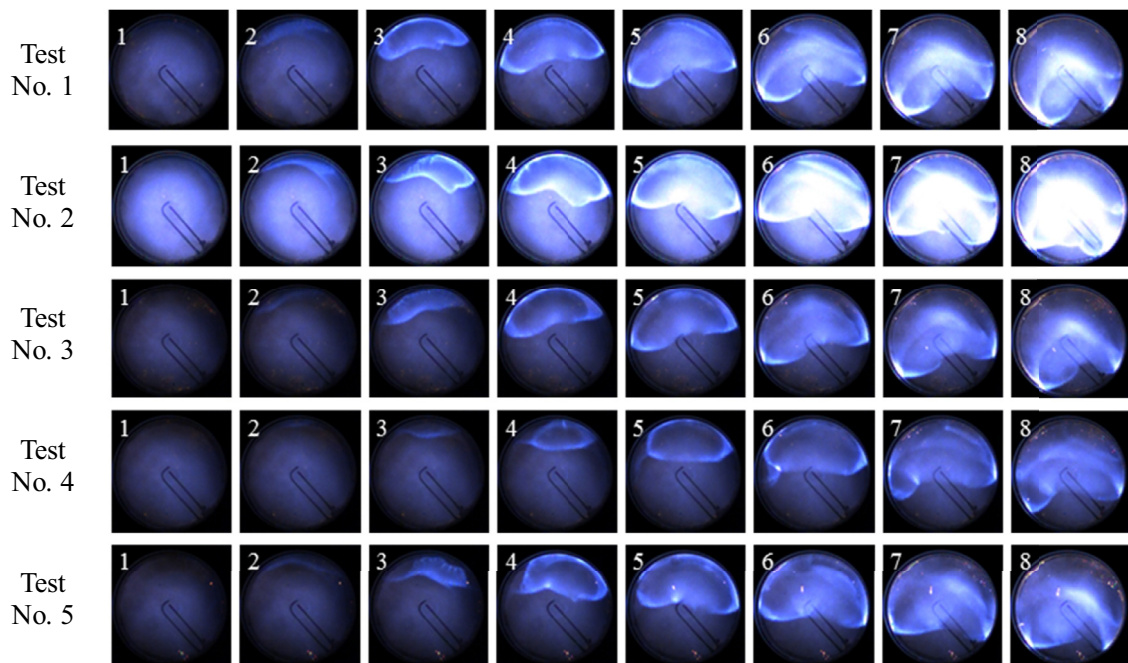


**Fig. 32.** Detonation of different tests at  $p_0 = 1.19$  bar (frame interval =  $3.47 \mu\text{s}$ ) (Reprinted from [78] with permission of Elsevier).

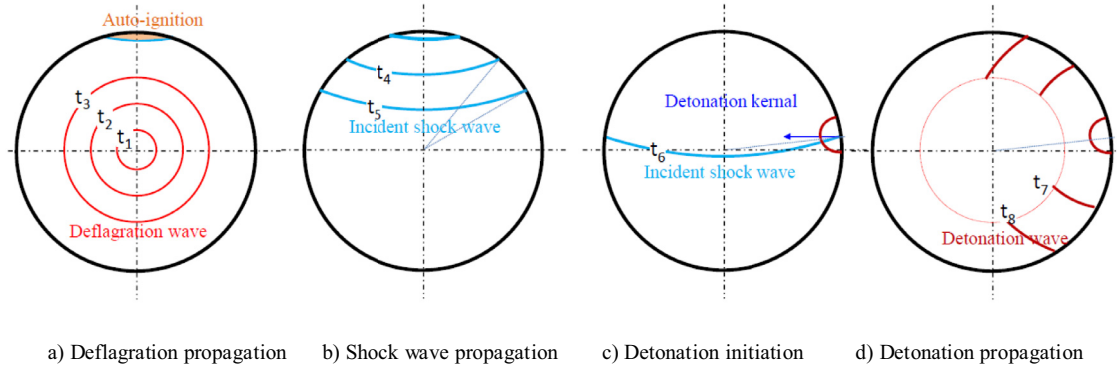


**Fig. 34.** Illustration of the SWRID initiation process (Reprinted from [247] with permission of Springer).

then suppress knock [267,268]. Injecting excessive fuel could increase the effect of charge cooling and decrease the temperature of the mixture, which could prolong the time to end-gas auto-ignition and finally suppress knock. However, under the condition of fuel enrichment, HC and CO emissions increase, and since the TWC can only work under stoichiometric conditions, this causes problems of fuel economy and emissions.

### 5.1.2. Exhaust gas recirculation

Exhaust gas recirculation (EGR) is regarded as an effective method [115,118,124,129,258,263,269–277] for suppressing knock in advanced SI engines due to the resulting increased  $\tau_2$ . Furthermore, cooled EGR has more potential in knock mitigation without a loss of output power [54,55,118,278,279]. Grandin et al. [118] demonstrated that by increasing the EGR ratio from 7% to 13%, the maximum BMEP increases with advanced spark timing. But, with further advanced spark timing, BMEP does not increase, since it is limited by knocking combustion. Increasing the EGR ratio reduces this limitation. Because an increase of cooled EGR lowers the gas temperature, and more fuel is consumed before reaching the knock temperature limit, therefore, it can further widen the ignition advance angle.

To quantify the effect of EGR on knock intensity, Alger et al. [129] conducted experiments on a 2.4 L boosted, MPI gasoline engine, equipped with a low-pressure loop (LPL) cooled EGR system. The results indicate that the improvement in effective AKI (anti-knock index) of the fuel from using EGR is about 0.5 RON per % of EGR for commercial grade gasoline fuels. Higher levels of EGR ( $EGR > 15\%$ ) have been shown to have a significant effect on engine efficiency by reducing knock, leading to improved combustion phasing [118,280–282] and the ability to operate at higher loads at compression ratios above 12 [283,284] (Fig. 35).

Combining the effects of boosting, increased compression ratio and cooled EGR [269] to further improve fuel economy, has also been investigated. Compared with CR 9.3 and no EGR, CR 10.9 and 18–25% cooled EGR could improve fuel economy by 6–9%. Among the contributing effects, the primary one is the theoretical thermal efficiency improvement caused by the increased ratio of specific heats and increased geometric CR, while the second one is the reduction in heat transfer loss due to lower combustion temperatures with EGR. On the contrary, high temperature internal EGR has a disadvantageous effect on knock suppression because of its heating effect, which should be avoided for gasoline engines. Mazda [285] used a 4-2-1 exhaust manifold timing sequence to reduce internal EGR and to decrease the temperature at TDC for suppressing knock.

### 5.1.3. Stratified mixtures

Use of stratified mixture is a flexible approach to suppress knock and is usually achieved using direct injection [109,111,112,114,

120,121,183,258,286–293]. Fuel directly injected in the cylinder can lower the combustion temperatures due to the cooling associated with fuel vaporization. Therefore, the cooling can lower knock sensitivity and the compression ratio can be increased [288–293].

A two-stage injection concept was proposed by Kuwahara et al. [289] and Yang et al. [294] for knock suppression and low speed torque improvement in DISI engines, but the proposed rich mixtures (A/F ratio = 12~12.5) would deteriorate fuel economy and exhaust emissions, which limited the application of this method. Use of stratified stoichiometric mixture has been demonstrated. Using a two-stage injection strategy in gasoline direct injection engine, Stratified Stoichiometric Mixture (SSM) could suppress knocking effectively compared with a Homogeneous Stoichiometric Mixture (HSM) case, as shown by the smooth pressure trace and lack of pressure oscillations in Fig. 36 [111]. Investigation of a two-stage strategy indicated that locally slightly rich mixtures due to a late injection helps to suppress auto-ignition by providing a local cooling effect and by enhancing the local flame propagation speed [55]. The assessment concludes that two-stage injection is an effective method for suppressing knock under high load operating conditions. However, the injection strategies and combustion systems need to be carefully designed and optimized to avoid soot emissions.

### 5.1.4. Dual-fuel spark ignition with DI and PFI

Dual-fuel spark ignition (DFSI) combustion is more flexible to suppress knock and improve efficiency [123,128,258,295–302], especially using gasoline and alcohols in SI engines. The potentials of ethanol direct-injection (DI) and dual-injection (PFI and DI) engines, to cool the charge and suppress knock were examined in Ref. [303].

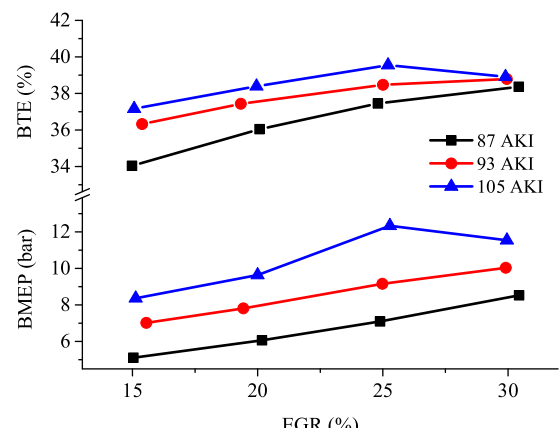


**Fig. 35.** Results of an EGR sweep at 1500 RPM for different AKI fuels (adapted from [129]).

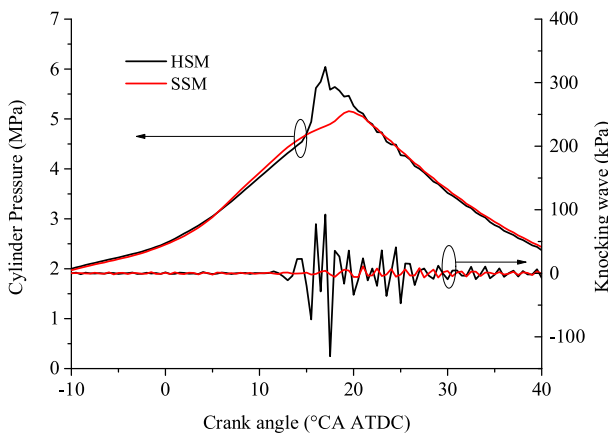


**Fig. 36.** Experimental results of Stratified Stoichiometric Mixture (SSM) and Homogeneous Stoichiometric Mixture (HSM) for knock suppression (adapted from [111]).

Dual-injection using PFI-gasoline with DI-E85 was developed on 'Ecoboost' gasoline turbocharged engines [156,304]. The engine efficiency was improved by suppressing knock at low-speed, high-load conditions. Higher volumetric efficiency by using ethanol and gasoline dual-injection was observed [305,306]. However, CO and HC emissions increased when the amount of ethanol was higher than 36% in the total fuel energy. Compared to the gasoline DI engine, the compression ratio of the dual-fuel engine was increased from 9.5 to 13.3 and it achieved significantly improved engine efficiency [307].

Alcohols-gasoline and gasoline-alcohols dual-fuel spark ignition (DFSI) combustion have been compared for knock suppression and higher engine efficiency using a high CR gasoline engine [143,308,309]. Alcohols-gasoline DFSI is organized using a PFI of high latent heat of vaporization, high octane number, and highly oxygenated fuel to suppress knock and a DI of high energy density fuel to extend engine load. Gasoline-alcohols DFSI was organized by gasoline PFI and alcohol DI, as shown in Fig. 37. It was found that both alcohols-gasoline DFSI and gasoline-alcohols DFSI are

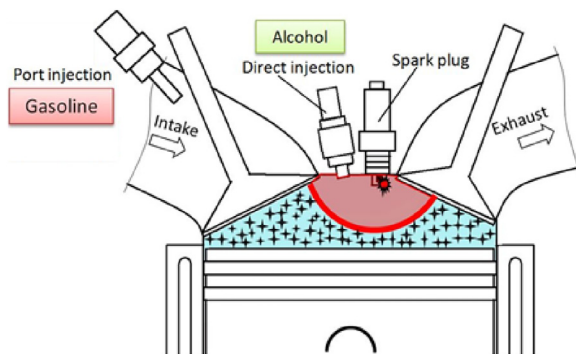


**Fig. 37.** Schematic of dual-fuel dual-injection spark ignition combustion.

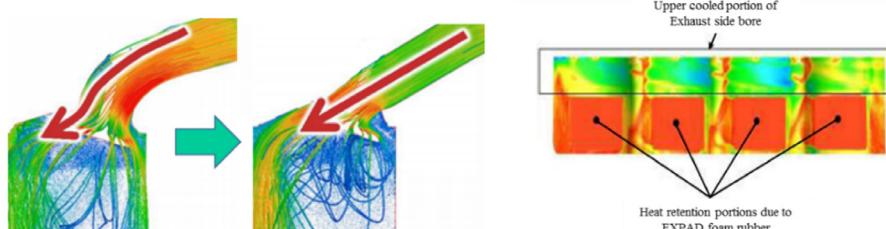


**Fig. 38.** High tumble intake-port and cooling water jacket for knock suppression (adapted from [155]).

promising methods of using alternative fuels in gasoline engines with significant improvements in thermal efficiency due to knock suppression. Gasoline-alcohols DFSI exhibited higher anti-knock performance than alcohols-gasoline DFSI. However, alcohols-gasoline DFSI is more practical for the automotive industry due to fewer engine modification requirements.

### 5.1.5. Other methods

**5.1.5.1. Turbulence** [205,258,310,311]. Increasing turbulence intensity usually suppresses engine knock. Once combustion has started, increased turbulence leads to fast combustion and decreases the tendency to knock [265,266,312]. However, at the start of combustion, increased turbulence also increases heat transfer from the spark electrode. To solve this problem, modern engines adopt high energy ignition (more than 100 mJ) to support strong turbulence. For example, through optimizing the geometry of the intake port as shown in Fig. 38, the tumble ratio of a dedicated engine for the Toyota Prius hybrid increased from 0.8 in the previous 2ZR-FXE model to 2.8 in the ESTEC 2ZR-FXE. Introduction of high tumble-induced-high-turbulence is accompanied by low tendency to knock.

**5.1.5.2. Cooling** [258,267,313–315]. Cooling of the combustion chamber walls is also an effective approach to reduce end-gas temperatures. An effective method to suppress knock is changing the coolant flow patterns to improve the distribution of wall temperatures [266]. However, increased heat transfer lowers the thermal efficiency. To suppress knock without a considerable loss of thermal efficiency, only the upper portion of the exhaust side bore should be cooled, and foam rubber can be utilized to provide heat insulation to maintain the temperature of the center and lower portions of the bore, as shown in Fig. 38 [155].

Cooling the intake charge is also useful for knock suppression. The initial condition of the end gas during a cycle is the intake air temperature. As expected by the Livengood-Wu correlation [92], the temperature history of the end-gas mixture plays an important role in engine knock. In addition, cooling the exhaust manifold is also important. A water-cooled exhaust manifold (WCEM) [316] with high cooling capacity was adopted to reduce the temperature of the exhaust valve surface and the EGR so as to suppress knock.

**5.1.5.3. Lowering effective compression ratio** [110,127,258,262,317–321]. Variable valve timing (VVT) is a practical way to change effective compression ratio at relatively low cost for the different engine operating regions. Late intake valve closure (LIVC) is commonly used at high load to achieve a lower effective compression ratio to avoid knock. Nissan developed a 1.2 L engine with such an Atkinson cycle, which uses LIVC to suppress knock.

Using a variable compression ratio (VCR) is a more ideal method, but the complex structure makes the cost increase significantly

[322]. However, FEV [323] has developed a VCR engine to suppress knock and improve fuel economy effectively.

### 5.2. Control strategy for super-knock

As reviewed in this article, there are two ways to avoid super-knock. One is to eliminate pre-ignition. The other is to decouple the shock wave and the heat release.

To suppress pre-ignition, the following factors should be established.

- 1) Oil intrusion: Oil intrusion into the combustion chamber can be reduced by using a larger chamfer piston edge [153], increased oil ring tension [224] or optimized ring orientation [324]. Use of a low volatility oil [153] and improved oil ventilation [197,324] are also helpful.
- 2) Oil/fuel mixing: Avoiding oil/fuel mixing in a gasoline direct injection engine can be achieved by adjusting the spray direction to reduce liner wall wetting, by employing a split injection strategy [153,204,325], or by adopting high tumble to enhance air motion [151] to reduce spray penetration.
- 3) Oil properties: Optimized oil formulations, including use of low calcium [152,324,326], Na [326], sulphated ash [227], and high ZnDTP [152] and MoDTC [147] oils.
- 4) Fuel properties: Optimized fuel formulation, including low aromatics [201,232], high ethanol addition [201], and low volatility [151,193,202].
- 5) Solid particles: Reduced flammable particles floating in the combustion chamber, including deposits [220,222], soot [204], and metal dusts [148] Fe, Cu, etc.
- 6) Combustion system: Optimized engine combustion systems to reduce end-of-compression temperatures by enriching the mixture or promoting gasoline evaporation via direct injection, or scavenging of the hot residual gas [214,327]

To suppress super-knock with a pre-ignition, the following factors should be established:

- 1) Adopting high octane fuels with higher laminar flame speeds, for example, gasoline/alcohol blends [3].
- 2) Optimized fuel formulations, including fuels with low aromatic content [149,201,202].
- 3) Decrease reactivity of the unburned mixture, by introducing cooler EGR [213], or ignition inhibitors as fuel additives, or even spraying water.
- 4) Increase mixture gradients by dual fuel direct injection to achieve fuel stratification [156].

Some practical solutions have been applied in gasoline engine production to control super-knock, and are summarized as follows:

#### 5.2.1. Cooled EGR

Besides suppression of conventional knock, engine tests indicate that light-to-moderate levels of EGR also dramatically suppresses super-knock.

EGR decreases the thermal load on the combustion chamber to suppress pre-ignition and then to suppress super-knock. Even adding small amounts of cooled EGR (6% or 10%) allows the reduction of super-knock frequency and intensity obviously, while also increasing BMEP, as shown in Fig. 39. Furthermore, under 10% EGR, it is possible to increase BMEP by 17% and thermal efficiency by 2% while decreasing super-knock frequency by 80%, when compared to the baseline without EGR [213].

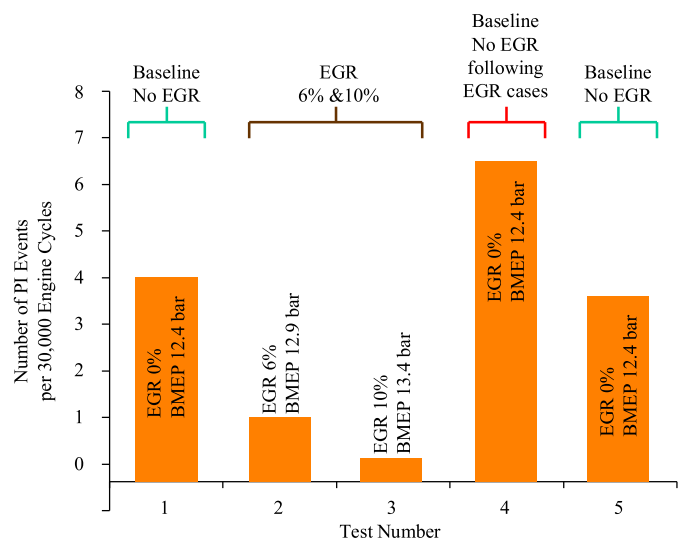


**Fig. 39.** LSPI (super-knock) frequency increase for non-EGR operation immediately following EGR test runs (adapted from [213]).

#### 5.2.2. Scavenging

Scavenging is a practical method for cooling combustion chamber walls. For boosted GDI engines, the scavenging process can be controlled using VVT technology.

The effectiveness of scavenging at high load for a turbocharged GDI engine under the conditions of stoichiometric [214] and lean [328] mixture combustion has been demonstrated using appropriate control of VVT parameters. It was also found that TGDI engines could be operated super-knock free, even when PI events were not eliminated completely. The pre-ignition cycles with scavenging were visualized using an endoscope [221]. It was found that scavenging has a positive effect to suppress pre-ignition. If some of the particles generated during the first pre-ignition cycle are not scavenged and remain inside the cylinder, the residual particles are heated during the subsequent combustion cycle and can induce the pre-ignition again.

#### 5.2.3. Injection strategy

The effects of injection strategies on super-knock have been comparatively investigated [116,204], as shown in Fig. 40. It was found that two-stage injections during the intake stroke (TSII, case 4) could eliminate super-knock due to a reduction of oil dilution via fuel impingement on the cylinder liner. In addition, fuel efficiency, exhaust temperature and emissions could be optimized by controlling the two injection timings, start of first injection (SOI1) and end of second injection (EOI2). The optimized injection strategy for a typical turbocharged gasoline direct injection engine is SOI1 in the middle of the intake stroke, EOI2 at the end of the intake stroke. If EOI2 occurs in the late compression stroke to form a stratified charge (Case 6), it decreased the super-knock frequency, but both fuel consumption and exhaust temperature increased. Obviously, this injection strategy is not suitable for long-term operation because of turbocharger durability considerations.

Mixture enrichment, stratification and scavenging strategies for super-knock suppression were also compared [204,328]. Mixture enrichment increased fuel consumption. Mixture stratification reduced super-knock frequency, but resulted in a remarkable increase of exhaust temperature. Scavenging by retarding the exhaust valve closing timing could suppress super-knock, but increase fuel consumption and CO emissions. TSII could eliminate super-knock while maintaining acceptable fuel consumption, emissions and exhaust temperatures. Thus, TSII has become a dominant injection strategy and has been widely applied in TC-GDI engine production in recent years [116,325]. More references about injection

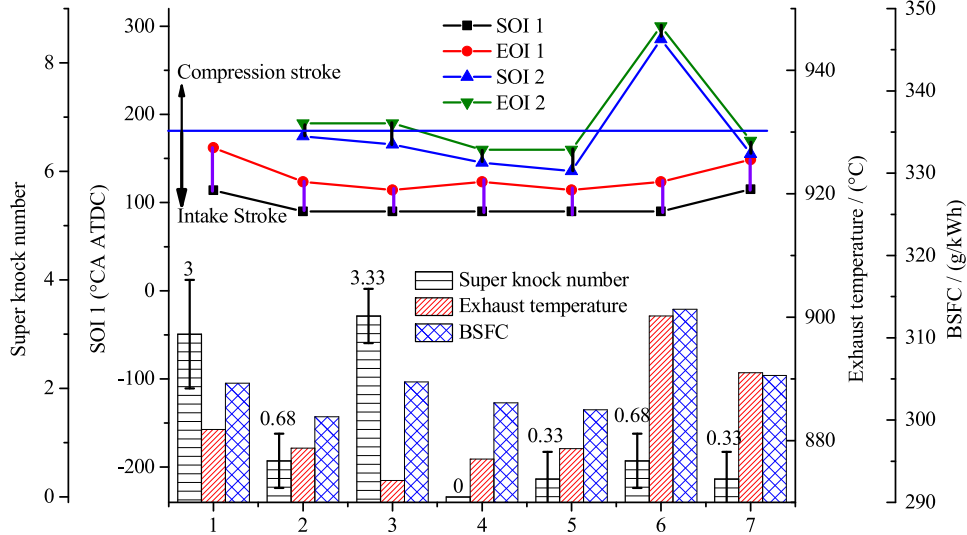


**Fig. 40.** Super-knock frequency, exhaust temperature and fuel consumption of different injection strategies (adapted from [116]) (Case 1: Homogeneous mode, Case 4: TSII mode, Case 6: stratified mode).

strategy effects on super-knock can be found in References [239,325,329–331].

#### 5.2.4. Integration of high tumble-high EGR-Atkinson/Miller cycle

To control both conventional knock and super-knock, several effective methods should be combined. Toyota recently developed a dedicated hybrid engine, the ESTEC 2ZR-FXE, for the fourth generation Prius. It is the first gasoline engine reported to achieve a maximum thermal efficiency of 40% [155]. Knocking combustion is successfully suppressed at full load with a geometrical compression ratio of 13. The main methods for improving combustion are the use of a high tumble ratio of 2.8, up to 25% EGR and a late IVC Atkinson cycle. Similar integration of EGR, the Miller cycle and a high compression ratio has been adopted to suppress pre-ignition and to improve fuel economy while realizing high load [324,332]. Experimental work was conducted in a four-cylinder turbocharged gasoline engine, with an additional supercharger to obtain higher boost pressures. The combustion strategy of a Miller cycle and low pressure EGR were studied and compared under a very high engine load condition, which can be seen in Fig. 41. An IMEPg of 3.0 MPa was achieved at 1500 rpm without pre-ignition using the Miller cycle concept. This result shows the possibility of further downsized engines in the near future.

## 6. Conclusions and future research directions

### 6.1. Conclusions

In summary, the knocking combustion research reviewed in this paper has revealed the following:

#### 6.1.1. Conventional knock

Knocking combustion in internal combustion engines is a phenomenon of pressure oscillations coupled with chemical kinetics, which originates from auto-ignition. High-speed optical diagnostics and advanced numerical simulations have been widely adopted to detect end-gas auto-ignition, intermediate combustion species, and pressure oscillations. It has been found that the in-cylinder local pressure is extremely uneven during the engine knocking process. Sequential auto-ignitions elevate the local pressure amplitude and form pressure waves. The pressure waves propagate and reflect from the chamber surfaces to generate pressure oscillations, which also enhance heat transfer due to the increased convective heat transfer associated with pressure oscillation-induced flows.

#### 6.1.2. Pre-ignition and super-knock

The occurrence of sporadic super-knock is a major obstacle in the development of advanced gasoline engines. Although pre-ignition is required for the occurrence of super-knock, pre-ignition does not always lead to super-knock. Pre-ignition could lead to super-knock, heavy knock, slight knock and non-knock. The knock intensity tends to increase with a knock onset that occurs near TDC.

A rapid compression machine is a suitable facility to investigate pre-ignition and super-knock under engine-like conditions with synchronous high-speed, high-resolution photography and pressure acquisition. In RCM experiments, super-knock was confirmed to be the result of detonation. The data reveal that the mechanism of pre-ignition to super-knock is due to a hotspot-induced deflagration transitioning to hotspot-induced detonation, followed by high-pressure oscillation.

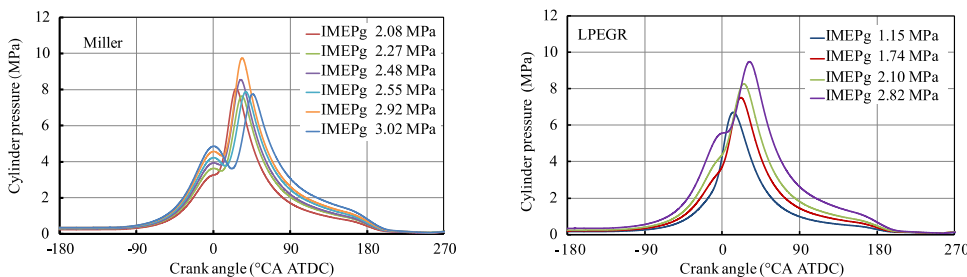


**Fig. 41.** Comparison of two concepts, p-θ diagram (adapted from [324]).

### 6.1.3. Knocking control strategies

SI engine fuel economy depends highly on mitigating knocking, and intensive experimental achievements have been used to control knock. Commonly used strategies include retarding spark timing, enriching the mixture, use of a high octane fuel, cooled EGR, cooled intake air, and enhancing turbulence in the combustion chamber. VVT, VGT and VCR have been applied in advanced gasoline engines with closed-loop control strategies. Thermal efficiency was further improved by more than 10% compared to current market engines (i.e., BTE from 35% to 40%). For gasoline direct injection engines, split injection is a promising knock suppression strategy to organize an optimal distribution of mixture concentration. A dual fuel spark ignition (DFSI) mode is useful for a moderate fuel stratification distribution. Combining PFI and GDI, the maximum achievable load exceeds 27 bar BMEP in production engines.

Eliminating pre-ignition is an effective approach to suppress super-knock. The main origins of pre-ignition include oil droplets and deposit particles. The composition and physicochemical properties of the fuel and oil seriously affect the frequency of occurrence of super-knock. It was found that oil additives have important effects on pre-ignition. CaSulfonate and NaSulfonate tend to promote pre-ignition, while the addition of ZnDDP and MoTDC tends to retard pre-ignition. Oil-induced pre-ignition and super-knock have a relatively greater probability to occur when the engine is highly boosted.

### 6.1.4. Combustion wave modes

Optical diagnostics have identified three end-gas combustion modes as no-autoignition, sequential autoignition, and detonation which appear under different initial conditions. The end-gas combustion mode is closely related to the mixture energy density in spite of temperature. As the mixture energy density increases, the end-gas combustion mode gradually transitions from no-autoignition to sequential autoignition, and then to detonation.

In a high temperature and high pressure closed combustion chamber, the local mixture auto-ignition generates a shock wave. Detonation initiations are usually associated with the shock wave. Shock wave reflection-induced detonation (SWRID) is the most frequently observed mode and the detonation is initiated near the wall because a local auto-ignition-generated shock wave is reflected by a concave cylinder wall. Before detonation is initiated the speed of the combustion wave front is less than that of a C-J detonation. Once the detonation is initiated, the speed of the combustion wave propagating in the unburned mixture is close to or exceeds the C-J detonation speed.

### 6.2. Future research directions

Over the past decade, great progress has been made in understanding knocking combustion and its characteristics. From the presented literature here it is inferred that there is scope for further research on knocking combustion, as listed below.

#### 6.2.1. Fundamental theory relating to knocking combustion

**Optical diagnostics of knocking combustion:** There are many influencing factors, including temperature stratification, random turbulence, shock wave compression and chemical reactivity, that serve to induce knocking combustion. However, a quantitative criterion for predicting knocking combustion is still unavailable. Thus, future directions for studying detonation initiation include: Utilizing modern optical diagnostics of PLIF and PIV spectra to detect intermediate species and combustion field details (temperature, pressure, and velocity distribution) during knocking combustion, identifying combustion wave modes, understanding shock wave propagation, reflection and intersection, and revealing the mechanism of deflagration-to-detonation transition under engine conditions.

**Single droplet and particle ignition in an ignitable mixture under high pressures:** To identify pre-ignition sources and to determine super-knock conditions, a RCM with optical accessibility is a suitable facility to investigate the phenomena under internal combustion engine conditions. It can not only be used to study auto-ignition combustion wave modes, but also to reveal the auto-ignition propensity of a single oil droplet or a particle in a stoichiometric gasoline-like fuel mixture. The effect of oil, additives, and fuel properties can be flexibly controlled to isolate the parameters that dominate under different thermodynamic conditions, including pressure, temperature and concentrations.

**Turbulence-shock-reaction interaction theory:** Detonations represent a highly nonlinear problem that couples turbulence, shock waves and chemical kinetics, and which involves strong discontinuities with multiple time and space scales. Its numerical simulation requires not only a high-resolution numerical scheme, but also requires treatment of numerical stiffness from multi-reaction time scales. Furthermore, the huge computational resources that are needed due to the high-resolution and large hydrocarbon fuel chemistry mechanism are unacceptable. Hence, it is essential to develop numerical methods with the ability to handle discontinuities and reaction stiffness, and auto-adaptive reaction mechanism reduction techniques and refined meshes for direct numerical simulation are needed.

#### 6.2.2. Detonation suppression and utilization

Super-knock is at present the major challenge for improving the power density in IC engines, not only for SI combustion, but also for HCCI combustion and dual fuel combustion if the premixed mixture concentration is high enough. A premixed charge is actually to some degree inhomogeneous in an engine combustion chamber, and this is likely to influence a developing detonation. There are two approaches to suppress super-knock. One is to eliminate pre-ignition sources, and the other is to avoid super-knock (detonation initiation). When a BMEP of up to 25 bar is desired in production engine, eliminating random pre-ignition becomes more-and-more of a challenge, and avoiding destructive detonation will be paid more attention. This may proceed by eliminating the transmission routes of shock waves, or by damping their amplitudes so as to suppress super-knock even with a pre-ignition (e.g., organizing a strong gradient of temperature and concentration, or introducing reaction inhibitors to prevent a shock wave coupled with heat release). Suppressing detonation prevents damage to the internal combustion engine, and the methods to be explored could also benefit industrial safety (e.g., preventing mine gas explosion and dust explosion accidents).

Since most detonations are initiated near the walls due to SWRID, a promising way to avoid super-knock is to remove radical species in the end gas near the walls. For instance, organizing pure air or EGR to be located at the periphery of the combustion chamber will help to avoid shock wave coupling with chemical kinetics near the wall. Or, organizing temporally-spatially distributed combustion, described as 1st stage combustion near walls, from burned gases without radicals such that the 2nd stage combustion occurs at the cylinder center.

Almost all existing knocking combustion studies focus on auto-ignition/detonation suppression, and the possibility of utilizing auto-ignition/detonation could be a future research direction. For instance, controllable HCCI is an example for utilizing lean mixture auto-ignition in internal combustion engines. Controlled detonation could be applied as for PDE/RDE (Pulse detonation engine or Rotary detonation engines) in the aerospace field. Some key scientific problems remain to be investigated, including detonation initiation. These problems include hotspot ignition, deflagration, sequential auto-ignition-detonation, detonation, and combustion mode

transition in ignitable mixtures over wide temperature and pressure ranges.

In order to suppress/utilize detonation, it is required to decouple/couple shock waves and reaction fronts. This may be accomplished by changing the amplitude and propagation direction of the shock wave via mixture stratification and reactivity distributions, or wall interactions. Such research will not only be helpful to improve the performance of internal combustion engines, but also may benefit the development of advanced aerospace engines.

### 6.2.3. Engine knock control and super-knock solution

Simulation works are effective to guide knock research and engine development in order to achieve high efficiency and high load operation. Utilizing a reduced surrogate fuel mechanism, a practical flame model and an accurate heat transfer model in 3D-CFD to capture auto-ignition ahead of the flame, will be helpful to evaluate knock intensity and optimize the combustion system in a spark-ignition engine.

Using direct injection of a second fuel, such as ethanol/methanol or gasoline blends, is an effective means to avoid knock in spark-ignited engines. Further study may focus on the dynamics of alcohol vaporization effects on the charge temperature of the unburned mixture at high loads above 25 bar BMEP.

Pre-ignition and super-knock will still be major obstacles for engine development in the next decades. For pre-ignition and super-knock suppression, two aspects should be paid close attention to: One is the properties of the lubricant oil and fuel, including their cleanliness, additives, laminar flame thickness, ignition delay, etc. The other concerns the engine design and optimization, including piston ring land structure, spray pattern, injection strategies, flow motion, sealing system, and cooling system, etc. To develop an effective solution, more research is necessary to clarify the detailed mechanisms of pre-ignition and super-knock, especially the role that oil droplets, fuel and deposits play in this process. With the understanding that future engine oil formulations will have to meet performance and durability requirements, besides suppressing pre-ignition, a critical balance must be maintained for a holistic solution. The effect of fuel properties, including olefin, aromatic, ethanol, and methanol content on pre-ignition and super-knock is also a productive future research direction.

Finally, integration of cooled EGR, Atkinson/Miller cycles and multi-stage boost is also a potential solution to achieve above 27 bar BMEP.

### Acknowledgments

This work was supported by the key project of National Natural Science Foundation of China (Grant No. 91541206: “Fundamental Investigation of Detonation Mode Transition and Control in Combustion Engines”). The authors gratefully acknowledge Dr. Yunliang Qi, Dr. Buyu Wang and Tanjin He for the useful discussion on near-wall detonation initiation, fuel chemistry and help on improving quality of figures. The authors also thanks to Prof. Xin He, Hongming Xu, Jianxin Wang and Shijin Shuai at Tsinghua University for the useful discussion on the paper structure.

### References

- [1] Heywood J. Internal combustion engine fundamentals. New York: McGraw-Hill Education; 1988.
- [2] Wang Z, Liu H, Song T, Qi Y, He X, Shuai S, et al. Relationship between super-knock and pre-ignition. *Int J Engine Res* 2015;16:166–80.
- [3] Kalghatgi GT. Developments in internal combustion engines and implications for combustion science and future transport fuels. *Proc Combust Inst* 2015;35:101–15.
- [4] Kalghatgi GT, Bradley D. Pre-ignition and ‘super-knock’ in turbo-charged spark-ignition engines. *Int J Engine Res* 2012;13:399–414.
- [5] Kim K, Zhang S, Salazar G, Jiang X. Design, fabrication and characterization of high temperature piezoelectric vibration sensor using YCOB crystals. *Sens Actuators A* 2012;178:40–8.
- [6] Pipitone E, D'Acquisto L. Development of a low-cost piezo film-based knock sensor. *Proc Inst Mech Eng Part D* 2003;217:691–9.
- [7] Klusacek S, Fialka J, Benes P, Havranek Z. An experimental study of temperature effect on material parameters of PZT ceramic ring used in knock sensors. In: Seventh International Conference on Sensing Technology (ICST); 2013. p. 863–8.
- [8] Cormier K, Isnard N, Disson JY, Mazoyer T, Fayet P. A multi sensors head gasket to detect and locate knock / last improvements. SAE Technical Paper 2008-36-0540, 2008.
- [9] Scholl D, Russ S, Stockhausen W. Detection of spark knock oscillations: dependence on combustion temperature. SAE Technical Paper 970038, 1997.
- [10] Giglio V, Police G, Rispoli N, di Gaeta A, Cecere M, Ragione LD. Experimental investigation on the use of ion current on SI engines for knock detection. SAE Technical Paper 2009-01-2745, 2009.
- [11] Carstens-Behrens S, Bohme JF. Fast knock detection using pattern signals. In: IEEE International Conference on Acoustics, Speech, and Signal Processing, 2001 Proceedings (ICASSP '01) 2001;5:3145–8.
- [12] Carstens-Behrens S, Wagner M, Bohme JF. Improved knock detection by time variant filtered structure-borne sound. In: IEEE International Conference on Acoustics, Speech, and Signal Processing, 1999 Proceedings 1999;4:2255–8.
- [13] Wang Y, Zhou L. Investigation of the detection of knock and misfire of a spark ignition engine with the ionic current method. *Proc Inst Mech Eng Part D* 2003;217:617–21.
- [14] Liu Z, Karim GA. Knock characteristics of dual-fuel engines fuelled with hydrogen fuel. *Int J Hydrogen Energy* 1995;20:919–24.
- [15] Ettefagh MM, Sadeghi MH, Piroupanah V, Arjmandi Tash H. Knock detection in spark ignition engines by vibration analysis of cylinder block: a parametric modeling approach. *Mech Syst Signal Process* 2008;22:1495–514.
- [16] Komachiya M, Sonobe H, Fumino T, Sakaguchi T, Kawakami K, Watanabe S, et al. Knocking detection of a gasoline engine by utilizing an optical fiber with specific refractive-index composition. *Appl Opt* 1998;37:1152–8.
- [17] Castagné M, Dumas JP, Henriot S, Lafossas FA, Mazoyer T. New knock localization methodology for SI engines. SAE Technical Paper 2003-01-1118, 2003.
- [18] Ollivier E, Bellettre J, Tazerout M. A non intrusive method for knock detection based on the exhaust gas temperature. SAE Technical Paper 2005-01-1129, 2005.
- [19] Mohammadpour J, Franchek M, Grigoriadis K. A survey on diagnostic methods for automotive engines. *Int J Engine Res* 2012;13:41–64.
- [20] Loubar K, Jrm Bellettre, Tazerout M. Unsteady heat transfer enhancement around an engine cylinder in order to detect knock. *J Heat Transf* 2005;127:278–5.
- [21] Borg JM, Cheok KC, Saikalis G, Oho S. Wavelet-based knock detection with fuzzy logic. *CIMSA 2005 IEEE international conference on computational intelligence for measurement systems and applications*; 2005. p. 26–31. 2005.
- [22] Nilsson Y, Frisk E, Nielsen L. Weak knock characterization and detection for knock control. *Proc Inst Mech Eng Part D* 2009;223:107–29.
- [23] Hettinger A, Kulzer A. A new method to detect knocking zones. *SAE Int J Engines* 2009;2:645–65.
- [24] Ortmann S, Rychetsky M, Glesner M, Groppo R, Tubetti P, Morra G. Engine knock estimation using neural networks based on a real-world database. SAE Technical Paper 980513, 1998.
- [25] Stotsky A. Frequency determination in control applications: excitation-based approach. *Proc Inst Mech Eng Part I* 2012;226:1142–8.
- [26] Boubal O, Oksman J. Knock acoustic signal estimation using parametric inversion. *IEEE Trans Instrum Meas* 2000;49:890–5.
- [27] Millo F, Ferraro CV. Knock in S.I. engines: a comparison between different techniques for detection and control. SAE Technical Paper 982477, 1998.
- [28] Molinaro F, Castané F. Signal processing pattern classification techniques to improve knock detection in spark ignition engines. *Mech Syst Signal Process* 1995;9:51–62.
- [29] Scholl D, Barash T, Russ S, Stockhausen W. Spectrogram analysis of accelerometer-based spark knock detection waveforms. SAE Technical Paper 972020, 1997.
- [30] Vulli S, Dunne JF, Potenza R, Richardson D, King P. Time-frequency analysis of single-point engine-block vibration measurements for multiple excitation-event identification. *J SoundVibr* 2009;321:1129–43.
- [31] Lezius U, Schultalbers M, Drewelow W, Lampe B. Improvements in knock control. In: MED '07 Mediterranean Conference on Control & Automation; 2007. p. 1–5.
- [32] Jones JCP, Spelina JM, Frey J. Likelihood-based control of engine knock. *IEEE Trans Control Syst Technol* 2013;21:2169–80.
- [33] Zurbriggen F, Ott T, Onder C, Guzzella L. Optimal control of the heat release rate of an internal combustion engine with pressure gradient, maximum pressure, and knock constraints. *J Dyn Syst Meas Control* 2014;136:061006.
- [34] Ham YY, Chun KM, Lee JH, Chang KS. Spark-ignition engine knock control and threshold value determination. SAE Technical Paper 960496, 1996.
- [35] Luo W, Chen B, Naber J, Glugla C. Stochastic knock detection, control, software integration, and evaluation on a V6 spark-ignition engine under steady-state operation. SAE Technical Paper 2014-01-1358, 2014.
- [36] Spelina JM, Peyton Jones JC, Frey J. Stochastic simulation and analysis of a classical knock controller. *Int J Engine Res* 2015;16:461–73.
- [37] Baik SH, Chun KM. A study on the transient knock control in a spark-ignition engine. SAE Technical Paper 981062, 1998.

- [38] Mangeruca L, Ferrari A, Sangiovanni-Vincentelli A, Pierantoni A, Pennese M. System level design of embedded controllers: knock detection, a case study in the automotive domain. Design, automation and test in Europe conference and exhibition; 2003. p. 232–7. 2003suppl.
- [39] Thomasson A, Eriksson L, Lindell T, Jones JCP, Spelina J, Frey J. Tuning and experimental evaluation of a likelihood-based engine knock controller. 52nd IEEE conference on decision and control; 2013. p. 6849–54.
- [40] Beccari S, Pipitone E, Gencchi G. Calibration of a knock prediction model for the combustion of gasoline-LPG mixtures in spark ignition engines. *Combust Sci Technol* 2015;187:721–38.
- [41] Misdaris A, Vermorel O, Poinsot T. LES of knocking in engines using dual heat transfer and two-step reduced schemes. *Combust Flame* 2015;162:4304–12.
- [42] Lecocq G, Richard S, Michel J-B, Vervisch L. A new LES model coupling flame surface density and tabulated kinetics approaches to investigate knock and pre-ignition in piston engines. *Proc Combust Inst* 2011;33:3105–14.
- [43] Chen L, Li T, Yin T, Zheng B. A predictive model for knock onset in spark-ignition engines with cooled EGR. *Energy Convers Manage* 2014;87:946–55.
- [44] Linse D, Kleemann A, Hasse C. Probability density function approach coupled with detailed chemical kinetics for the prediction of knock in turbocharged direct injection spark ignition engines. *Combust Flame* 2014;161:997–1014.
- [45] Sileghem L, Wallner T, Verhelst S. A quasi-dimensional model for SI engines fueled with gasoline–alcohol blends: knock modeling. *Fuel* 2015;140:217–26.
- [46] Richard S, Bougrine S, Font C, Lafossas FA, Le Berr F. Réduction d'un modèle de combustion 3D en vue d'obtenir un modèle 0D physique permettant de simuler le dégagement d'énergie, le cliquetis et les émissions de polluants des moteurs à allumage commandé. *Oil Gas Sci Technol - Rev IFP* 2009;64:223–42.
- [47] Pipitone E, Beccari S, Gencchi G. A refined model for knock onset prediction in spark ignition engines fueled with mixtures of gasoline and propane. *J Eng Gas Turbines Power* 2015;137:111501.
- [48] Liu Z, Chen R. A zero-dimensional combustion model with reduced kinetics for SI engine knock simulation. *Combust Sci Technol* 2009;181:828–52.
- [49] Vancollie J, Sileghem L, Verhelst S. Development and validation of a quasi-dimensional model for methanol and ethanol fueled SI engines. *Appl Energy* 2014;132:412–25.
- [50] Yao A, Xu H, Yao C. Analysis of pressure waves in the cone-type combustion chamber under SI engine knock. *Energy Convers Manage* 2015;96:146–58.
- [51] Wei H, Shang Y, Chen C, Gao D, Feng D. A numerical study on pressure wave-induced end gas auto-ignition near top dead center of a downsized spark ignition engine. *Int J Hydrogen Energy* 2014;39:21265–74.
- [52] Di Gaeta A, Giglio V, Police G, Rispoli N. Modeling of in-cylinder pressure oscillations under knocking conditions: a general approach based on the damped wave equation. *Fuel* 2013;104:230–43.
- [53] Wei H, Wei J, Shu G. Calculation on cylinder pressure fluctuation by using the wave equation in KIVA program. *Chin J Mech Eng* 2012;25:362–9.
- [54] Liang L. Multidimensional modeling of combustion and knock in spark ignition engines with detailed chemical kinetics. University of Wisconsin-Madison; 2006.
- [55] Liang L, Reitz RD, Iyer CO, Yi J. Modeling knock in spark-ignition engines using a G-equation combustion model incorporating detailed chemical kinetics. *SAE Technical Paper* 2007-01-0165, 2007.
- [56] Robert A, Richard S, Colin O, Poinsot T. LES study of deflagration to detonation mechanisms in a downsized spark ignition engine. *Combust Flame* 2015;162: 2788–807.
- [57] Fontanesi S, d'Adamo A, Rutland CJ. Large-eddy simulation analysis of spark configuration effect on cycle-to-cycle variability of combustion and knock. *Int J Engine Res* 2015;16:403–18.
- [58] Robert A, Richard S, Colin O, Martinez L, De Francqueville L. LES prediction and analysis of knocking combustion in a spark ignition engine. *Proc Combust Inst* 2015;35:2941–8.
- [59] Zhen X, Wang Y, Zhu Y. Study of knock in a high compression ratio SI methanol engine using LES with detailed chemical kinetics. *Energy Convers Manage* 2013;75:523–31.
- [60] Richard S, Dulbecko A, Angelberger C, Truffin K. Development of a one-dimensional computational fluid dynamics modeling approach to predict cycle-to-cycle variability in spark-ignition engines based on physical understanding acquired from large-eddy simulation. *Int J Engine Res* 2014.
- [61] Seok Kwon O, Lim OT. Effect of boost pressure on thermal stratification in HCCI engine using the multi-zone model. *J Mech Sci Technol* 2010;24:399–406.
- [62] Shivapuri AM, Dasappa S. Experiments and zero D modeling studies using specific Wiebe coefficients for producer gas as fuel in spark-ignited engines. *Proc Inst Mech Eng Part C* 2013;227:504–19.
- [63] Liberman MA, Ivanov MF, Valiev DM, Eriksson LE. Hot spot formation by the propagating flame and the influence of EGR on knock occurrence in SI engines. *Combust Sci Technol* 2006;178:1613–47.
- [64] Lee Y, Pae S, Min K, Kim ES. Prediction of knock onset and the autoignition site in spark-ignition engines. *Proc Inst Mech Eng Part D* 2000;214:751–63.
- [65] Lee J, Lee Y, Huh KY, Kwon H, Park JI. Quasi-dimensional analysis of combustion, emissions and knocking in a homogeneous GDI engine. *Int J Automot Technol* 2015;16:877–83.
- [66] Zhen X, Wang Y, Xu S, Zhu Y. Study of knock in a high compression ratio spark-ignition methanol engine by multi-dimensional simulation. *Energy* 2013;50: 150–9.
- [67] Bozza F, Siano D, Costa M. Heat transfer, knock modeling and cyclic variability in a “downsized” spark-ignition turbocharged engine. *Adv Appl Math Mech* 2011;3:310–26.
- [68] Rostampour A, Toosi AN. Numerical investigation of the effect of knock on heat transfer in a turbocharged spark ignition engine. *J Eng Gas Turbines Power* 2015;137:121502.
- [69] Han Z, Reitz RD. A temperature wall function formulation for variable-density turbulent flows with application to engine convective heat transfer modeling. *Int J Heat Mass Transf* 1997;40:613–25.
- [70] Wang Z, Wang Y, Reitz RD. Pressure oscillation and chemical kinetics coupling during knock processes in gasoline engine combustion. *Energy Fuels* 2012;26:7107–19.
- [71] Holly WE, Lauer T, Schuemie HA, Murakami S. Prediction of the knocking combustion and NOx formation for fuel gases with different methane numbers. *Int J Engine Res* 2016;17:35–43.
- [72] Rakopoulos CD, Michos CN. Development and validation of a multi-zone combustion model for performance and nitric oxide formation in syngas fueled spark ignition engine. *Energy Convers Manage* 2008;49:2924–38.
- [73] Dahl D, Andersson M, Denbratt I. The origin of pressure waves in high load HCCI combustion: a high-speed video analysis. *Combust Sci Technol* 2011;183: 1266–81.
- [74] Katsumata M, Morikawa K, Tanabe M. Behavior of shock wave and pressure wave of SI knocking with super rapid compression machine. *SAE Technical Paper* 2011-01-1875, 2011.
- [75] Kawahara N, Tomita E. Visualization of auto-ignition and pressure wave during knocking in a hydrogen spark-ignition engine. *Int J Hydrogen Energy* 2009;34:3156–63.
- [76] He X, Qi Y, Wang Z, Wang J, Shuai S, Tao L. Visualization of the mode shapes of pressure oscillation in a cylindrical cavity. *Combust Sci Technol* 2015;187: 1610–9.
- [77] Wang Z, Qi YL, He X, Wang JX, Shuai SJ, Law CK. Analysis of pre-ignition to super-knock: hotspot-induced deflagration to detonation. *Fuel* 2015;144:222–7.
- [78] Qi Y, Wang Z, Wang J, He X. Effects of thermodynamic conditions on the end gas combustion mode associated with engine knock. *Combust Flame* 2015;162:4119–28.
- [79] Merola SS, Sementa P, Tornatore C, Vaglieco BM. Optical investigations of the abnormal combustion in a boosted spark-ignition PFI engine. *SAE Int J Engines* 2009;2:632–44.
- [80] Pöschl M, Sattelmayer T. Influence of temperature inhomogeneities on knocking combustion. *Combust Flame* 2008;153:562–73.
- [81] Spicher U, Kröger H, Ganser J. Detection of knocking combustion using simultaneously high-speed Schlieren cinematography and multi optical fiber technique. *SAE Technical Paper* 912312, 1991.
- [82] Konig G, Sheppard CGW. End gas autoignition and knock in a spark ignition engine. *SAE Technical Paper* 902135, 1990.
- [83] Miller CD. Roles of detonation waves and autoignition in spark - ignition engine knock as shown by photographs taken at 40,000 and 200,000 frames per sec. *SAE Technical Paper* 470207, 1947.
- [84] Schießl R, Dreizler A, Maas U, Grant AJ, Ewart P. Double-pulse PLIF imaging of self-ignition centers in an SI engine. *SAE Technical Paper* 2001-01-1925, 2001.
- [85] Merola SS, Vaglieco BM. Knock investigation by flame and radical species detection in spark ignition engine for different fuels. *Energy Convers Manage* 2007;48:2897–910.
- [86] Ma X, Wang Z, Jiang C, Jiang Y, Xu H, Wang J. An optical study of in-cylinder CH<sub>2</sub>O and OH chemiluminescence in flame-induced reaction front propagation using high speed imaging. *Fuel* 2014;134:603–10.
- [87] Schießl R, Maas U. Analysis of endgas temperature fluctuations in an si engine by laser-induced fluorescence. *Combust Flame* 2003;133:19–27.
- [88] Kawahara N, Tomita E, Ohnishi K, Goto K. In-situ unburned gas temperature measurement in a spark ignition engine using laser interferometry. *SAE Technical Paper* 2005-01-0646, 2005.
- [89] Bood J, Bengtsson P-E, Mauss F, Burgdorf K, Denbratt I. Knock in spark-ignition engines: end-gas temperature measurements using rotational CARS and detailed kinetic calculations of the autoignition process. *SAE Technical Paper* 971669, 1997.
- [90] Suzuki R, Shoji H, Yoshida K, Iijima A. Analysis of knocking in an SI engine based on in-cylinder: spectroscopic measurements and visualization. *SAE Technical Paper* 2010-32-0092, 2010.
- [91] Hernández JJ, Lapuerta M, Sanz-Argent J. Autoignition prediction capability of the Livengood–Wu correlation applied to fuels of commercial interest. *Int J Engine Res* 2014;15:817–29.
- [92] Livengood JC, Wu PC. Correlation of autoignition phenomena in internal combustion engines and rapid compression machines. *Symposium (International) on combustion*, 5; 1955. p. 347–56.
- [93] Pan J, Zhao P, Law CK, Wei H. A predictive Livengood–Wu correlation for two-stage ignition. *Int J Engine Res* 2015.
- [94] Kurtz MD, Regele JD. Acoustic timescale characterisation of a one-dimensional model hot spot. *Combust Theory Modell* 2014;18:532–51.
- [95] Rudloff J, Zaccardi JM, Richard S, Anderlohr JM. Analysis of pre-ignition in highly charged SI engines: emphasis on the auto-ignition mode. *Proc Combust Inst* 2013;34:2959–67.
- [96] Qi C, Dai P, Yu H, Chen Z. Different modes of reaction front propagation in n-heptane/air mixture with concentration non-uniformity. *Proc Combust Inst* 2017;36:3633–41.
- [97] Misdaris A, Vermorel O, Poinsot T. A methodology based on reduced schemes to compute autoignition and propagation in internal combustion engines. *Proc Combust Inst* 2015;35:3001–8.
- [98] Gu XJ, Emerson DR, Bradley D. Modes of reaction front propagation from hot spots. *Combust Flame* 2003;133:63–74.

- [99] Dai P, Chen Z, Chen SY, Ju YG. Numerical experiments on reaction front propagation in n-heptane/air mixture with temperature gradient. *Proc Combust Inst* 2015;35:3045–52.
- [100] D'Anna A, Mercoguano R, Barbella R, Ciajolo A. Low temperature oxidation chemistry of iso-octane under high pressure conditions. *Combust Sci Technol* 1992;83:217–32.
- [101] Curran HJ, Pitz WJ, Westbrook CK, Callahan GV, Dryer FL. Oxidation of automotive primary reference fuels at elevated pressures. *Symposium (International) on combustion*, 27; 1998. p. 379–87.
- [102] Pan J, Shu G, Zhao P, Wei H, Chen Z. Interactions of flame propagation, autoignition and pressure wave during knocking combustion. *Combust Flame* 2016;164:319–28.
- [103] Boubal O, Oksman J. Knock acoustic signal estimation using parametric inversion. *Instrumentation and measurement technology conference, 1999 IMTC/99 proceedings of the 16th IEEE*, 3; 1999.
- [104] Qi Y, He X, Wang Z, Wang J. Frequency domain analysis of knock images. *Meas Sci Technol* 2014;25:125001.
- [105] Yang F, Zhang H, Chen Z, Kong W. Interaction of pressure wave and propagating flame during knock. *Int J Hydrogen Energy* 2013;38:15510–9.
- [106] Irimescu A, Merola SS, Tornatore C, Valentino G. Development of a semi-empirical convective heat transfer correlation based on thermodynamic and optical measurements in a spark ignition engine. *Appl Energy* 2015;157:777–88.
- [107] Attard WP, Toulson E, Watson H, Hamori F. Abnormal combustion including mega knock in a 60% downsized highly turbocharged PFI engine. *SAE Technical Paper* 2010-01-1456, 2010.
- [108] Duarte J, Amador G, Garcia J, Fontalvo A, Vasquez Padilla R, Sanjuan M, et al. Auto-ignition control in turbocharged internal combustion engines operating with gaseous fuels. *Energy* 2014;71:137–47.
- [109] Wang Z, Liu H, Long Y, Wang J, He X. Comparative study on alcohols–gasoline and gasoline–alcohols dual-fuel spark ignition (DFSI) combustion for high load extension and high fuel efficiency. *Energy* 2015;82:395–405.
- [110] Luisi S, Doria V, Stroppiana A, Millo F, Mirzaeian M. Experimental investigation on early and late intake valve closures for knock mitigation through Miller cycle in a downsized turbocharged engine. *SAE Technical Paper* 2015-01-0760, 2015.
- [111] Y-I Bai, J-x Wang, Wang Z, Shuai S-j. Knocking suppression by stratified stoichiometric mixture with two-zone homogeneity in a DISI engine. *J Eng Gas Turbines Power* 2012;135:012803.
- [112] Costa M, Sementa P, Sorge U, Catapano F, Marseglia G, Vaglieco BM. Split injection in a GDI engine under knock conditions: an experimental and numerical investigation. *SAE Technical Paper* 2015-24-2432, 2015.
- [113] Hoppe F, Thewes M, Baumgarten H, Dohmen J. Water injection for gasoline engines: potentials, challenges, and solutions. *Int J Engine Res* 2016;17:86–96.
- [114] Liu H, Wang Z, Wang J, Wang M, Yang W. Controlled SSCI with moderate end-gas auto-ignition for fuel economy improvement and knock suppression. *J Eng Gas Turbines Power* 2015;137:101508.
- [115] Potteau S, Lutz P, Leroux S, Moroz S, Tomas E. Cooled EGR for a turbo SI engine to reduce knocking and fuel consumption. *SAE Technical Paper* 2007-01-3978, 2007.
- [116] Wang Z, Liu H, Song T, Xu Y, Wang J-X, Li D-S, et al. Investigation on pre-ignition and super-knock in highly boosted gasoline direct injection engines. *SAE Technical Paper* 2014-01-1212, 2014.
- [117] Dahnz C, Spicher U. Irregular combustion in supercharged spark ignition engines – pre-ignition and other phenomena. *Int J Engine Res* 2010;11:485–98.
- [118] Grandin B, Ångström H-E, Stålhammar P, Olofsson E. Knock suppression in a turbocharged SI engine by using cooled EGR. *SAE Technical Paper* 982476, 1998.
- [119] Zaccardi J-M, Escudié D. Overview of the main mechanisms triggering low-speed pre-ignition in spark-ignition engines. *Int J Engine Res* 2015;16:152–65.
- [120] Li Y, Zhao H, Leach B, Ma T. Development of a fuel stratification spark ignition engine. *Proc Inst Mech Eng Part D* 2005;219:923–34.
- [121] Yeom K, Bae C. Stratified liquefied petroleum gas–dimethyl ether compression ignition engine combustion at various intake valve open timings. *Int J Engine Res* 2010;11:187–97.
- [122] Laget O, Richard S, Serrano D, Soleri D. Combining experimental and numerical investigations to explore the potential of downsized engines operating with methane/hydrogen blends. *Int J Hydrogen Energy* 2012;37:11514–30.
- [123] Chintala V, Subramanian KA. Experimental investigations on effect of different compression ratios on enhancement of maximum hydrogen energy share in a compression ignition engine under dual-fuel mode. *Energy* 2015;87:448–62.
- [124] Teodosio L, De Bellis V, Bozza F. Fuel economy improvement and knock tendency reduction of a downsized turbocharged engine at full load operations through a low-pressure EGR system. *SAE Int J Engines* 2015;8:1508–19.
- [125] Dalla Nora M, Zhao H. High load performance and combustion analysis of a four-valve direct injection gasoline engine running in the two-stroke cycle. *Appl Energy* 2015;159:117–31.
- [126] Vavra J, Bohac SV, Manofsky L, Lavoie G, Assanis D. Knock in various combustion modes in a gasoline-fueled automotive engine. *J Eng Gas Turbines Power* 2012;134:082807.
- [127] Li T, Gao Y, Wang J, Chen Z. The Miller cycle effects on improvement of fuel economy in a highly boosted, high compression ratio, direct-injection gasoline engine: EIVC vs. LIVC. *Energy Convers Manage* 2014;79:59–65.
- [128] Kim N, Cho S, Min K. A study on the combustion and emission characteristics of an SI engine under full load conditions with ethanol port injection and gasoline direct injection. *Fuel* 2015;158:725–32.
- [129] Alger T, Mangold B, Roberts C, Gingrich J. The interaction of fuel anti-knock index and cooled EGR on engine performance and efficiency. *SAE Int J Engines* 2012;5:1229–41.
- [130] Bade Shrestha SO, Rodrigues R. Effects of diluents on knock rating of gaseous fuels. *Proc Inst Mech Eng Part A* 2008;222:587–97.
- [131] Bradley D, Head RA. Engine autoignition: the relationship between octane numbers and autoignition delay times. *Combust Flame* 2006;147:171–84.
- [132] Cerri T, D'Errico G, Onorati A. Experimental investigations on high octane number gasoline formulations for internal combustion engines. *Fuel* 2013;111:305–15.
- [133] Rahmouni C, Brecq G, Tazerout M, Le Corre O. Knock rating of gaseous fuels in a single cylinder spark ignition engine. *Fuel* 2004;83:327–36.
- [134] Rankovic N, Bourhis G, Loos M, Dauphin R. Understanding octane number evolution for enabling alternative low RON refinery streams and octane boosters as transportation fuels. *Fuel* 2015;150:41–7.
- [135] Splitter DA, Szymbist JP. Experimental investigation of spark-ignited combustion with high-octane biofuels and EGR. 2. Fuel and EGR effects on knock-limited load and speed. *Energy Fuels* 2014;28:1432–45.
- [136] Haas FM, Chaos M, Dryer FL. Low and intermediate temperature oxidation of ethanol and ethanol–PRF blends: an experimental and modeling study. *Combust Flame* 2009;156:2346–50.
- [137] Gersen S, van Essen M, van Dijk G, Levinsky H. Physicochemical effects of varying fuel composition on knock characteristics of natural gas mixtures. *Combust Flame* 2014;161:2729–37.
- [138] Moore NPW, Roy BN. Studies of autoignition and knock with propane as an engine fuel. *Combust Flame* 1959;3:421–35.
- [139] Rothamer DA, Jennings JH. Study of the knocking propensity of 2,5-dimethylfuran–gasoline and ethanol–gasoline blends. *Fuel* 2012;98:203–12.
- [140] Morganti KJ, Brear MJ, da Silva G, Yang Y, Dryer FL. The autoignition of liquefied petroleum gas (LPG) in spark-ignition engines. *Proc Combust Inst* 2015;35:2933–40.
- [141] Bradley D. Combustion and the design of future engine fuels. *Proc Inst Mech Eng Part C* 2009;223:2751–65.
- [142] Qiao X, Hou J, Wang Z, Zhou J, Huang Z. Knock investigation of a direct injection–homogeneous charge compression ignition engine fueled with dimethyl ether and liquefied petroleum gas. *Energy Fuels* 2009;23:2006–12.
- [143] Liu H, Wang Z, Long Y, Wang J. Dual-fuel spark ignition (DFSI) combustion fuelled with different alcohols and gasoline for fuel efficiency. *Fuel* 2015;157:255–60.
- [144] Liu H, Wang Z, Long Y, Xiang S, Wang J, Wagnon SW. Methanol–gasoline dual-fuel spark ignition (DFSI) combustion with dual-injection for engine particle number (PN) reduction and fuel economy improvement. *Energy* 2015;89:1010–7.
- [145] Mack JH, Rapp VH, Broeckelmann M, Lee TS, Dibble RW. Investigation of biofuels from microorganism metabolism for use as anti-knock additives. *Fuel* 2014;117(Part B):939–43.
- [146] Dagaur P, Koch R, Cathonnet M. The oxidation of N-heptane in the presence of oxygenated octane improvers: MTBE and ETBE. *Combust Sci Technol* 1997;122:345–61.
- [147] Fujimoto K, Yamashita M, Hirano S, Kato K, Watanabe I, Ito K. Engine oil development for preventing pre-ignition in turbocharged gasoline engine. *SAE Int J Fuels Lubr* 2014;7:869–74.
- [148] Hirano S, Yamashita M, Fujimoto K, Kato K. Investigation of engine oil effect on abnormal combustion in turbocharged direct injection – spark ignition engines (part 2). *SAE Technical Paper* 2013-01-2569, 2013.
- [149] Long Y, Wang Z, Qi Y, Xiang S, Zeng G, Zhang P, et al. Effect of oil and gasoline properties on pre-ignition and super-knock in a thermal research engine (TRE) and an optical rapid compression machine (RCM). *SAE Technical Paper* 2016-01-0720, 2016.
- [150] Miyasaka T, Miura K, Hayakawa N, Ishino T, Iijima A, Shoji H, et al. A study on the effect of a calcium-based engine oil additive on abnormal SI engine combustion. *SAE Int J Engines* 2014;8:206–13.
- [151] Palaveev S, Magar M, Kubach H, Schiessl R, Spicher U, Maas U. Premature flame initiation in a turbocharged DISI engine – numerical and experimental investigations. *SAE Int J Engines* 2013;6:54–66.
- [152] Takeuchi K, Fujimoto K, Hirano S, Yamashita M. Investigation of engine oil effect on abnormal combustion in turbocharged direct injection – spark ignition engines. *SAE Int J Fuels Lubr* 2012;5:1017–24.
- [153] Zahdeh A, Rothenberger P, Nguyen W, Anbarasu M, Schmuck-Soldan S, Schaefer J, et al. Fundamental approach to investigate pre-ignition in boosted SI engines. *SAE Int J Engines* 2011;4:246–73.
- [154] Affleck WS, Fish A. Knock: flame acceleration or spontaneous ignition? *Combust Flame* 1968;12:243–52.
- [155] Matsuo S, Ikeda E, Ito Y, Nishiura H. The new Toyota inline 4 cylinder 1.8L ESTEC 2ZR-FXE gasoline engine for hybrid car. *SAE Technical Paper* 2016-01-0684, 2016.
- [156] Stein RA, House CJ, Leone TG. Optimal use of E85 in a turbocharged direct injection engine. *SAE Int J Fuels Lubr* 2009;2:670–82.
- [157] He X, Donovan MT, Zigler BT, Palmer TR, Walton SM, Wooldridge MS, et al. An experimental and modeling study of iso-octane ignition delay times under homogeneous charge compression ignition conditions. *Combust Flame* 2005;142:266–75.

- [158] Amann M, Alger T. Lubricant reactivity effects on gasoline spark ignition engine knock. *SAE Int J Fuels Lubr* 2012;5:760–71.
- [159] ASTM International. Annual book of ASTM standards 05.01–05.05. PA: West Conshohocken; 2012.
- [160] Mehl M, Chen JY, Pitz WJ, Sarathy SM, Westbrook CK. An approach for formulating surrogates for gasoline with application toward a reduced surrogate mechanism for CFD engine modeling. *Energy Fuels* 2011;25:5215–23.
- [161] Kalghatgi GT. Fuel anti-knock quality- part II. Vehicle studies - how relevant is motor octane number (MON) in modern engines? SAE Technical Paper 2001-01-3585, 2001.
- [162] Kalghatgi GT. Fuel anti-knock quality - part I. Engine studies. SAE Technical Paper 2001-01-3584, 2001.
- [163] Mittal V, Heywood JB. The relevance of fuel RON and MON to knock onset in modern SI engines. SAE Technical Paper 2008-01-2414, 2008.
- [164] Kalghatgi GT, Nakata K, Mogi K. Octane appetite studies in direct injection spark ignition (DISI) engines. SAE Technical Paper 2005-01-0244, 2005.
- [165] Kalghatgi GT. Auto-ignition quality of practical fuels and implications for fuel requirements of future SI and HCCI engines. SAE Technical Paper 2005-01-0239, 2005.
- [166] Orlebar CN, Joedicke A, Studzinski W. The effects of octane, sensitivity and K on the performance and fuel economy of a direct injection spark ignition vehicle. SAE Technical Paper 2014-01-1216, 2014.
- [167] Mittal V, Heywood JB. The shift in relevance of fuel RON and MON to knock onset in modern SI engines over the last 70 years. *SAE Int J Engines* 2009;2:1–10.
- [168] Remmert S, Campbell S, Cracknell R, Schuetze A, Lewis A, Giles K, et al. Octane appetite: the relevance of a lower limit to the MON specification in a down-sized, highly boosted DISI engine. *SAE Int J Fuels Lubr* 2014;7:743–55.
- [169] Kalghatgi G, Risberg P, Angstrom H-E. A method of defining ignition quality of fuels in HCCI engines. SAE Technical Paper 2003-01-1816, 2003.
- [170] Risberg P, Kalghatgi G, Angstrom H-E. Auto-ignition quality of gasoline-like fuels in HCCI engines. SAE Technical Paper 2003-01-3215, 2003.
- [171] Kalghatgi GT, Head RA. The available and required autoignition quality of gasoline - like fuels in HCCI engines at high temperatures. SAE Technical Paper 2004-01-1969, 2004.
- [172] Boot MD, Tian M, Hensen EJM, Mani Sarathy S. Impact of fuel molecular structure on auto-ignition behavior – design rules for future high performance gasolines. *Prog Energy Combust Sci* 2017;60:1–25.
- [173] ASTM. Standard test method for research octane number of spark-ignition engine fuel. ASTM D2699-16, 2016.
- [174] ASTM. Standard test method for motor octane number of spark-ignition engine fuel. ASTM D2700-16a, 2016.
- [175] Amer A, Babiker H, Chang J, Kalghatgi G, Adomeit P, Brassat A, et al. Fuel effects on knock in a highly boosted direct injection spark ignition engine. *SAE Int J Fuels Lubr* 2012;5:1048–65.
- [176] Zádor J, Taatjes CA, Fernandes RX. Kinetics of elementary reactions in low-temperature autoignition chemistry. *Prog Energy Combust Sci* 2011;37:371–421.
- [177] Ciecki HK, Adomeit G. Shock-tube investigation of self-ignition of n-heptane-air mixtures under engine relevant conditions. *Combust Flame* 1993;93:421–33.
- [178] Bugler J, Marks B, Mathieu O, Archuleta R, Camou A, Grégoire C, et al. An ignition delay time and chemical kinetic modeling study of the pentane isomers. *Combust Flame* 2016;163:138–56.
- [179] Zhang P, Ji W, He T, He X, Wang Z, Yang B, et al. First-stage ignition delay in the negative temperature coefficient behavior: experiment and simulation. *Combust Flame* 2016;167:14–23.
- [180] Ji W, Zhao P, He T, He X, Farooq A, Law CK. On the controlling mechanism of the upper turnover states in the NTC regime. *Combust Flame* 2016;164:294–302.
- [181] Martz JB, Lavoie GA, Im HG, Middleton RJ, Babajimopoulos A, Assanis DN. The propagation of a laminar reaction front during end-gas auto-ignition. *Combust Flame* 2012;159:2077–86.
- [182] Kawahara N, Tomita E, Sakata Y. Auto-ignited kernels during knocking combustion in a spark-ignition engine. *Proc Combust Inst* 2007;31:2999–3006.
- [183] Pan J, Sheppard CGW, Tindall A, Berzins M, Pennington SV, Ware JM. End gas inhomogeneity, autoignition and knock. SAE Technical Paper 982616, 1998.
- [184] Dowling AP, Stow SR. Acoustic analysis of gas turbine combustors. *J Propul Power* 2003;19:751–64.
- [185] Keller JJ. Thermoacoustic oscillations in combustion chambers of gas turbines. *AIAA J* 1995;33:2280–7.
- [186] Draper CS. Pressure waves accompanying detonation in the internal combustion engine. *J Aeronaut Sci (Inst Aeronaut Sci)* 1938;5:219–26.
- [187] Wang Z, Shuai S, Wang B. Simulation and experiments of advanced gasoline engine combustion modes from spark ignition to compression ignition. *Int J Powertrains* 2016.
- [188] Yi J, Wooldridge S, Coulson G, Hilditch J, Iyer CO, Moilanen P, et al. Development and optimization of the Ford 3.5L V6 EcoBoost combustion system. *SAE Int J Engines* 2009;2:1388–407.
- [189] Kalghatgi G, Bradley D, Andrae J, Harrison AJ. The nature of 'super knock' and its origins in SI engines. In: IMechE conference on internal combustion engines: performance, fuel economy and emissions; 2009.
- [190] Prochazka G, Hofmann P, Geringer B, Willand J, Jelitto C, Schafer O. Autoignition on a highly supercharged gasoline engine and preventive measures. In: 26th international Vienna motor symposium; 2005.
- [191] Winklhofer E, Hirsch A, Kapus P, Kortschak M, Philipp H. TC GDI engines at very high power density? Irregular combustion and thermal risk. SAE Technical Paper 2009-24-0056, 2009.
- [192] Amann M, Alger T, Mehta D. The effect of EGR on low-speed pre-ignition in boosted SI engines. *SAE Int J Engines* 2011;4:235–45.
- [193] Chapman E, Davis R, Studzinski W, Geng P. Fuel octane and volatility effects on the stochastic pre-ignition behavior of a 2.0L gasoline turbocharged DI engine. *SAE Int J Fuels Lubr* 2014;7:379–89.
- [194] Bradley D, Morley C, Gu XJ, Emerson DR. Amplified pressure waves during auto-ignition: relevance to CAI engines. SAE Technical Paper 2002-01-2868, 2002.
- [195] Bradley D, Kalghatgi GT. Influence of autoignition delay time characteristics of different fuels on pressure waves and knock in reciprocating engines. *Combust Flame* 2009;156:2307–18.
- [196] Bansal G, Im HG. Autoignition and front propagation in low temperature combustion engine environments. *Combust Flame* 2011;158:2105–12.
- [197] Inoue T, Inoue Y, Ishikawa M. Abnormal combustion in a highly boosted SI engine - the occurrence of super knock. SAE Technical Paper 2012-01-1141, 2012.
- [198] Amann M, Alger T. Lubricant reactivity effects on gasoline spark ignition engine knock. *SAE Int J Fuels Lubr* 2012;5:760–71.
- [199] Sasaki N, Nakata K, Kawatake K, Sagawa S, Watanabe M, Sone T. The effect of fuel compounds on pre-ignition under high temperature and high pressure condition. SAE Technical Paper 2011-01-1984, 2011.
- [200] Haenel P, Seyfried P, Kleberg H, Tomazic D. Systematic approach to analyze and characterize pre-ignition events in turbocharged direct-injected gasoline engines. SAE Technical Paper 2011-01-0343, 2011.
- [201] Amann M, Mehta D, Alger T. Engine operating condition and gasoline fuel composition effects on low-speed pre-ignition in high-performance spark ignited gasoline engines. *SAE Int J Engines* 2011;4:274–85.
- [202] Dahm C, Han K-M, Spicher U, Magar M, Schiessl R, Maas U. Investigations on pre-ignition in highly supercharged SI engines. *SAE Int J Engines* 2010;3:214–24.
- [203] Zaccardi J-M, Duval L, Pagot A. Development of specific tools for analysis and quantification of pre-ignition in a boosted SI engine. *SAE Int J Engines* 2009;2:1587–600.
- [204] Wang Z, Xu Y, Wang J. Suppression of super-knock in TC-GDI engine using two-stage injection in intake stroke (TSII). *Sci China Technol Sci* 2014;57:80–5.
- [205] Peters N, Kerschgens B, Paczko G. Super-knock prediction using a refined theory of turbulence. *SAE Int J Engines* 2013;6:953–67.
- [206] Goyal G, Maas U, Warnatz J. Simulation of the transition from deflagration to detonation. SAE Technical Paper 900026, 1990.
- [207] Willand J, Daniel M, Montefrancesco E, Geringer B, Hofmann P, Kieberger M. Limits on downsizing in spark ignition engines due to pre-ignition. *MTZ Worldwide* 2009;70:56–61.
- [208] Zhang Z, Shu G, Liang X, Liu G, Yang W, Wang Z. Super knock and preliminary investigation of its influences on turbocharged GDI engine. *Trans CSICE* 2011;29:422–6.
- [209] Wang J, Wang Z. Research progress of high efficient and clean combustion of automotive gasoline engines. *J Automot Saf Energy* 2010;1:167–78.
- [210] Downs D, Pignéguy JH. An experimental investigation into pre-ignition in the spark-ignition engine. *Proc Inst Mech Eng* 1950;4:125–49.
- [211] Downs D, Theobald FB. The effect of fuel characteristics and engine operating conditions on pre-ignition. *Proc Inst Mech Eng* 1963;178:89–108.
- [212] Shibata G, Nagaiishi H, Oda K. Effect of intake valve deposits and gasoline composition on SI engine performance. SAE Technical Paper 922263, 1992.
- [213] Amann M, Alger T, Mehta D. The effect of EGR on low-speed pre-ignition in boosted SI engines. *SAE Int J Engines* 2011;4:235–45.
- [214] Luo X, Teng H, Hu T, Miao R, Cao L. Mitigating intensities of super knocks encountered in highly boosted gasoline direct injection engines. SAE Technical Paper 2015-01-0084, 2015.
- [215] Qi Y, Xu Y, Wang Z, Wang J. The effect of oil intrusion on super knock in gasoline engine. SAE Technical Paper 2014-01-1224, 2014.
- [216] Welling O, Moss J, Williams J, Collings N. Measuring the impact of engine oils and fuels on low-speed pre-ignition in downsized engines. *SAE Int J Fuels Lubr* 2014;7:1–8.
- [217] Ohtomo M, Miyagawa H, Koike M, Yokoo N, Nakata K. Pre-ignition of gasoline-air mixture triggered by a lubricant oil droplet. *SAE Int J Fuels Lubr* 2014;7:673–82.
- [218] Dingle SF, Cairns A, Zhao H, Williams J, Williams O, Ali R. Lubricant induced pre-ignition in an optical SI engine. SAE Technical Paper 2014-01-1222, 2014.
- [219] Wang Z, Long Y, Wang J. Research progress of pre-ignition and super-knock in boost gasoline engine. *J Automot Saf Energy* 2015;6:17–29.
- [220] Okada Y, Miyashita S, Izumi Y, Hayakawa Y. Study of low-speed pre-ignition in boosted spark ignition engine. *SAE Int J Engines* 2014;7:584–94.
- [221] Kuboyama T, Moriyoshi Y, Morikawa K. Visualization and analysis of LSPI mechanism caused by oil droplet, particle and deposit in highly boosted SI combustion in low speed range. *SAE Int J Engines* 2015;8:529–37.
- [222] Lauer T, Heiss M, Bobicic N, Holly W, Pritze S. A comprehensive simulation approach to irregular combustion. SAE Technical Paper 2014-01-1214, 2014.
- [223] Moriyoshi Y, Yamada T, Tsunoda D, Xie M, Kuboyama T, Morikawa K. Numerical simulation to understand the cause and sequence of LSPI phenomena and suggestion of CaO mechanism in highly boosted SI combustion in low speed range. SAE Technical Paper 2015-01-0755, 2015.
- [224] Magar M, Spicher U, Palaveev S, Gohl M, Müller G, Lensch-Franzen C, et al. Experimental studies on the occurrence of low-speed pre-ignition in turbocharged GDI engines. *SAE Int J Engines* 2015;8:495–504.
- [225] Wang Z, Qi Y, Liu H, Long Y, Wang J-X. Experimental study on pre-ignition and super-knock in gasoline engine combustion with carbon particle at

- elevated temperatures and pressures. SAE Technical Paper 2015-01-0752, 2015.
- [226] Kalghatgi G. Fuel/engine interactions. Warrendale PA: SAE International; 2013.
- [227] Yang Y, Zhou Z, Liu H, Cheng C, Hu Y. Effect of engine oil on low-speed stochastic pre-ignition from turbocharged DI gasoline engine. *Chin Intern Combust Engine Eng* 2015;36:58–61.
- [228] Welling O, Collings N, Williams J, Moss J. Impact of lubricant composition on low-speed pre-ignition. SAE Technical Paper 2014-01-1213, 2014.
- [229] Kassai M, Torii K, Shiraishi T, Noda T, Goh TK, Wilbrandt K, et al. Research on the effect of lubricant oil and fuel properties on LSPI occurrence in boosted S. I. engines. SAE Technical Paper 2016-01-2292, 2016.
- [230] Kassai M, Shiraishi T, Noda T, Hirabe M, Wakabayashi Y, Kusaka J, et al. An investigation on the ignition characteristics of lubricant component containing fuel droplets using rapid compression and expansion machine. *SAE Int J Fuels Lubr* 2016;9:469–80.
- [231] Hayakawa N, Miura K, Miyasaka T, Ishino T, Iijima A, Shoji H, et al. A study on the effect of Zn- and Mo-based engine oil additives on abnormal SI engine combustion using in-cylinder combustion visualization. *SAE Int J Engines* 2014;8:214–20.
- [232] Mansfield AB, Chapman E, Briscoe K. Impact of fuel octane rating and aromatic content on stochastic pre-ignition. SAE Technical Paper 2016-01-0721, 2016.
- [233] Pischinger S, Günther M, Budak O. Abnormal combustion phenomena with different fuels in a spark ignition engine with direct fuel injection. *Combust Flame* 2017;175:123–37.
- [234] Li Y, Ping Y, Yin Q. Experimental study on preignition and megaknock in turbocharged DI gasoline engine. *Chin Intern Combust Engine Eng* 2012;33:63–6.
- [235] Hülser T, Grünenfeld G, Brands T, Günther M, Pischinger S. Optical investigation on the origin of pre-ignition in a highly boosted SI engine using bio-fuels. SAE Technical Paper 2013-01-1636, 2013.
- [236] Kalghatgi GT. Deposits in gasoline engines - a literature review. SAE Technical Paper 902105, 1990.
- [237] Cracknell R, DAVIES T, Kalghatgi G. Fuel formulations. US Patent 20110271926, 2011.
- [238] Kalghatgi G, Algunaibet I, Morganti K. On knock intensity and superknock in SI engines. SAE Technical Paper 2017-01-0689, 2017.
- [239] Mayer M, Hofmann P, Geringer B, Williams J, Moss J. Influence of different fuel properties and gasoline - ethanol blends on low-speed pre-ignition in turbocharged direct injection spark ignition engines. *SAE Int J Engines* 2016;9:841–8.
- [240] Zheng J, Miller D, Cernansky N, Liu D. The effect of active species in internal EGR on preignition reactivity and on reducing UHC and CO emissions in homogeneous charge engines. SAE Technical Paper 2003-01-1831, 2013.
- [241] Sasaki N, Nakata K. Effect of fuel components on engine abnormal combustion. SAE Technical Paper 2012-01-1276, 2012.
- [242] Hamilton LJ, Rostedt MG, Caton PA, Cowart JS. Pre-ignition characteristics of ethanol and E85 in a spark ignition engine. *SAE Int J Fuels Lubr* 2008;1:145–54.
- [243] Chan EC, Evans RL, Davy MH, Cordiner S. Pre-ignition characterization of partially-stratified natural gas injection. SAE Technical Paper 2007-01-1913, 2007.
- [244] Zel'Dovich YB. Regime classification of an exothermic reaction with nonuniform initial conditions. *Combust Flame* 1980;39:211–4.
- [245] Bates L, Bradley D, Paczko G, Peters N. Engine hot spots: modes of auto-ignition and reaction propagation. *Combust Flame* 2016;166:80–5.
- [246] Di HS, He X, Zhang P, Wang Z, Wooldridge MS, Law CK, et al. Effects of buffer gas composition on low temperature ignition of iso-octane and n-heptane. *Combust Flame* 2014;161:2531–8.
- [247] Wang Z, Qi Y, Liu H, Zhang P, He X, Wang J. Shock wave reflection induced detonation under high pressure and temperature condition in closed cylinder. *Shock Waves* 2016.
- [248] Wang Z, Qi Y, He X, Wang J, Shuai S, Law CK. Analysis of pre-ignition to super-knock: hotspot-induced deflagration to detonation. *Fuel* 2015;144:222–7.
- [249] Kalghatgi GT, Bradley D. Pre-ignition and 'super-knock' in turbocharged spark-ignition engines. *Int J Engine Res* 2012;13:399–414.
- [250] Ra Y, Reitz RD. A reduced chemical kinetic model for IC engine combustion simulations with primary reference fuels. *Combust Flame* 2008;155:713–38.
- [251] Liu H, Wang Z, Wooldridge M, Fatouriae M, Jia Z, Qi Y, et al. Highly turbocharged gasoline engine and rapid compression machine studies of super-knock. *SAE Int J Engines* 2016;9.
- [252] Stiebels B, Schreiber M, Sakak AS. Development of a new measurement technique for the investigation of end-gas autoignition and engine knock. SAE Technical Paper 960827, 1996.
- [253] Griffiths JF, Whitaker BJ. Thermokinetic interactions leading to knock during homogeneous charge compression ignition. *Combust Flame* 2002;131:386–99.
- [254] Qi Y. Experimental research on super knock mechanism of gasoline engine (in Chinese). Beijing: Tsinghua University; 2015.
- [255] Ben-Dor G. Shock wave reflection phenomena. Springer; 2007.
- [256] Xiang S, Qi Y, Wang Z, Wang J. Numerical simulation of detonation initiation induced by shock wave reflection in a rapid compression machine (in Chinese). *Sci Sin Tech* 2016;46:1287–95.
- [257] Lim G, Lee S, Park C, Choi Y, Kim C. Effect of ignition timing retard strategy on NO<sub>x</sub> reduction in hydrogen-compressed natural gas blend engine with increased compression ratio. *Int J Hydrogen Energy* 2014;39:2399–408.
- [258] Chen X, Wang Y, Xu S, Zhu Y, Tao C, Xu T, et al. The engine knock analysis – an overview. *Appl Energy* 2012;92:628–36.
- [259] Abu-Qudais M. Exhaust gas temperature for knock detection and control in spark ignition engine. *Energy Convers Manage* 1996;37:1383–92.
- [260] Whelan DE, Schmidt GK, Hischier ME. An acceleration based method to determine the octane number requirement of knock sensor equipped vehicles. SAE Technical Paper 982721, 1998.
- [261] Haghgoie M. Effects of fuel octane number and inlet air temperature on knock characteristics of a single cylinder engine. SAE Technical Paper 902134, 1990.
- [262] Swarts A, Yates A, Viljoen C, Coetzer R. A further study of inconsistencies between autoignition and knock intensity in the CFR octane rating engine. 2005.
- [263] Grandin B, Denbratt I, Bood J, Brackmann C, Bengtsson P-E, Gogan A, et al. Heat release in the end-gas prior to knock in lean, rich and stoichiometric mixtures with and without EGR. SAE Technical Paper 2002-01-0239, 2002.
- [264] Ayala FA, Gerty MD, Heywood JB. Effects of combustion phasing, relative air-fuel ratio, compression ratio, and load on SI engine efficiency. SAE Technical Paper 2006-01-0229, 2006.
- [265] Russ S. A review of the effect of engine operating conditions on borderline knock. SAE Technical Paper 960497, 1996.
- [266] Towers JM, Hoekstra RL. Engine knock, a renewed concern in motorsports - a literature review. SAE Technical Paper 983026, 1998.
- [267] Lanzaferme R. Water injection effects in a single-cylinder CFR engine. SAE Technical Paper 1999-01-0568, 1999.
- [268] Böhm M, Mährle W, Bartelt H-C, Rubbert S. Functional integration of water injection into the gasoline engine. *MTZ* 2016;77.
- [269] Su J, Xu M, Li T, Gao Y, Wang J. Combined effects of cooled EGR and a higher geometric compression ratio on thermal efficiency improvement of a downsized boosted spark-ignition direct-injection engine. *Energy Convers Manage* 2014;78:65–73.
- [270] Wei H, Zhu T, Shu G, Tan L, Wang Y. Gasoline engine exhaust gas recirculation – a review. *Appl Energy* 2012;99:534–44.
- [271] Kumano K, Yamaoka S. Analysis of knocking suppression effect of cooled EGR in turbo-charged gasoline engine. SAE Technical Paper 2014-01-1217, 2014.
- [272] Qi Y, Srinivasan KK, Krishnan SR, Yang H, Midkiff KC. Effect of hot exhaust gas recirculation on the performance and emissions of an advanced injection low pilot-ignited natural gas engine. *Int J Engine Res* 2007;8:289–303.
- [273] Galloni E, Fontana G, Palmaccio R. Effects of exhaust gas recycle in a downsized gasoline engine. *Appl Energy* 2013;105:99–107.
- [274] Hoepke B, Jannsen S, Kasseris E, Cheng WK. EGR effects on boosted SI engine operation and knock integral correlation. *SAE Int J Engines* 2012;5:547–59.
- [275] Diana S, Giglio V, Iorio B, Police G. Evaluation of the effect of EGR on engine knock. SAE Technical Paper 982479, 1998.
- [276] Westin F, Grandin B, Ångström H-E. The influence of residual gases on knock in turbocharged SI-engines. SAE Technical Paper 2000-01-2840, 2000.
- [277] Parsons D, Akehurst S, Brace C. The potential of catalysed exhaust gas recirculation to improve high-load operation in spark ignition engines. *Int J Engine Res* 2015;16:592–605.
- [278] Grandin B, Ångström H-E. Replacing fuel enrichment in a turbo charged SI engine: lean burn or cooled EGR. SAE Technical Paper 1999-01-3505, 1999.
- [279] Fontana G, Galloni E. Experimental analysis of a spark-ignition engine using exhaust gas recycle at WOT operation. *Appl Energy* 2010;87:2187–93.
- [280] Alger T, Chauvet T, Dimitrova Z. Synergies between high EGR operation and GDI systems. *SAE Int J Engines* 2008;1:101–14.
- [281] Cairns A, Blaxill H, Irlam G. Exhaust gas recirculation for improved part and full load fuel economy in a turbocharged gasoline engine. SAE Technical Paper 2006-01-0047, 2006.
- [282] Duchaussou Y, Lefebvre A, Bonetto R. Dilution interest on turbocharged SI engine combustion. SAE Technical Paper 2003-01-0629, 2003.
- [283] Alger T, Hanhe S, Roberts CE, Ryan TW. The heavy duty gasoline engine - a multi-cylinder study of a high efficiency, low emission technology. SAE Technical Paper 2005-01-1135, 2005.
- [284] Roberts CE, Snyder JC, Stovell C, Dodge LG, Ryan TW, Stanglmaier RH. The heavy-duty gasoline engine - an alternative to meet emissions standards of tomorrow. SAE Technical Paper 2004-01-0984, 2004.
- [285] Goto T, Isobe R, Yamakawa M, Nishida M. The new Mazda gasoline engine Sky-activ-G. *ATZ Auto-Technol* 2011;11:40–7.
- [286] Li Y, Zhao H, Ma T. Stratification of fuel for better engine performance. *Fuel* 2006;85:465–73.
- [287] Liu H, Wang Z, Wang J, Wang M, Yang W. Controlled ASSCI with moderate auto-ignition for engine knock suppression in a GDI engine with high compression ratio. *ASME 2014 internal combustion engine division fall technical conference, ICEF2014-5434, 2014.*
- [288] Kume T, Iwamoto Y, Iida K, Murakami M, Akishino K, Ando H. Combustion control technologies for direct injection SI engine. SAE Technical Paper 960600, 1996.
- [289] Kuwahara K, Ueda K, Ando H. Mixing control strategy for engine performance improvement in a gasoline direct injection engine. SAE Technical Paper 980158, 1998.
- [290] Mohammadi A, Shioji M, Nakai Y, Ishikura W, Tabo E. Performance and combustion characteristics of a direct injection SI hydrogen engine. *Int J Hydrogen Energy* 2007;32:296–304.
- [291] Schwarz C, Schünemann E, Durst B, Fischer J, Witt A. Potentials of the spray-guided BMW DI combustion system. SAE Technical Paper 2006-01-1265, 2006.
- [292] Suzuki Y, Oki H, Kuroshima S. Gasoline SI. Engine combustion and knocking analysis on the mixture formation in the various direct injection fuel spray patterns. SAE Technical Paper 2006-01-0230, 2006.

- [293] Töpfer G, Reissing J, Weimar HJ, Spicher U. Optical investigation of knocking location on S.I.-engines with direct-injection. SAE Technical Paper 2000-01-0252, 2000.
- [294] Yang J, Anderson RW. Fuel injection strategies to increase full-load torque output of a direct-injection SI engine. SAE Technical Paper 980495, 1998.
- [295] Kassner E, Heywood JB. Charge cooling effects on knock limits in SI DI engines using gasoline/ethanol blends: part 1-quantifying charge cooling. SAE Technical Paper 2012-01-1275, 2012.
- [296] Abdelaal MM, Rabee BA, Hegab AH. Effect of adding oxygen to the intake air on a dual-fuel engine performance, emissions, and knock tendency. *Energy* 2013;61:612–20.
- [297] Cho S, Kim N, Chung J, Min K. The effect of ethanol injection strategy on knock suppression of the gasoline/ethanol dual fuel combustion in a spark-ignited engine. SAE Technical Paper 2015-01-0764, 2015.
- [298] Abd Alla GH, Soliman HA, Badr OA, Abd Rabbo MF. Effect of pilot fuel quantity on the performance of a dual fuel engine. *Energy Convers Manage* 2000;41:559–72.
- [299] Zhuang Y, Hong G. Effects of direct injection timing of ethanol fuel on engine knock and lean burn in a port injection gasoline engine. *Fuel* 2014;135:27–37.
- [300] Parlak A, Ayhan V, Deniz C, Kolip A, Koksal S. Effects of M15 blend on performance and exhaust emissions of spark ignition engine with thermal barrier layer coated piston. *J Energy Inst* 2008;81:97–101.
- [301] Khalifa AE, Antar MA, Farag MS. Experimental and theoretical comparative study of performance and emissions for a fuel injection SI engine with two octane blends. *Arabian J Sci Eng* 2015;40:1743–56.
- [302] Selim MYE. Sensitivity of dual fuel engine combustion and knocking limits to gaseous fuel composition. *Energy Convers Manage* 2004;45:411–25.
- [303] Bromberg L, Cohn D. Alcohol fueled heavy duty vehicles using clean, high efficiency engines. SAE Technical Paper 2010-01-2199, 2010.
- [304] Whitaker P, Shen Y, Spanner C, Fuchs H, Agarwal A, Byrd K. Development of the combustion system for a flexible fuel turbocharged direct injection engine. *SAE Int J Engines* 2010;3:326–54.
- [305] Zhuang Y, Hong G. Investigation to leveraging effect of ethanol direct injection (EDI) in a gasoline port injection (GPI) engine. SAE Technical Paper 2013-01-1322, 2013.
- [306] Zhuang Y, Hong G. The effect of direct injection timing and pressure on engine performance in an ethanol direct injection plus gasoline port injection (EDI+GPI) SI engine. SAE Technical Paper 2013-01-0892, 2013.
- [307] Kim N, Cho S, Choi H, Song HH, Min K. The efficiency and emission characteristics of dual fuel combustion using gasoline direct injection and ethanol port injection in an SI engine. SAE Technical Paper 2014-01-1208, 2014.
- [308] Liu H, Wang Z, Long Y, Xiang S, Wang J, Fatouraie M. Comparative study on alcohol gasoline and gasoline alcohol dual-fuel spark ignition (DFSI) combustion for engine particle number (PN) reduction. *Fuel* 2015;159:250–8.
- [309] Liu H, Wang Z, Wang J. Methanol-gasoline DFSI (dual-fuel spark ignition) combustion with dual-injection for engine knock suppression. *Energy* 2014;73: 686–93.
- [310] Hirooka H, Mori S, Shimizu R. Effects of high turbulence flow on knock characteristics. SAE Technical Paper 2004-01-0977, 2004.
- [311] Radwan MS, Helali AHB, Elfeky SM, Attai YA. An investigation on knock and pre-ignition with tumble induced turbulence. SAE Technical Paper 2007-01-3557, 2007.
- [312] Takahashi D, Nakata K, Yoshihara Y, Ohta Y, Nishiura H. Combustion development to achieve engine thermal efficiency of 40% for hybrid vehicles. SAE Technical Paper 2015-01-1254, 2015.
- [313] Shih S, Itano E, Xin J, Kawamoto M, Maeda Y. Engine knock toughness improvement through water jacket optimization. SAE Technical Paper 2003-01-3259, 2003.
- [314] Boretti A. Stoichiometric H2ICEs with water injection. *Int J Hydrogen Energy* 2011;36:4469–73.
- [315] Wang Li-S, Yang S. Turbo-cool turbocharging system for spark ignition engines. *Proc Inst Mech Eng Part D* 2006;220:1163–75.
- [316] Turner JWG, Popplewell A, Patel R, Johnson TR, Darnton NJ, Richardson S, et al. Ultra boost for economy: extending the limits of extreme engine downsizing. SAE Technical Paper 2014-01-1185, 2014.
- [317] Baek H-K, Lee SW, Han D, Kim J, Lee J, Aino H. Development of valvetrain system to improve knock characteristics for gasoline engine fuel economy. SAE Technical Paper 2014-01-1639, 2014.
- [318] Gottschalk W, Lezius U, Mathusall L. Investigations on the potential of a variable Miller cycle for SI knock control. SAE Technical Paper 2013-01-1122, 2013.
- [319] Ling Z, Burluka A, Azimov U. Knock properties of oxygenated blends in strongly charged and variable compression ratio engines. SAE Technical Paper 2014-01-2608, 2014.
- [320] Rabia SM, Korah NS. Knocking phenomena in a gasoline engine with late-intake valve closing. SAE Technical Paper 920381, 1992.
- [321] Shaik A, Moorthy NSV, Rudramoorthy R. Variable compression ratio engine: a future power plant for automobiles - an overview. *Proc Inst Mech Eng Part D* 2007;221:1159–68.
- [322] Clenci AC, Descombes G, Podevin P, Hara V. Some aspects concerning the combination of downsizing with turbocharging, variable compression ratio, and variable intake valve lift. *Proc Inst Mech Eng Part D* 2007;221:1287–94.
- [323] Schwaderlapp M, Habermann K, Yapici KI. Variable compression ratio - a design solution for fuel economy concepts. SAE Technical Paper 2002-01-1103, 2002.
- [324] Morikawa K, Moriyoshi Y, Kuboyama T, Imai Y, Yamada T, Hatamura K. Investigation and improvement of LSPI phenomena and study of combustion strategy in highly boosted SI combustion in low speed range. SAE Technical Paper 2015-01-0756, 2015.
- [325] Xu Z, Zhou Z, Wu T, Li T, Cheng C, Yin H. Investigations of smoke emission, fuel dilution and pre-ignition in a 2.0L turbo-charged GDI engine. SAE Technical Paper 2016-01-0698, 2016.
- [326] Ritchie A, Boese D, Young AW. Controlling low-speed pre-ignition in modern automotive equipment part 3: identification of key additive component types and other lubricant composition effects on low-speed pre-ignition. *SAE Int J Engines* 2016;9:832–40.
- [327] Luo X, Teng H, Hu T, Miao R, Cao L. An experimental investigation on low speed pre-ignition in a highly boosted gasoline direct injection engine. *SAE Int J Engines* 2015;8:520–8.
- [328] Xu Y, Wang Z, Wang J, Li D. Suppression strategies for super-knock of turbocharged GDI engines. *Trans CSICE* 2014;32:26–31.
- [329] Amann M, Alger T, Westmoreland B, Rothmaier A. The effects of piston crevices and injection strategy on low-speed pre-ignition in boosted SI engines. *SAE Int J Engines* 2012;5:1216–28.
- [330] Han L, Zhu T, Qiao H, Zhang D, Fu D, Zhang J. Investigation of low-speed pre-ignition in boosted spark ignition engine. SAE Technical Paper 2015-01-0751, 2015.
- [331] Mayer M, Hofmann P, Geringer B, Williams J, Moss J, Kapus P. Influence of different oil properties on low-speed pre-ignition in turbocharged direct injection spark ignition engines. SAE Technical Paper 2016-01-0718, 2016.
- [332] Fraisl G. Gasoline engine 2020. SAE 2015 high efficiency IC engine symposium; 2015.